

CRANFIELD INSTITUTE OF TECHNOLOGY

School of Mechanical Engineering

Ph.D. Thesis

Academic Years 1974-76

G. E. LORENZETTO

INFLUENCE OF LIQUID PROPERTIES ON

PLAIN-JET AIRBLAST ATOMIZATION

SUPERVISOR : Professor A.H. LEFEBVRE

April, 1976

ProQuest Number: 10820920

All rights reserved

INFORMATION TO ALL USERS

The quality of this reproduction is dependent upon the quality of the copy submitted.

In the unlikely event that the author did not send a complete manuscript and there are missing pages, these will be noted. Also, if material had to be removed, a note will indicate the deletion.



ProQuest 10820920

Published by ProQuest LLC (2019). Copyright of the Dissertation is held by Cranfield University.

All rights reserved.

This work is protected against unauthorized copying under Title 17, United States Code
Microform Edition © ProQuest LLC.

ProQuest LLC.
789 East Eisenhower Parkway
P.O. Box 1346
Ann Arbor, MI 48106 – 1346

SUMMARY

This thesis reports the results of a detailed programme of research on airblast atomization carried out using a specially designed plain-jet atomizer in which the fuel is injected into a high velocity airstream in the form of a discrete jet. Because recent studies on airblast atomization have been mainly confined to sheet and then subjected on both sides to the atomizing action of high velocity air, information was needed to carry out a comparison between the two mechanisms of atomization. It was in order to obtain such information that the present investigation was undertaken and the study essentially resolved into a detailed experimental exploration of the spray characteristics of 'plain-jet' airblast atomizers.

Specially prepared liquids were employed to distinguish between the separate effects on S.M.D. (Sauter Mean Diameter of spray) of viscosity, surface tension and density. The liquids employed represented a range of values of viscosity from 1.0 to 76×10^{-3} Kg/ms, while surface tension and density were varied between 26 and 73×10^{-3} N/m and 794 and 2180 Kg/m^3 respectively. Atomizing air velocities covered the range of practical interest to the designers of continuous combustion systems and varied between 70 and 180 m/s. The effect of scale on S.M.D. was studied using several different fuel injectors varying in orifice diameter between 0.39 and 1.58 mm.

A detailed description of the light-scattering technique for drop size measurement is included.

Analysis of the experimental data showed that they could be described to a reasonable order of accuracy by the following dimensionally correct empirical expression:

$$\text{S.M.D.} = 950 \times 10^3 \frac{(\sigma_1 W_1)^{0.33}}{v_r \rho_1^{0.37} \rho_a^{0.30}} (1 + \frac{1}{\text{AFR}})^{1.7} + 127 \times 10^3 \eta_l \left(\frac{D_o}{\sigma_1 \rho_1} \right)^{0.5} (1 + \frac{1}{\text{AFR}})^{1.8}$$

The ability of this equation to predict values of S.M.D. over the above range of air and liquid properties is also demonstrated.

■ ■ ■ ■

X

ACKNOWLEDGEMENTS

The author wishes to record his sincere appreciation to Professor A.H. Lefebvre for his assistance and guidance at every stage of this work.

He also wishes to express his gratitude to Monsieur Jean Corrihons (Sté Creusot-Loire, France), without whom his stay at Cranfield would not have been possible.

Thanks are due to the supporting staff of the School of Mechanical Engineering and in particular to Mr. H.D. Bambury who always provided all possible assistance in making 'things working'. Thanks are also due to Mr. B.R. Moffit for his expertise in helping with the many electronics problems.

A special word of thanks to Mrs. Todd for neat typing of the thesis.

Cet ouvrage est dédié à
Bernadette qui a bien
mérité ce doctorat ... par
sa compréhension admirable
et son sacrifice de tant
d'heures de solitude.

CONTENTS

	Page
Summary	i
Acknowledgements	ii
Contents	iii
List of Tables	vi
List of Figures	vii
List of Plates	xi
Nomenclature	xii
Chapter 1:	
INTRODUCTION	1
1.1 : Pressure Atomizers	1
1.2 : Vaporisers	2
1.3 : Airblast Atomizers	2
1.4 : Scope of the Present Work	4
Chapter 2:	
LITERATURE REVIEW	6
2.1 : Nukiyama and Tanasawa	6
2.2 : Wigg	8
2.3 : Rizkalla-Lefebvre	11
2.4 : Other Relevant Work on Airblast Atomization	14
Chapter 3:	
PROCESS OF DROPS FORMATION AND LIQUID JET BREAK UP	17
3.1 : Shattering of Liquid Drops	17
3.2 : Atomization of Liquid Sheets and Jets.	21
Chapter 4:	
EXPERIMENTAL TECHNIQUE AND APPARATUS	25
4.1 : The Spray	25
4.2 : Optical Method for Mean Droplet Size	26

	Page
4.3 : The Opto-Electronic Apparatus	27
4.4 : Readout of Illumination Profile	30
4.5 : Air System	31
4.6 : Liquid System	32
4.7 : Atomizer	32
 Chapter 5: TESTS RESULTS	 33
5.1 : A.F.R. Effect	34
5.2 : Effect of Atomizing Air Velocity	35
5.3 : Atomizer Scale Effect	36
5.4 : Effect of Liquid Flow Rate	36
5.5 : Effect of Liquid Viscosity	37
5.6 : Effect of Liquid Surface Tension	37
5.7 : Effect of Liquid Density	37
 Chapter 6: ANALYSIS OF DATA RESULTS	 39
6.1 : Empirical Results	39
6.1.1: The Effects of the Atomizer Linear Dimensions on Spray Atomization	40
6.1.2: The Effect of Other Variables on S.M.D.	41
6.2 : Dimensional Analysis	43
6.3 : Analysis of Drop-Size Data	46
6.4 : Comparison between Experimental Data Points and Equation (24)	49
6.5 : Comparison with Rizkalla-Lefebvre's Measured Results	50
6.6 : Comparison with Nukiyama and Tanasawa's Calculated Results (Ref. 39)	50
6.7 : Comparison with Wigg's (Ref. 52) Calculated Results	51

	Page
Chapter 7:	
CONCLUSIONS	52
7.1 : Suggestions for Future Work	55
REFERENCES	56
APPENDICES	
A	
ATOMIZATION EFFICIENCY	63
B	
CALIBRATION AND OPERATING PROCEDURE OF THE LOGARITHMIC AMPLIFIER	66
TABLES	68
FIGURES	
PLATES	

LIST OF TABLES

- (1) Solutions of the Synthetic Hydrocarbon Polymer, Hyvis Polybutene No. 05 in kerosine to obtain a Wide Range of Viscosity.
- (2) Mixtures of Sec-Butyl Alcohol (Butan-2-ol) with Water to obtain Different Values of Surface Tension.
- (3) Dibromo-Ethane (Ethylene Dibromide) diluted with Methylated Spirit to obtain a Wide Range of Density.

LIST OF FIGURES

1. Airblast Atomizer Used in Present Study.
2. Airblast Atomizer Used by Rizkalla and Lefebvre (Refs. 43 & 45).
3. Nukiyama and Tanasawa's Atomizers (Ref. 39).
4. N.G.T.E. Airblast Atomizer.
5. N.R.L. Canada Convergent Nozzles.
6. Early N.G.T.E. High Pressure Air Atomizers.
7. Rolls-Royce 'DART' Airspray Atomizer.
8. The Optical Bench used by Rizkalla and Lefebvre (Ref. 43).
9. Godbole's No. 3 (Ref. 13) and Bryan's (Ref. 3) Atomizer.
10. Graphs Illustrating Inverse Relationship between S.M.D. and Air Pressure from Rizkalla and Lefebvre's Work. (Ref. 45).
11. Optical Bench as Used by Dobbins, Crocco and Glassman. (Ref. 9).
12. Mean Theoretical Illumination Profile (Dobbins, Crocco and Glassman - Ref. 9).
13. Mean Theoretical Illumination Profile (Roberts and Webb - Refs. 46 and 47).
14. The Optical Bench in Diagrammatic Form as used in Present Study.
15. Beam Expanding and Collimating Telescope.
16. Block Diagram of Light Scattering Instrumentation.
17. Optical Receiving System.
18. E.M.I. - 9658 MR Photomultiplier Spectral Response.
19. Typical X-Y Recorder Plot.
20. Typical X-Y Recorder Plot.
21. Typical X-Y Recorder Plot.
22. S.M.D. Vs. Traverse Distance 'r' for 60 cm Focal Length Lens and 6328Å Wavelength.
23. Air Nozzles Flow Characteristics.
24. Typical Plain-Jet Atomizer.
25. Typical Convergent Air Nozzle.

26. 3-D Impression of 'Plain-Jet' Atomizer Performance.
27. Influence on S.M.D. of Air Velocity and Air/Water Mass Ratio (A.F.R.)
28. Influence on S.M.D. of Air Velocity and Air/Kerosine Mass Ratio.
29. Influence on S.M.D. of Air/Liquid Mass Ratio for Water and Kerosine.
30. Influence on S.M.D. of Air Velocity alone (Water).
31. Influence on S.M.D. of Air Velocity alone (Kerosine).
32. Influence on S.M.D. of Air Velocity for large A.F.R. - Air Nozzles Used: 25.4 and 19.05 mm (Water).
33. Influence on S.M.D. of Air Velocity for large A.F.R. - Air Nozzle Used: 25.4 mm (Kerosine).
34. Influence on S.M.D. of Air Velocity for a 12.70 mm Air Nozzle (Water).
35. Influence on S.M.D. of Air Velocity for a 12.70 mm Air Nozzle (Kerosine).
36. Influence on S.M.D. of Fuel Orifice Diameter: Scale Effect (Water).
37. Influence on S.M.D. of Fuel Orifice Diameter: Scale Effect (Kerosine).
38. Influence on S.M.D. of Fuel Orifice Diameter: Scale Effect (High Viscosity Liquid).
39. Influence on S.M.D. of Liquid Flow Rate (Water).
40. Influence on S.M.D. of Liquid Flow Rate (Kerosine).
41. Influence on S.M.D. of Liquid Viscosity at Constant Air Velocity.
42. Influence on S.M.D. of Liquid Viscosity at Constant Liquid Flow Rate.
43. Influence on S.M.D. of Air/Liquid Mass Ratio at High Viscosity Liquid for Constant Air Velocity.
44. Influence on S.M.D. of Air/Liquid Mass Ratio at High Viscosity Liquid for Constant Liquid Flow Rate.

45. Influence on S.M.D. of Air/Liquid Mass Ratio for High Viscosity Liquid at Large Air Flow Rates.
46. Influence on S.M.D. of Liquid Surface Tension at Constant Air Velocity.
47. Influence on S.M.D. of Liquid Surface Tension at Constant Liquid Flow Rate.
48. Influence on S.M.D. of Liquid Density at Constant Air Velocity.
49. Influence on S.M.D. of Liquid Density at Constant Liquid Flow Rate.
50. Influence of Air/Liquid Mass Ratio for Low Viscosity Liquid in Log-Plot Form.
51. Influence of Liquid Flow Rate for Low Viscosity Liquids in Log-Plot Form.
52. Influence of Liquid Surface Tension in Log-Plot Form.
53. Influence of Liquid Density in Log-Plot Form.
54. Influence of Fuel Orifice Diameter (Scale Effect) for High Viscosity Liquid in Log-Plot Form.
55. Influence of Air/Liquid Mass Ratio for High Viscosity Liquids in Log-Plot Form.
56. Influence of Liquid Viscosity in Log-Plot Form.
57. Comparison of Calculated and Experimental Values of S.M.D. for Water and Kerosine.
58. Comparison of Calculated and Experimental Values of S.M.D. (Liquid Viscosity Data).
59. Comparison of Calculated and Experimental Values of S.M.D. (Liquid Surface Tension Data).
60. Comparison of Calculated and Experimental Values of S.M.D. (Liquid Density Data).
61. Comparison of Experimental Values of S.M.D.: Rizkalla-Lefebvre's (Ref. 45) Vs. Present Work for Kerosine at Variable A.F.R.
62. Comparison of Experimental Values of S.M.D.: Rizkalla-Lefebvre's (Ref. 43) Vs. Present Work for High Viscosity Liquids at Variable A.F.R.

63. Comparison of Experimental Values of S.M.D.: Rizkalla-Lefebvre's (Ref. 45) Vs. Present Work for Kerosine at Variable Air Velocity.
64. Comparison of Experimental Values of S.M.D.: Rizkalla-Lefebvre's (Ref. 45) Vs. Present Work for High Viscosity Liquids at Variable Air Velocity.
65. Comparison of Experimental and Calculated Values of S.M.D.: Rizkalla-Lefebvre's (Ref. 45) Vs. Present Work for Low Viscosity Liquids as a Function of Weber No.
66. Comparison of Predicted (Nukiyama and Tanasawa, Ref. 39 and Eq. 1) Vs. Measured (Present Study) Values of S.M.D. for Low Viscosity Liquids.
67. Comparison of Predicted (Wigg, Ref. 51, Eq. 7) Vs. Measured (Present Study) Values of S.M.D. for Low Viscosity Liquids.

LIST OF PLATES

- (1) General View of the Test Rig.
- (2) View of the Receiving Opto-Electronic Traversing System.
- (3) General View of the Light Intensity Profile Recording System.
- (4) View of the Air Supply System.
- (5) View of the Control Panel, Kerosine and Special Liquids Reservoirs and Part of the Recording System.
- (6) Close-up of a Kerosine Spray from a Plain-Jet Atomizer at 120 m/s Air Velocity.
- (7) View of the Fuel Orifices used Throughout the Present Work.
- (8) View of Some Air Nozzles.
- (9) Kerosine Spray: $W_1 = 1 \text{ gr/s} - V_r = 100 \text{ m/s} - D = 0.794 \text{ mm.}$
- (10) Kerosine Spray: $W_1 = 1 \text{ gr/s} - V_r = 100 \text{ m/s} - D = 1.588 \text{ mm.}$
- (11) Kerosine Spray: $W_1 = 2 \text{ gr/s} - V_r = 100 \text{ m/s} - D_n = 5.83 \text{ mm.}$
- (12) Kerosine Spray: $W_1 = 2 \text{ gr/s} - V_r = 100 \text{ m/s} - D_n = 6.85 \text{ mm.}$
- (13) Kerosine Spray: $W_1 = 2 \text{ gr/s} - V_r = 100 \text{ m/s} - D_n = 12.7 \text{ mm.}$
- (14) Kerosine Spray: $W_1 = 2 \text{ gr/s} - V_r = 70 \text{ m/s} - D_n = 6.85 \text{ mm.}$
and $D = 1.191 \text{ mm.}$
- (15) Kerosine Spray: $W_1 = 2 \text{ gr/s} - V_r = 100 \text{ m/s} - D_n = 6.85 \text{ mm.}$
and $D = 1.191 \text{ mm.}$
- (16) Kerosine Spray: $W_1 = 2 \text{ gr/s} - V_r = 140 \text{ m/s} - D_n = 6.85 \text{ mm.}$
and $D = 1.191 \text{ mm.}$

NOMENCLATURE

\AA	=	Angstrom, ($1 \text{\AA} = 10^{-7} \text{mm}$)
A_1	=	Liquid jet surface area, m^2
A_2	=	Total surface area of spray droplets, m^2
A.F.R.	=	Atomizing Air/Liquid Mass Flow Ratio
D	=	Diameter of plain-jet fuel orifice, mm
D_n	=	Diameter of air nozzle, mm
\bar{D}	=	Most probable droplet diameter, micron
D_∞	=	Maximum droplet diameter, micron
\bar{D}/D_∞	=	Skewness in U.L.D.F.
$D_{+\frac{1}{2}}, D_{-\frac{1}{2}}$	=	Droplet diameters occurring at half the frequency of the most probable droplet diameter.
$\frac{D_{+\frac{1}{2}} - D_{-\frac{1}{2}}}{\bar{D}}$	=	Spread in U.L.D.F.
d_{32}	=	Volume to surface area mean diameter, = $\frac{\sum nd^3}{\sum nd^2}$
d	=	Droplet diameter, micron
f	=	Focal length (also mathematical function), cm
H.T.	=	High Tension Power
$I(\theta)$	=	Intensity of light at angular displacement θ radiant.

- M.M.D. = Mass Median Diameter (≈ 1.2 S.M.D.), micron
- n = Number of drops, the diameter of which is 'd'
(also slope of straight lines in log-log graphs)
- P_1 = Total pressure upstream the air nozzle, N/m^2
- P_2 = Ambient pressure (downstream the air nozzle), $\frac{N}{m^2}$
- Q = Volume flow rate, m^3/s
- r = Photomultiplier traverse distance corresponding to 1/10th I (θ)
- Re = Reynolds No, $VaD \rho_a / \eta_1$ $\frac{\rho V d}{\eta}$
- S.M.D. = Sauter Mean Diameter, micron = $\frac{\sum nd^3}{\sum nd^2}$
- S = Surface area created by atomization of liquid jet into droplets: $S = A_2 - A_1$
- T = Absolute temperature, $^{\circ}K$
- U.L.D.F. = Upper Limit Distribution Function
- V = Velocity, m/s
- W = Mass flow rate, gr/s
- We = Weber No, $\rho_a V_a^2 D / \sigma_1$

GREEK SYMBOLS

μ	=	Micron, ($1 \mu = 10^{-3} \text{ mm}$)
η	=	Absolute viscosity, Kg/ms ($= 10^3$ centipoise)
ν	=	Kinematic viscosity, m^2/s ($= 10^6$ centistokes)
σ_l	=	Liquid surface tension, N/m ($= 10^3$ dyn/cm)
ρ	=	Density, Kg/m^3 ($= 10^{-3}$ gr/cm^3)
θ	=	Angular displacement of monochromatic light beam, rad.
λ	=	Wavelength, Angstroms
τ	=	External force acting on droplets (dynamic pressure)
ϵ	=	Energy associated to droplets, Nm

SUBSCRIPTS

a	=	Air
l	=	Liquid
r	=	Relative
s	=	Spray
n	=	Nozzle

CHAPTER 1

I N T R O D U C T I O N

CHAPTER 1

INTRODUCTION

The subject of investigation is that of "liquid atomization" which has many practical applications such as spray drying and crop spraying, and is widely used in engines and furnaces as a means of fuel injection.

The fuel injector is one of the most critical components of a combustion chamber. Rapid liquid fuel evaporation is a main requisite for a gasturbine combustor and in general finely atomised and well distributed fuels must be provided.

1.1 - Pressure Atomizers

The pressure atomizer, which is still widely used in gasturbine combustors, depends almost entirely on fuel pressure for the quality of the spray. In the pressure atomizer the potential energy of the fuel is converted into kinetic energy and applied to the process of disintegration. When the injection pressure is increased the droplets become smaller and the size is found to be proportional to p^n , where n normally is smaller than 0.5 (Ref. 12).

The gasturbine is essentially a high power unit, with a correspondingly high rate of fuel consumption. It is desirable to avoid very high fuel injection pressures in order to increase reliability in service. At the same time good atomization is necessary to maintain the stability of the flame under varying conditions of service. The range of fuel flow needed to cover all working conditions can be of the order of 50 to 1 for a high performance aircraft gas turbine. Since fuel flow is proportional to the square root of the pressure drop across the nozzle, the required range of fuel pump pressures for a single nozzle is beyond the capability of practical fuel pumps.

To avoid excessive pressure variations, different types of "wide-range" atomizers have been developed, of which the "duplex" and the "duple" (or dual-orifice) atomizer are the most important. The latter uses a small flow number pilot atomizer which fits inside a larger main atomizer. At low fuel flows all the fuel is supplied from the pilot atomizer but when the fuel pressure exceeds

d

X

a certain level, fuel is also supplied by the main atomizer.

Lefebvre and Miller (Ref. 29) have pointed out that with pressure atomizers the exhaust temperature traverse is dependent on fuel flow, since the fuel distribution is largely governed by fuel momentum rather than chamber aerodynamics, and this may affect turbine blade life. Furthermore, pressure swirl atomizers create a fuel rich region in the centre of the flame tube adjacent to the atomizer. At high chamber pressures this zone becomes even richer because of a reduction in fuel penetration. This fuel-rich zone is responsible for one of the main drawbacks of this system namely, the production of large amounts of soot, but it also provides wide stability limits (Ref. 28).

It has been reported by Mock and Ganger (Ref. 34) that the attainment of a high degree of atomization and uniformity of distribution, particularly at low fuel rates, are major needs for gas turbine combustors. Similarly, Lawrence (Ref. 24) stated that a well atomized fuel is required when the fuel flow rate is low. Thus, an important characteristic of an atomizer is to ensure the quality of atomization at low as well as at high fuel flow rates.

1.2 - Vaporisers

The fuel, together with some air, is injected into the vaporiser tube which is commonly of a walking stick shape. The fuel-air mixture is heated up by the tube walls and emerges as a mixture of air and vaporised fuel.

The main criticism^{is} of this controversial means of fuel injection is the mechanical reliability of the vaporising tubes, especially at high combustion pressures (Lefebvre, Ref. 27). It seems likely that vaporising systems will pose formidable mechanical problems due to overheating of the vaporising tubes by the intense radiation associated with high combustion pressures (Ref. 27).

Further disadvantages of vaporising systems are the need for auxiliary fuel jets for starting, slow response to changes in fuel flow and fairly narrow stability limits.

1.3 - Airblast Atomizers

The "pneumatic" or "two-fluid atomization", as sometimes airblast atomization is referred to, is a method of liquid spray production by the disruptive action of a high velocity compressible fluid on thin liquid films, or straight jets, by friction forces.

It is particularly well suited to the production of sprays having average drops diameters below 50 microns.

The present study is confined to "plain-jet atomizers" which consist of a small diameter tube discharging a liquid jet along the axis of a high-velocity gas stream.

Such atomizers were previously studied by Nukiyama and Tanasawa (Ref. 39). In an alternative form of airblast atomizer the fuel is caused to spread over a "prefilmer" surface into a thin attenuated sheet of uniform thickness. As the liquid sheet flows over the edge of the prefilmer it is shattered into fine droplets by high velocity air which then enters the combustion zone. An example of this "thin sheet" airblast atomizer is shown in Fig. 2. Such an airblast atomizer was used by Rizkalla and Lefebvre (Ref. 45).

Lefebvre and Miller (Ref. 29) investigated the performance of an airblast atomizer at the conditions encountered in gasturbine combustion chambers. They concluded that the airblast atomizer was capable of producing fuel droplets comparable in size to those obtained from a swirl atomizer.

The continuing trend towards gasturbine engines of higher pressure ratios promoted the interest in airblast atomization. In this system, droplet size is less dependent on fuel flow rate and droplet momentum is less important, the spray being largely airborne, its distribution throughout the combustion zone being dictated by the airflow pattern.

Fuel pressures therefore, can be low. Because the fuel enters the combustion zone premixed with air the combustion is characterized by a blue flame of low radiation and a minimum of exhaust smoke. Moreover, the airblast-atomizer is continuously cooled by the high velocity air flowing over it at compressor outlet temperature and fuel-rich zones close to the fuel spray, as occur with pressure atomizers, are prevented by the early mixing of fuel and air before entering the combustion zone.

The most important advantages associated with airblast atomization can be summarized as follows:-

- (a) The fuel droplets entering the combustion zone remain completely airborne, their distribution is dictated mainly by the air-flow pattern and is unaffected by fuel flow, hence the spray angle and penetration are relatively constant over a wide range of fuel flows. This also prevents deposition of liquid on solid surfaces.

- (b) The ensuing combustion is characterized by very low soot formation and a blue flame of low luminosity, resulting in relatively cool flame-tube walls and reductions in exhaust smoke.
- (c) The fuel distribution pattern which controls the combustion pattern, and hence the temperature traverse quality at the chamber outlet, remains fairly insensitive to changes of fuel flow.
- (d) Atomizer component parts are protected from overheating by the fuel and air flowing over them.
- (e) Low fuel pressure requirements.

However, since the air used for atomization mixes well with the atomized fuel, the performance results in quite narrow stability limits and it is essential to keep the air required for atomization to a minimum to get acceptable stability limits.

1.4 - Scope of the Present Work.

A great deal of effort has been devoted to investigating airblast atomizer performances with a view to establishing relationships between the various design and operating parameters and the most important liquid spray characteristics: the Sauter Mean Diameter (S.M.D.). Most of the research in this field, so far, has been carried out at atmospheric pressure using "thin sheet" airblast atomizers. Since the pioneer work of Nukiyama and Tanasawa, very little work has been done to study the performance of "plain-jet" airblast atomizers which, by virtue of their simplicity and ease of manufacture, may represent a very attractive solution to the fuel injection problem in both gas turbine engines (Wigg Ref. 52) and furnaces. Nukiyama and Tanasawa investigated with their photomicrographic technique the performance of such plain jet atomizers (Fig. 3) only within a restricted range of liquid properties.

This thesis describes a programme of research carried out in order to extend the scope of Nukiyama and Tanasawa's work and to include a wider range of

flow conditions. A more modern optical technique was used, due to Dobbins, Crocco and Glassman, (Ref. 9) based on the scattering of a monochromatic beam of laser light by the spray under investigation. Other objectives were to study the effect of atomizer size on S.M.D., to improve the prediction of S.M.D. for this particular system of atomization and to attempt some performance comparisons with thin sheet airblast atomizers over an extended range of liquid properties.

CHAPTER 2

L I T E R A T U R E R E V I E W

CHAPTER 2

LITERATURE REVIEW

The scientific literature on the subject of airblast atomization is abundant, but the information available on S.M.D. prediction for a range of liquid properties and flow conditions is quite small.

2.1 - Nukiyama and Tanasawa

It is largely recognized that one of the most fundamental researches in pneumatic atomisation, certainly the best known and the most widely quoted research in this field, is that of Nukiyama and Tanasawa (Ref. 39). By measuring droplet S.M.D. and drop size distributions for a range of liquid properties, flow conditions and nozzle sizes and configurations (Fig. 3), they delineated three successive stages in the atomization of a liquid jet by the action of an air stream: A) "Dropwise atomisation" where at very low relative air velocities the liquid jet is bead-like, swollen and contracted with continuously increasing amplitude, until the liquid jet finally breaks up into several separated drops. B) "Twisted ribbon-like atomization" whereby an increase in relative air velocity will create a fluttering action on the jet with the effect of shaping the liquid jet as a twisted ribbon (a portion of the ribbon is caught up and drawn out into a fine ligament), and C) "Filmwise atomization" which is reached when the relative air velocity is increased still further. This causes the flattening action of the horizontal part of the twisted ribbon and thus forms a cobweb-like film, which is so thin that it tears itself apart into microdroplets.

By studying the atomization of gasoline, water, oils and solutions of alcohol and glycerine by compressed air jets, Nukiyama and Tanasawa developed their well known empirical equation for Sauter Mean Diameter:

$$S.M.D. = 585 \frac{\sqrt{\sigma_l}}{v_r \sqrt{\rho_l}} + 597 \left(\frac{\mu_l}{\sqrt{\sigma_l \rho_l}} \right)^{0.45} \left(1000 \frac{Q_l}{Q_a} \right)^{1.5} \quad (1)$$

where: ρ_l = liquid density (gr/cc)
 σ_l = liquid surface tension (dyn/cm)
 μ_l = coefficient of viscosity (poise)
 V_r = relative air velocity (m/sec)
 Q_l = liquid volumetric flow rate (cm³/sec)
 Q_a = air volumetric flow rate (cm³/sec)

X X Droplet diameters were measured by taking microphotographs of droplets collected on oil-coated small glass slides and then counted and measured to obtain the mean diameter understood as:

$$d_{32} = \frac{\sum n d^3}{\sum n d^2} \quad \begin{matrix} 4.1 \\ (2) \end{matrix}$$

where: n = number of droplets
 d = diameter of droplets.

←
The correlating formula shows that liquid viscosity has little or no effect on S.M.D. as long as the air to liquid volumetric ratio is high, but with smaller air flows S.M.D. increases with viscosity. It was also found that, within experimental error, S.M.D. is independent of the size of the liquid and air nozzles and depends only on the volumetric flow ratio Q_a/Q_l . For liquids of low viscosity, such as water and gasoline, the first term of the empirical equation is predominant, and S.M.D. depends only on liquid density and liquid surface tension, and shows an inverse proportionality law with relative air velocity. When Q_a/Q_l decreases, S.M.D. is mainly governed by the second term of the equation and the surface tension has only a slight influence on mean drop size.

X

The Nukiyama-Tanasawa's equation is dimensionally inconsistent and it is only valid for the following range of liquid properties:

Liquid viscosity : from 1.0 to 30 centipoise

Liquid surface tension : from 30 to 73 $\frac{\text{dyn}}{\text{cm}}$

Liquid density : from 0.8 to 1.2 $\frac{\text{gr}}{\text{cm}^3}$

In 1948 Lewis, Goglia, Edwards, Rice and Smith (Ref. 31) succeeded in correlating their experimental results obtained with different atomizers. They found that at very high values of air/liquid volumetric ratios the liquid surface tension was a controlling parameter. In their research programme they used atomizing gases such as nitrogen, ethylene and helium and found that gas density also plays a role as a parameter affecting droplet size.

For example, for constant gas viscosity, Q_a/Q_l and relative air velocity, if the gas pressure were reduced to one-seventh of its original value, the diesel oil droplets were found to increase by a factor of two.

2.2 - Wigg

The work done by Wigg and published in 1959 and 1964 (Ref. 51, 52) represents one of the most valuable contributions towards a better understanding of airblast atomisation in recent years.

He investigated the performance of three large airblast atomizers, geometrically similar, made to the same design with values of $D = 1.27, 2.54$ and 3.59 cm (Fig. 4). The standard design has air swirlers, which have been omitted in the figure. A large number of tests was carried out to show the variation of mass median diameter (≈ 1.2 S.M.D.) with water/air ratio. A linear relationship was obtained of the form:-

$$\text{M.M.D.} = 4 + (58 + 55 D^{1.5}) / (W_a / W_l) \quad (3)$$

where D is the inner body diameter. This relationship is in line with the Japanese approach also. By comparing his experimental results with some of the results obtained by Golitzine et al (Ref. 15 and Fig. 5) and by Clare and Radcliffe (Ref. 5 and Fig. 6), he found that geometric scale had an effect on mean drop size only through its influence on liquid mass flow rate.

Wigg's paper also gave a theoretical account of the atomization processes based on kinetic energy considerations and momentum sharing principles. The following expression:

$$\text{M.M.D.} \propto \eta_l^{0.5} W_l^{0.05} (1 + W_l/W_a)^{0.5} / V_r \quad (4)$$

was derived. Wigg also suggested that coalescence (or droplet recombination) should be taken into account when the number of droplets per unit volume of air containing the spray becomes significant and an extra term should be considered:

$$\text{M.M.D.} \propto \left[1 + 2 \left(\frac{W_l}{W_a} \right)^{0.7} W_l^{0.25} \right] \quad (5)$$

The complete empirical correlation of the data from sprays with recombination then becomes:

$$\text{M.M.D.} = 2300 \left[\eta_l^{0.5} W_l^{0.05} \left(1 + \frac{W_l}{W_a} \right)^{0.5} / V_r \right] \cdot \left[1 + 2 \left(\frac{W_l}{W_a} \right)^{0.7} W_l^{0.25} \right] \quad (6)$$

where the first bracketed parameter is suitable for comparing atomizer performances when there is little or no recombination.

In a later work Wigg (Ref. 52), selecting as the most likely correlating parameter to have an effect on mean drop size the loss of kinetic energy (i.e. the difference between the inlet air energy and the spray energy), was able to correlate the results obtained by Wood (Ref. 55 and Fig. 7), and by Clare and Radcliffe (Ref. 5 and Fig. 6) using a correlating parameter similar to equation (4). From dimensional analysis considerations in order to take into account liquid properties, Wigg proposed the following dimensionally consistent formula:

$$\text{M.M.D.} = 200 \frac{v_1^{0.5} W_1^{0.1} \left(1 + \frac{W_1}{W_a}\right)^{0.5} h^{0.1} \sigma_1^{0.2}}{\rho_a^{0.3} v_r} = N \quad (7)$$

where h = height of air annulus (cm), as in Figs. 4 and 5, and ρ_a = air density (gr/cm³).

This formula succeeded in correlating Wood's and Clare's results because they used molten wax which hardens before recombination occurs and the coalescence effect does not have to be taken into account.

Application of the parameter N to water sprays, where recombination of droplets could occur, gave no overall correlation. Wigg, in order to take the coalescence effect into account, added an extra term to his previous expression and by proposing the following expression:

$$\text{M.M.D.} = 200 N \left[1 + 2.5 \left(\frac{W_1}{W_a} \right)^{0.6} W_1^{0.1} \right] \quad (8)$$

he was able to correlate reasonably well the results obtained by Golitzine, Sharp and Badham (Ref. 15), by Nukiyama and Tanasawa (Ref. 39) and his own results, using water sprays.

He correlated also the results quoted in the report by Ingebo and Foster (Ref. 20) who photographed droplets formed by cross-current break-up of iso-octane, JP-5, benzene, carbon tetrachloride ($\rho_1 = 1.59 \frac{\text{gr}}{\text{cm}^3}$) and water,

although in this case there is some doubt about the linear dimension "h" used in the calculation of the parameter N, which may account for some discrepancy encountered in evaluating MMD. In fact "h" was taken as the distance the liquid penetrated into the air stream at a reference plane downstream of the injection hole.

The work done by Wigg on the correlation he achieved with the results of many researchers in this field to arrive at general empirical expressions, is a significant one. The main criticism of his relationships is that they only cover a restricted range of liquid physical properties. In fact, for example, equation (8) "does not predict the results of Nukiyama and Tanasawa when spraying mixtures of glycerine and water, the effect of liquid viscosity being greater than the measured effect" as Wigg himself puts it.

2.3 - Rizkalla-Lefebvre

Another fundamental step towards a thorough understanding of the airblast atomization process has been made by Rizkalla and Lefebvre (Ref. 43) and (Ref. 45) who investigated the performance of an airblast atomizer (Fig. 2) that is much more representative of current gas turbine practice than the types used by previous researchers. In this specially-designed atomizer, the liquid is first spread into a thin sheet and then exposed on both sides to high velocity air, following a technique that was first devised by Lefebvre and Miller (Ref. 29). As reported in Ref. 43, the following mechanism for drop formation is envisaged:

- (1) Spreading of the liquid across a "pre-filming" surface to focus a thin continuous sheet at the atomizing edge.
- (2) Disintegration of the liquid sheet by aerodynamic forces to form ligaments.
- (3) Break up of the ligaments into drops and acceleration of the drops.
- (4) Agglomeration of drops by collision, occurring simultaneously with evaporation of drops in the air stream.

The first phase of the work (Ref. 43) was confined to the influence of liquid physical properties on mean drop size in the following ranges:

- a) surface tension from 26 to 73 $\frac{\text{dyn}}{\text{cm}}$
- b) absolute viscosity from 1.3 to 124 centipoise
- c) density from 0.8 to 1.8 $\frac{\text{gr}}{\text{cm}^3}$
- d) atomizing air velocities from 60 to 125 $\frac{\text{m}}{\text{sec}}$

Drop sizes were obtained using the well-established light scattering technique due to Dobbins, Crocco and Glassman (Ref. 9) which has the advantage, apart from its reliability, that it does not disturb the droplet flow pattern as do mechanical devices. A description of the method will be given in a following chapter, because this method has been used also in the present work in exploring the spray characteristics of 'plain-jet' airblast atomizers. The optical apparatus as used by Rizkalla and Lefebvre is shown in diagrammatic form in Fig. 8. Analysis of the experimental data led to the following empirical expression for mean drop size:

$$\begin{aligned} \text{S.M.D.} = & \frac{521 \sigma_1^{0.5} \rho_1^{0.75}}{V_a} \left(1 + \frac{W_1}{W_a}\right) + \\ & + 0.037 \eta_1^{0.85} (\sigma_1 \rho_1)^{1.2} \left(1 + \frac{W_1}{W_a}\right)^2 \end{aligned} \quad (9)$$

These findings, which were all obtained at atmospheric pressure, are in broad agreement with the results obtained by Nukiyama and Tanasawa and by Wigg with different atomizers. However, atomizer performance should be experimentally determined

at high ambient air pressure since modern gasturbines use high pressure ratios and must operate free from smoke.

Neya, (Ref. 36) and (Ref. 37), found that for a swirl atomizer the mean droplet size increased as the ambient pressure increased due to the spray shrinking and causing droplet coalescence. Different results were obtained by Popov (Ref. 40) who found that raising the density of the gaseous medium around the swirl atomizer reduced the mean droplet size. Godbole (Ref. 13), using the atomizer shown in Fig. 9, carried out tests under varying ambient pressures and concluded that "the effect of increase in the ambient air pressure at a constant air/fuel ratio, and atomizing air stream velocity, is generally to reduce the mean droplet size of the spray. The S.M.D. varies with ambient pressure according to a power law of index - 0.6". Godbole's results are in good agreement with the results of Weiss and Worsham (Ref. 49), but the average value of the pressure exponent is higher than that derived by Wigg (Ref. 52).

The question of the effect of ambient pressure (and of air properties in general) on spray characteristics brought Rizkalla and Lefebvre to undertake the second phase of their research programme (Ref. 45), which was mainly devoted to the influence of air properties, notably density, on atomization quality using the same airblast atomizer referred to in Ref. 43 and shown in Fig. 2.

The two main liquids used were kerosine and water, and the tests were run at constant levels of air velocity and temperature, over a range of liquid flow rates from 0.005 to 0.039 Kg/sec, at various levels of ambient air pressure from 10^5 to $10^6 \frac{N}{m^2}$. Fig. 10 shows the inverse law of

proportionality relating S.M.D. and air pressure, at least for liquids of low viscosity. Again the drop sizes were measured using the light-scattering technique as described in Ref. 44. Taking into account the results obtained by separating the effects on S.M.D. of different liquid properties, Rizkalla and Lefebvre were able to derive a dimensionally consistent empirical formula for mean drop size in terms of all the relevant air and liquid properties, as follows:-

$$S.M.D. = A \frac{(t \sigma_1 \rho_1)^{0.5}}{v_a \rho_a} \left(1 + \frac{W_1}{W_a}\right) + B \left(\frac{\eta_1^2}{\sigma_1 \rho_a}\right)^{0.425} \cdot t^{0.575} \left(1 + \frac{W_1}{W_a}\right)^2 \quad (10)$$

where A and B are constants and "t" is the liquid film thickness at the prefilming lip. It was also shown that increase in air temperature had a deleterious effect on atomization. Consistently with Nukiyama and Tanasawa and Wigg's findings, S.M.D. was inversely proportional to the atomizing air velocity, and spray quality was affected also by the liquid/air mass ratio. The atomization quality starts to decline when the air/liquid ratio falls below about four and deteriorates much further at air/liquid ratio below about two.

Consistently also with Nukiyama and Tanasawa's work, liquid viscosity has an effect which is independent from that of air velocity and this suggests a form of equation in which S.M.D. is expressed as the sum of two terms, the first term being dominated by air velocity, density and surface tension and the second term by liquid viscosity.

Because no measurements were made of the liquid film thickness, evaluation of the constants A and B was impossible. However, Lefebvre made the assumption that the liquid film thickness is proportional to the diameter of the prefilmer "D" and the equation could then be rewritten more conveniently in the form:

$$\begin{aligned}
 \text{S.M.D.} = & 0.33 \frac{(\sigma_l \rho_l D)^{0.5}}{v_a \rho_a} (1 + W_l/W_a) + 0.157 \times \\
 & \times \left(\frac{\eta_l^2}{\sigma_l \rho_a} \right)^{0.425} D^{0.575} (1 + W_l/W_a)^2 \quad (11)
 \end{aligned}$$

This empirical formula proved able to predict values of S.M.D. over wide ranges of liquid viscosity, air velocity and air/liquid ratio within 5% of the experimental values.

2.4 - Other Relevant Work on Airblast Atomization

Weiss and Worsham (Ref. 49) found that the mean droplet diameter for an airblast liquid spray was primarily dependent upon the relative air velocity, the physical properties of the liquid playing a less critical part in controlling the fineness of the spray. The range of droplet diameters found in a spray depended primarily on the range of excitable wavelengths on the surface of the liquid sheet. The short wavelength limit was due to viscous damping while the long wavelengths were limited due to inertia. On the basis of this theory the mean droplet diameter of the spray ought to be dependent on the air

velocity and the liquid properties as follows:

$$\begin{aligned}
 \text{S.M.D.} &\propto V_r^{-4/3} \\
 &\propto \rho_l^{1/3} \\
 &\propto \rho_a^{-2/3} \\
 &\propto \eta_l^{2/3}
 \end{aligned}
 \tag{12}$$

The experimental results obtained confirmed the air velocity response, but gave slightly different indices for effects of liquid surface tension, liquid viscosity and air density.

Gretzinger and Marshall, Jr. (Ref. 17) produced sprays of an aqueous solution of a black dye sampled in mineral oil by using a converging airblast nozzle, which was very similar to that used by Nukiyama and Tanasawa, for liquid rates from 5.25×10^{-7} to $5.25 \times 10^{-6} \frac{\text{m}^3}{\text{s}}$ (0.5 to 5 gal/hr.).

The following correlating equation was suggested:

$$\text{M.M.D.} = 2600 \left[\left(\frac{W_l}{W_a} \right) \left(\frac{\eta_a}{V_a L} \right) \right]^{0.4}
 \tag{13}$$

where L = diameter of the circular surface where the air and liquid streams come into contact. The authors concluded that the above correlation was specific to the liquid used and was only valid for MMD's between 5 and 30 microns.

Bryan (Ref. 3) and (Fig. 9) found that a combination of swirling fuel with air streams acting on both sides of the atomizing lip produced an atomizer with good fuel distribution characteristics at low air and fuel flows and reasonable starting performance. The effect of shroud air in controlling the cone angle and in improving the fineness of spray was also established.

X

Wetzel and Marshall (Ref. 58), experimenting with venturi injection type atomizers and using molten wax, density 0.38 gr/cm^3 , viscosity $9 \times 10^{-3} \text{ Kg/ms}$ (9 centipoise), surface tension $29.5 \times 10^{-3} \text{ N/m}$ (29.5 dyn/cm), expressed their results as:

$$\text{M.M.D.} = 4.2 \times 10^6 V_r^{-1.68} D^{0.35} \quad (14)$$

where: V_r (relative air velocity) is expressed in ft/sec

and D is the diameter of the injection orifice in inches. Their results show good agreement with Nukiyama and Tanasawa when wax was used and the air velocity was above 120 m/s, but no agreement was obtained when spraying a high density, high surface tension molten alloy.

CHAPTER 3

PROCESS OF DROPS FORMATION AND LIQUID JET BREAK UP

CHAPTER 3

PROCESS OF DROPS FORMATION AND LIQUID JET BREAK UP.

The literature includes several hundred papers and reports on the atomization of liquids and care must be taken to select the most pertinent and fundamental ones.

Joyce (Ref. 22) points out that the surface area of 1 cm³ of liquid in the form of a single sphere is only 4.83 cm²; whereas the same volume of liquid in a normal spray containing 10 million particles, ranging from 5 microns up to 500 microns in diameter, has a surface area that may range up to 1200 cm². The energy associated to the droplets and defined as:-

$$\mathcal{E} = s \sigma_1 \quad (15)$$

(where s = droplet surface area and σ_1 = surface tension)

is small. However, because the efficiency of atomization is usually very small considerable energy is required to accomplish a high degree of atomization, (Appendix A).

3.1- Shattering of Liquid Drops

When a liquid droplet is in relative motion with respect to the surrounding gaseous medium, there exists a system of aerodynamic forces acting upon the surface of the droplet, conflicting against internal forces made up of surface tension and shear stresses due to viscosity. Following a change in the droplet shape, the pressure distribution around it will also change such that, either a new equilibrium state is reached or a further deformation occurs. This last situation may eventually favour the splitting of the droplet up to a point where no more sub-division is possible because of prevailing forces due to droplet internal pressures (Klüsener).

It is known from experimental work that surface tension and liquid viscosity tend to oppose the splitting of the droplets. Following Giffen and Muraszew's (Ref. 12) approach to this subject, the properties of the surrounding medium that might play a role in determining drop size are air density and air viscosity.

X

Rizkalla and Lefebvre's work (just to mention one of the most recent researches) has proved that an increase in air density will cause a decrease in droplet size just as it appears in the expressions for air resistance derived by Giffen and Muraszew:

(up to $Re = 2$)	Laminar flow	$R = 3\pi \eta_a V d$	
($2 < Re < 500$)	Semiturbulent flow	$R = \pi (0.05 \rho_a V^2 d^2 + 5 \eta_a V d)$	(16)
($Re > 500$)	Turbulent flow	$R = 0.055 \pi \rho_a V^2 d^2$	

where:

- d = droplet diameter
- η_a = air viscosity
- R = air resistance
- Re = Reynolds number $\frac{V d \rho}{\eta}$
- V = droplet relative velocity

The equations (16) for laminar and semiturbulent flow show that the air viscosity would have a similar effect to air density, but there appears to be little or no direct evidence on the effect of the air viscosity on the droplet size.

Lane (Ref. 23) made a series of flash photographs of single droplets of uniform size which were allowed to fall into a vertical tube of transparent material along with a stream of air drawn at a known velocity. The measured minimum air velocity for droplet disruption was about 23 m/sec. The droplet seemed first flattened to form a circular ring with a thin membrane in the centre. This membrane was then blown out into a hollow bag which burst and produced a shower of fine droplets. The bursting of the central bag proceeded as a wave travelling back towards the thicker rim; when the wave struck the rim the latter threw off small droplets and then itself broke into larger droplets.

Hinze (Ref. 19) considers three different ways in which liquid globule can split up depending upon the flow pattern around it:

- (a) the globule is flattened, forming in the initial stages an oblate ellipsoid (lenticular deformation) which may deform into a torus, which, after stretching, breaks into many small droplets.
- (b) the globule becomes more and more elongated, forming in the initial stages a prolate ellipsoid, until ultimately a long cylindrical thread is formed which bursts into droplets (cigar-shaped deformation).
- (c) as the surface of the globule is deformed locally, bulges and protuberances occur and parts of the globule become bodily separated (bulgy deformation).

If τ is an external force per unit surface area acting on an isolated globule to cause deformation, σ_1 the interfacial tension counteracting the deformation, D the diameter of the globule, μ_d and ρ_d are the viscosity and the density of the droplets, then according to Hinze the break-up point of a globule is dependent on two dimensionless groups:

$$N_{We} = \tau D / \sigma_1 \quad (\text{generalized Weber group})$$

$$N_{Vi} = \mu_d / \sqrt{\rho_d \sigma_1 D} \quad (\text{viscosity group})$$

The greater value of N_{We} , that is, the greater the external force τ (viscous stress or dynamic pressure) compared with the counteracting interfacial-tension force σ_1/D , the greater the deformation. At a critical value (N_{We})_{crit.}, break-up occurs.

Work on droplet disintegration by the shattering action

X

of strong shock waves was reported by Ranger and Nicholls (Ref. 42). According to them the main function of the shock is to produce the high-speed convective flow that is responsible for the disintegration. A drop which is originally spherical is deformed into a planetary ellipsoid with its major axis perpendicular to the direction of flow. The shearing action exerted by the high-speed flow causes a boundary layer to form on the surface of the liquid and the stripping away of this layer accounts for the break-up. They found that the break-up time is proportional to the droplet diameter, inversely proportional to the velocity and proportional to the square root of the liquid-to-gas density ratio. In order to photograph the sequence of events leading to the shattering of water drops, of 750 ± 4000 microns diameters, by the impact of Mach 1.5 to Mach 3.5 shock waves, they used a collimated beam of high intensity light to back-light the drops with both image converter and rotating-drum type cameras. A series of individual shadow and streak photographs taken at different time intervals after the shock wave had intercepted the drop, showed that the drop displacement is a smooth, continuously varying function of time and thus the drop velocity is also a continuous function of time.

The shattering of liquid drops behind normal shock waves in shock tubes has also been studied experimentally by Engel (Ref. 10), Hansom, Domich, and Adams (Ref. 18), and by Wolfe and Andersen (Ref. 53). It seems that the parameters playing a major role in the high-speed disintegration of droplets are the liquid properties, the dynamic pressure of the convective flow and the drop diameter.

Dickerson and Schuman (Ref. 8) used a high-speed motion camera (14,500 frames/sec) to observe the volume loss rate of a kerosine droplet of known initial conditions as a function of the flowing gas properties and liquid droplet characteristics. They proposed a relationship relating the mass loss rate of the droplet to the Weber number and modified Reynold's number as following:

$$\dot{M} = 3.53 \times 10^{-5} (Re')^{2.8} (We)^{-0.42} \quad (17)$$

where:

- \dot{M} = Mass number = $\dot{m} D/A_d \rho_d$
- \dot{m} = mass loss rate, gr/sec
- D = droplet average diameter, cm.
- A_d = droplet surface area, cm^2

X

η_d = droplet viscosity, centipoise

Re' = modified Reynold's number :

$$Re' = D V_{rel} \rho_g \rho_d^{1/2} / \eta_d$$

V_{rel} = relative air velocity, cm/sec

ρ_g, ρ_d = density of gas and droplet respectively.
 $\frac{gr}{cm^3}$

We = Weber number = $\rho_g V_{rel}^2 D / \sigma_d$

σ_d = liquid droplet surface tension, dynes/cm.

The liquid used was a Kerosine RP-1 with $\sigma_d = 26 \frac{dyn}{cm}$ and viscosity 1.71 centipoise, and the validity of equation (17) should be restricted to liquids of similar characteristics.

3.2 - Atomization of Liquid Sheets and Jets

Lord Rayleigh (Ref. 59) carried out the first theoretical investigation concerning the breakup of liquid jets. Actually, Rayleigh treated this problem as one of instability. In the case of jets of heavy liquids, as well as for water projected into air, the cause of the instability is due to capillary force, or surface tension, which renders the cylinder unstable and favours its breakup into detached masses of large diameter, the aggregate surface of which is less than that of the cylinder. In this particular case, the principal problem was to determine the wavelength of the disturbance from which may be determined the number of masses into which a given length of jet may be expected to break up. Rayleigh showed that the growth rate of the disturbance caused by surface tension was at a maximum when the

wavelength was 4.508 times the diameter of the jet. It must be pointed out that Rayleigh's theoretical work to predict droplet initial sizes only applies to cases of disintegrating low-velocity jets, and in no way can his theory be applied to cases of atomization.

According to Castleman (Ref. 4) the actual process of atomization is explained by his "ligament theory". A portion of the large mass of liquid is caught up by the air and, being anchored by the other end, it is drawn out into a fine ligament. This ligament is quickly cut off by the rapid growth of a dent in its surface and the detached mass, being quite small, is quickly drawn up into a spherical drop. Atomization occurs at the surface under the influence of the relative motions of gas and liquid. According to Castleman, a minimum drop size is reached at a speed ranging from 100 to 120 m/s. The minimum diameter that he reported for water droplets was about 10 microns when atomized in a high-speed air stream.

A large number of excellent photomicrographs of fuel sprays were taken by Lee and Spencer (Ref. 25) who studied the structure of sprays and the process of spray formation. These investigators supported the theory advanced by Castleman and they observed that with injected sprays the fuel leaves the nozzle as an unbroken column, becomes ruffled and then is torn into small irregular ligaments by the action of air. The ligaments are then quickly drawn up into drops by the surface tension of the fuel. They found that the degree of disintegration of the jet increases with the distance from the nozzle, the air density, the fuel velocity, or the fuel turbulence, but decreases with increase of fuel viscosity, surface tension, or nozzle-orifice diameter.

As discussed by Marshall (32), the effect of liquid properties and jet velocity on the mechanism of atomization has been studied from the standpoint of dimensional analysis. For the case of atomization of a liquid jet breaking up without the influence of the surrounding air, the mechanism of break up can be predicted to be dependent on jet diameter, jet velocity, liquid density, surface tension and viscosity. The break up mechanism of a jet, as predicted by dimensional analysis, would appear to be a function of the jet Reynolds number, $V d \rho_1 / \mu_1$, Z_1

and a dimensionless group $\mu_1 / \sqrt{\sigma_1 \rho_1} d$, sometimes referred to as the Z-number (or viscosity group).

Frazer (Ref. 11) predicts that for a jet in laminar flow, disintegration will occur if triggered by a vibration in the jet or an external disturbance. When the jet is in turbulent condition, the disintegration will occur without any external

influence when the liquid surface tension is no longer able to cope with the radial components of the jet velocity. In any case, the break up of the jet is enhanced by higher air density. The process of sheet disintegration and drop formation is obtained through the formation of ligaments or fine threads which are broken up by the reaction effect of impinging air. Three modes of disintegration of the liquid sheet are proposed:

- 1) "Rim" disintegration. Threads are pulled out from the rim during contraction and these produce quite large drops. This mode of disintegration is peculiar to low velocity, high surface tension and high viscosity liquids.
- 2) "Perforated" sheet disintegration. In this mode the leading edge disintegrates into a network of threads. Disturbances on the sheet puncture it, create holes which expand until they coalesce into long disintegrating threads.
- 3) "Wavy" sheet disintegration. In this mode, major waves disturbances caused by the atmosphere disintegrate the sheet by tearing whole surfaces away.

A similar "wavy" theory is proposed by Briffa and Dombrowski (Ref. 2) who tested a flat spray of the fan type. The experiments were carried out with iso-octane and tetralin. For iso-octane the air velocities ranged from 0.23 to 1.55 m/sec and differential ejection pressures from 7.6 to 118 psi, the intervals being selected to provide equal velocity increments. For tetralin tests the differential pressures ranged from 45.5 to 118 psi at a single air velocity of 5.8 m/sec. Rapidly growing waves were produced on the sheet which subsequently broke down at the crest. Fragments of sheet then rapidly contracted into ligaments which broke down into drops. A number of drops were also produced at the point of fragmentation; these drops had an additional velocity component resulting from the accelerating wave crest.

York, Stubbs and Tek (Refs. 56, 57) made a mathematical and experimental analysis of the disintegration of a plane sheet of liquid of finite thickness. They showed that instability and wave formation at the interface are the major factors in the break-up of the sheet of liquid into drops. The most useful result of this study was the development of an equation for predicting roughly the size of the drops in the spray from swirl nozzles. From plots of the maximum rate of growth of the waves on the surface of the sheet of liquid, the wavelength of the predominant disturbance can be determined. This disturbance grows until the sheet disintegrates into rings, after which the

X

rings break into drops by the action of surface tension. The drop size of the spray may be approximated by calculating the diameter of the spray resulting from the typical successive disintegration, recognizing that a range of drop sizes is actually produced. The resulting equation for drop size is:

$$r \approx 1.06 \sqrt{\frac{b W^* \sigma_L}{\rho_A V^2}} \quad (18)$$

where b is the thickness of the undisturbed sheet, σ_L is the liquid surface tension, ρ_A is the mass density of the gas phase, V is the velocity of the bulk of the gas phase relative to the liquid phase and W^* is the Weber number based on the wavelength of disturbance for maximum growth rate. W^* can be determined from the density ratio of the gas to the liquid and the Weber number equal to $V^2 b \rho_A / 2 \sigma_L$. The major problem is estimation of the sheet thickness at the breakup distance. In spite of many assumptions in the analysis, the results are reasonable and have been verified qualitatively by short-exposure photographs and high-speed motion pictures.

X

CHAPTER 4

EXPERIMENTAL TECHNIQUE AND APPARATUS

CHAPTER 4

EXPERIMENTAL TECHNIQUE AND APPARATUS

4.1 - The Spray

The sprays produced by airblast atomizers are polydispersions of droplets with upper and lower limits of size. Different mean diameters can be defined so that an imaginary uniform spray can be thought of consisting of droplets of that mean diameter.

For the atomization of fuels it is common practice to use the Sauter Mean Diameter (S.M.D.) already expressed in previous equations, with total volume and total surface area of the uniform imaginary spray equal to those of the real spray.

The distribution of droplets around the mean size could completely describe the spray characteristics. Without going into the details of mathematical functions proposed in the past to fit best the frequency distribution obtained in a spray, it is worth mentioning one of the most commonly accepted, namely the Upper Limit Distribution Function.

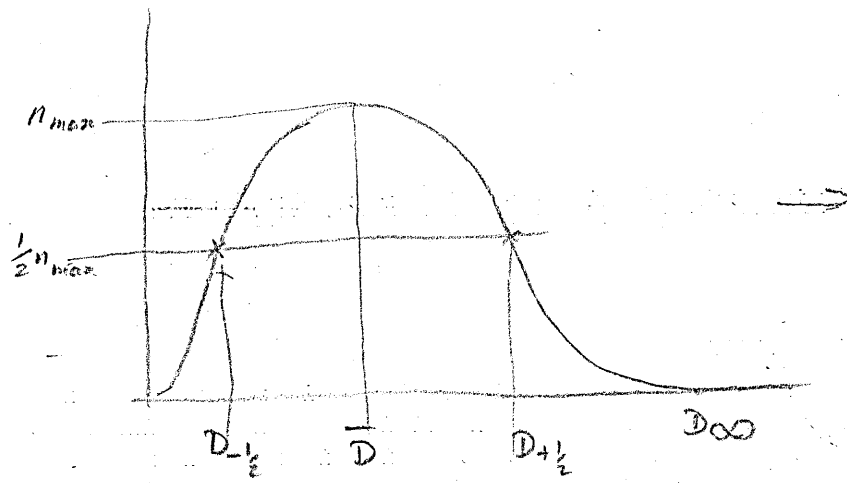
The Upper Limit Distribution Function (U.L.D.F.) has been defined by Mugele and Evans (Ref. 35) to overcome the shortcomings of the conventional exponential types of distribution functions, e.g. Rosin-Rammler or Nukiyama-Tanasawa expressions, that do not admit a maximum particle size. Using Dobbins's terminology, "the relative frequencies of occurrence of particles of a given diameter D are distributed according to a distribution function $N_r(D)$, defined in such a way that the integral of $N_r(D)$ over a given diameter interval represents the probability of occurrence of particles within the specified interval". Consistently, the U.L.D.F. form becomes:

$$N_r(D) = C \frac{\exp - \left\{ \delta \ln \left[aD / (D_\infty - D) \right] \right\}^2}{D^4 (D_\infty - D)} \quad (19)$$

where C is defined such that

$$\int_0^{D_\infty} N_r(D) dD = 1$$

The parameters 'a' and δ can be replaced by two variables of more immediate geometrical significance. Two such variables



are:

(skewness factor) \bar{D} / D_{∞} (ratio of most probable to max. droplet diameter)

(spread factor) $(D_{+\frac{1}{2}} - D_{-\frac{1}{2}}) / \bar{D}$ (width of the distribution function at the two half peak values divided by the most probable diameter).

4.2 - Optical Method for Mean Droplet Size

A technique for drop size measurements which implies no interference with the spray is that of direct photography which was used extensively by Nukiyama and Tanasawa. To obtain a sample, a large number of photographs have to be taken which is costly and time consuming. Moreover, the residence time of a droplet in a microscopic volume is so short that extremely high shutter speeds are required.

Eliminating the disadvantages of direct photography, while still avoiding sampling on coated slides is the aim of the various indirect optical techniques. One of these which has drawn the attention of quite a few investigators in the recent years, is the one developed at Princeton by Dobbins, Crocco and Glassman (Ref. 9) utilizing the diffractive light-scattering properties of a polydispersion of non-absorbing spherical particles of non-uniform size. A review of their paper is also given in Ref. 6.

The optical method due to Dobbins, Crocco and Glassman is based on the forward diffractive scatter of monochromatic light due to the spray. The Sauter Mean Diameter of the spray under investigation is obtained from the intensity of a recorded scattered light profile. The optical apparatus used by Dobbins et al is illustrated in Fig. 11. They found that for sprays described by an upper limit distribution function defined by Mugele and Evans (Ref. 35), having characteristic parameters of spread and skewness within specified limits, the scattered light intensity profiles were coincident and that S.M.D. could be obtained from the distance traversed to have 1/10th of the intensity of scattered light at the optical axis. The mean theoretical illumination profile of Dobbins et al is shown in Fig. 12. Roberts and Webb (Refs. 46-47) extended the work to widen the spread and skewness in the U.L.D.F. making it possible to apply the method to sprays produced by an airblast atomizer. The mean theoretical illumination profile of Roberts and Webb is shown in Fig. 13. The 1/10th intensity is chosen for Sauter

Mean Diameter evaluation, as it is known from the work of Roberts and Webb that this point gives the least deviation.

4.3 - The Opto-Electronic Apparatus

In order to obtain an illumination profile, a highly collimated monochromatic beam of light should be directed through the spray and the diffractively scattered light should be focussed on a receiving plane (the photomultiplier sensitive surface) some distance from the particles.

The optical apparatus is shown diagrammatically in Fig.14 and the optical bench in Plates 1 and 2. As a light source it uses a 5 mW - Helium/Neon Laser by Spectra Physics (Model 120), working at 632.8 nm (6328 Å) wavelength.

Some of its characteristics are:

Beam Amplitude Noise (1 to 100 KHz) < 0.5% r.m.s.

Beam Amplitude Ripple (120 Hz) < 0.2% r.m.s.

Beam Polarization:Linear to better than 1 part per thousand.

Plane of Polarization: Vertical

Beam Diameter: 0.65 mm at $1/e^2$ points

Beam Divergence: 1.7 milliradians at $1/e^2$ points

The laser beam is spatially filtered and collimated by an optical assembly (Fig. 15) (Model 332/Model333 by Spectra Physics) screwed to the laser head. The first optical unit (Model 332) is a "spatial filter" which employs an aperture placed at the focus of an expanding lens to pass only the fundamental laser mode. In order to match the output beam diameter of the laser at $1/e^2$ points (0.65 mm), which becomes the input beam diameter for the "spatial filter" unit, an aperture diameter of 22 μ was selected together with a 12.8 mm focal length expanding lens. The aperture assembly position in the optical unit may be adjusted in the X and Y positions by two adjustment knobs and in the Z position (axial alignment) by a rotational lock ring. Spatial filtering to remove spatial noise is accomplished by the expanding lens which focuses the laser beam through the aperture. Its diameter has been calculated (and the aperture chosen accordingly) to be close to the diffraction-limited spot size for the focusing lens using the relationship:

$$a_f = \frac{\lambda}{\pi a} f \quad (20)$$

where: f = equivalent focal length of the expanding lens,

a = radius of the laser beam at which the intensity falls to $1/e^2$ of the central intensity,

$$\lambda = 6328 \text{ \AA}$$

The aperture placed at this point will pass the fraction of the total power:

$$P = 1 - e^{-2r^2 / a^2 f} \quad (21)$$

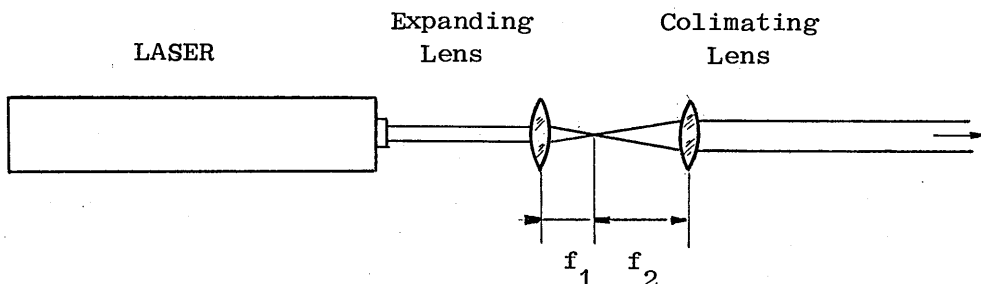
where: r = radial distance from beam centre.

The second optical unit (Model 333) screwed to Model 332 is a "Beam Expanding Telescope" which produces a highly collimated beam provided some adjustments are carried out on the collimating lens. The output beam diameter is determined by the initial beam diameter (0.65 mm) and by the multiplication factor i.e. the ratio of focal lengths of the collimating and expanding lenses: $85/12.8 = 6.64$. A beam diameter of 4.32 mm is then obtained at $1/e^2$ points. The reason to seek such an enlargement of the beam is to reduce the beam divergence or spread. The laser beam intensity profile is Gaussian and the diffraction limited, far-field pattern of the Gaussian wave-front is also a Gaussian. The beam spread is given by:

$$\theta = \frac{2\lambda}{\pi a} \quad (22)$$

where θ is the full cone angle to the $1/e^2$ intensity points, λ is the wavelength of the radiation and 'a' is the initial beam radius defined above. In the projection of the beam to large distances it is often desirable to reduce the divergence from the value given by (22) and this is accomplished by enlargement

of the beam before transmission as in the following sketch:



Technique for Reducing Divergence

In this case, equation (22) still applies, but since the beam has been enlarged in the ratio f_2/f_1 , the divergence is reduced by the same factor.

The incident and collimated light beam is then chopped by a rotating perforated disc. The light from a small lamp is also chopped in a synchronous way by the rotating disc and the pulsed signals are sent to a "Gate Circuit Rectifier" in a "Synchronous Demodulator" by a photo-cell transducer (Fig. 16). By passing the electrical signals produced by the photomultiplier tube into the Gate Circuit synchronized with the chopped incident reference light, via an electronic filter, the unwanted output of the phototube due to stray light in the system is reduced and sensitivity is increased.

The beam of light passes at right angles to the spray axis and it is essential to ensure that the light beam crosses the spray at the same distance away from the atomizer to ensure that under all test conditions the spray sampled by the beam is in the same state of development.

This parallel beam of monochromatic light of 6328 \AA is diffracted through the spray under investigation and focussed by a 60 cm focal length receiver lens onto a 22 microns aperture. This aperture assembly, with X and Y adjustment knobs, is a Spectra-Physics Model 332 stripped of its condensing lens. The light will eventually travel the distance to the photomultiplier cathode through the eyepiece mounting and the shutter assembly shielding the photomultiplier tube (Fig. 17). The line of sight of the eyepiece is inclined 36° for more comfortable viewing of the concentric-circle and cross-line eyepiece graticule which has been added to the sliding plunger of the shutter assembly.

This viewing optical system facilitates the lengthy trial-and-error process of alignment of the optical components, and is necessary for accurate results.

The Photomultiplier tube (located in a PR-1400RF photomultiplier housing by "Products for Research, Inc.") is of the type 9658R, manufactured by E.M.I., and has 11 venetian blind dynodes having highly stable CsSb secondary emitting surfaces. The 44mm diameter cathode is of the S-20 (trialkali) type which provides very high quantum efficiency in the red, the spectral response extending out to approximately 8500Å (Fig. 18). The end window is internally corrugated and this enhances the red sensitivity due to multiple reflection of the incident light. With this tube at $\lambda = 6328 \text{ \AA}$ a Quantum Efficiency of 11.4% and a Responsivity of 57 mA/w was achieved. The test ticket supplied by the manufacturer shows a cathode sensitivity of 378 $\mu\text{A/L}$ and a dark current at 20°C of 4 nA.

Due to the high sensitivity of the phototube, and because it was suggested not to exceed a mean anode current of 10 μA for highest stability, an interchangeable neutral density filter was located in front of the photo-tube and a constant 750V voltage supply to the photomultiplier was maintained.

The electrical signal from the photomultiplier is passed into the Synchronous Demodulator (Fig. 16) and (Plate 3) where it is processed successively in a Band-Pass Filter, A.C. Amplifier, Gate Circuit Rectifier, Low-Pass Filter, and finally in a D.C. Amplifier.

4.4 - Readout of Illumination Profile

The signal eventually reaches an X-Y plotter (type Bryans 26001, main frame A4, single pen), Plate 3, where it is amplified by a logarithmic amplifier module (type Bryans 26236). This arrangement allows a direct reading of the 1/10th intensity point of the maximum intensity of the illumination profile on the Y-axis. The X-axis displacement of the plotter is electrically connected to a Hewlett-Packard 7 DCDT-1000 linear displacement transducer which is mechanically linked (Plate 2) to the photomultiplier trolley. The movement of the trolley is obtained either manually or by means of a 1 R.P.M. electric motor (Plate 2) in such a way that the traversing plane is maintained at right angles with respect to the optical axis. The combination of the X and Y displacements allow the light intensity profile to be plotted. The position of the light beam (i.e. of the photomultiplier trolley) is indicated on the X-axis of the plotter while the Y-axis records its intensity $I(\theta)$ (θ is the angular displacement; $\theta = 0$ corresponds to the optical axis position). Typical plots of the light intensity profile are shown in Figs. 19, 20 and 21. In order to find from the illumination profile

the traverse distance "r" to $0.1 I(\Theta)_{\max}$ it is required to extrapolate the curve towards the centre line for that portion of the graph corresponding to the unscattered beam profile. In the present work this unavoidable "guessing" procedure was quite straightforward because it would only cover a "r" range usually not exceeding 0.5 mm. This favourable situation is probably due to the very small aperture in front of the photomultiplier although other favourable causes may also be involved.

The S.M.D. of the spray tested was then obtained by using the curve shown in Fig. 22 which has been calculated for conditions of $\lambda = 6328 \text{ \AA}$ and $f_c = 60 \text{ cm}$ (focal length of condensing lens) from the curve of Fig. 13 due to Roberts and Webb (Ref. 46).

All readouts have been constantly monitored with a D.V.M. and an Oscilloscope to watch for the scattered light intensity.

All the optical components were mounted on a rigid and heavily framed bench, free from external vibrations emanating from the floor because antivibration mounts were used. Where possible, all the components were shielded from stray light and all enclosing surfaces painted matt black to reduce the possibility of unwanted reflections.

All tests were carried out for a light beam position in the spray at 200 mm from the air nozzle exit plane.

4.5 - Air System

A two stage fan (Plate 4) supplied air up to $20.68 \times 10^3 \text{ N/m}^2$ ($\approx 3 \text{ psig}$). The air flow characteristics versus air velocity for different air nozzles are given in Fig. 23. The air flow was fed through a straight pipe towards the test section. The air mass flow was measured using an orifice plate fitted with D and D/2 pressure tappings in accordance with B.S. 1042. The air velocity was measured at the air nozzle exit with two pitot tubes. The air temperature was recorded by means of a thermocouple (with reference junction at 0°C) before and after the expansion through the air nozzle.

In order to achieve higher atomizing air velocities (up to 180 m/s), a supply air pipe, and isolating valve, was branched off the main air pipe on the rig and higher pressure air was occasionally supplied to the test section from a compressor out of the test house.

4.6 - Liquid System

The two liquids used most extensively throughout the present work were water and kerosine. Water came directly to the atomizer from the test house water supply. Kerosine was fed to the atomizer from a reservoir (Plate 5) pressurized by a bottle of nitrogen. The special liquids were contained in a smaller reservoir and fed to the atomizer again by pressurizing with nitrogen. (Plate 5). All liquids were made to flow to the atomizer (Plate 6) via a filter, isolation valves and Fisher & Porter flow-meters (calibrated for all liquids) located on the control panel.

The sprays discharged into a 101.6 mm (4 inches) pipe (Plate 1) which was open at the upstream end and was free to induce air along with the spray. Most of the liquid deposited on the pipe wall and was collected in a container outside the test house.

4.7 - Atomizer

Cross-section representations of the airblast atomizer assembly and of the "plain-jet" straight atomizer are shown in Figs. 1 and 24.

In order to study the scale effect, four brass "plain-jet" atomizers were made with diameters: 0.397, 0.794, 1.191 and 1.588 mm (Plate 6), the smallest diameter being obtained by fitting an hypodermic tube. The length "l" of the straight tubular portion for each atomizer was 6 mm and the l/D values were: 12.60, 6.30, 4.20 and 3.15, where "D" is the orifice diameter.

In order to separate the effect of liquid flow rate alone from the effect of air/liquid ratio, ten air nozzles, of $\frac{1}{4}$ of a circle profile, were made to the following diameters: 5.84, 6.85, 8.89, 11.43, 12.70, 13.97, 14.98, 16.76, 19.05 and 25.40 mm, Fig. 25 and Plate 8.

CHAPTER 5

TESTS RESULTS

CHAPTER 5

TESTS RESULTS

The experimental results obtained from tests conducted on "plain-jet" airblast atomizers (Fig. 1) are shown on graphs in Figs. 27 to 49. They represent the main characteristics of sprays, expressed as Sauter Mean Diameter of the droplets, under different air flows and different liquid physical properties. The choice of liquid flow rates from 0.5 to 4 gr/s was dictated by atomizer dimensions or by liquid jet velocity which was restricted to 6 m/s, although the vast majority of tests were conducted at liquid velocities less than 5 m/s.

All the data in the present work were obtained by conducting the tests at atmospheric pressure and room temperature and the effects of each property on atomization are presented separately.

All air velocities are 'relative' to liquid velocity and they were obtained as: $V_r = V_a - V_l$, where V_a and V_l are the axial air and liquid velocities at nozzles exit planes.

The two main liquids employed during the entire experimental programme were:-

$$\text{Water } (\eta_1 = 10^{-3} \text{ Kg/ms; } \rho_1 = 1 \text{ gr/cc; } \sigma_1 = 73.4 \times 10^{-3} \text{ N/m)}$$

$$\text{Kerosine } (\eta_1 = 1.293 \times 10^{-3} \text{ Kg/ms; } \rho_1 = 0.784 \text{ gr/cc;}$$

$$\sigma_1 = 27.7 \times 10^{-3} \text{ N/m}).$$

The purpose of the present research was to establish a relationship between S.M.D. and the main parameters involved in the atomization process such as: air velocity, liquid mass flow rate, air to liquid mass ratio, liquid density, liquid surface tension, liquid viscosity and scale effect. The tests were run with the purpose of establishing the effect of each particular variable on S.M.D. and to determine the values of the exponents in the following S.M.D. predicting formula:

$$SMD = f (V_r^a, W_l^b, W_l/W_a^c, \rho_l^d, \sigma_l^e, \eta_l^f, D^g) \quad (23)$$

In order to achieve this, all parameters were varied independently of all the others to separate each effect.

The special liquids used were the same that Rizkalla and Lefebvre used (Ref. 43) to establish their empirical formula. They made a large number of different trial solutions to obtain wide variations in each of the three liquid properties while maintaining the other two approximately constant. The liquids and solutions found to fulfill the above requirements are presented in Tables 1, 2 and 3.

5.1 - A.F.R. Effect

The influence of A.F.R. as illustrated in Figs. 27, 28, 29 for water and kerosine. Tests were carried out for A.F.R.'s ranging from 1 to 36, and for liquid flow rates from 1.5 to 3 gr/s. In order to separate the A.F.R. effect from the effects of other parameters, use has been made of ten air nozzles of different diameters. Each of them supplied a different air flow, at constant air velocity, and consequently they allowed ten different points to be plotted (when possible) in each case to describe the variation of S.M.D. as a function of A.F.R. Two conclusions can be drawn from the graphs:

- a) decreasing the amount of atomizing air flow, compared to the liquid flow rate injected, causes a sharp increase of S.M.D., which amounts to saying that the performance of the atomizer deteriorates when A.F.R. decreases. This is certainly the case for A.F.R.'s smaller than 3.
- b) Increasing the amount of atomizing air flow, compared to the liquid flow rate, does not seem to affect the droplet sizes at least for A.F.R.'s larger than 7. For this upper range, no matter how large was the air nozzle at a given velocity the droplet sizes remained fairly constant and the purpose of Fig. 29 is to show this peculiarity for A.F.R. as high as 36.

Figs. 43 and 44 show a similar behaviour but plotted as a function of the nondimensional group $(1 + \frac{1}{AFR})$ for liquids of high viscosity. For the high viscosity test results illustrated in Fig. 43, A.F.R. varied between 1.68 and 8.40 as a consequence of a variation of liquid flow rate at constant air flow rate.

(Values reproduced from test results represented in Fig. 41). The test results illustrated in Fig. 44 were obtained by using six different air nozzles at 1.5 gr/s liquid flow rate. In both cases the relative air velocity was so adjusted as to give 100 m/s. In this situation also, where high viscosity liquids were used (from 19×10^{-3} Kg/ms = 19 centipoise to 76×10^{-3} Kg/ms = 76 centipoise), the influence of A.F.R. is such that as it decreases, S.M.D. increases.

5.2 - Effect of Atomizing Air Velocity

This effect is clearly shown in Figs. 30 and 31, for the case of water and kerosine. The influence of all other parameters has been neutralized by selecting those air nozzles which, at a given liquid flow rate, and at the appropriate air velocities, will determine a constant A.F.R. which has been selected to be equal to 3. Liquid flow rates did not exceed 4 gr/s and the range covered was made to start at 1 gr/s.

Figs. 32 and 33 show the influence of air velocity on S.M.D. for water and kerosine, with the difference, compared to the previous situation, that the A.F.R. was allowed to vary due to the fact that only one air nozzle was used (two in the case of water tests). The air nozzles used (25.40 and 19.05 mm) were purposely selected to deliver high air flow rates in order to keep the nondimensional group $(1 + \frac{1}{AFR})$ as close as

possible to unity. This nondimensional group has been selected because it is thought to play a major role in a S.M.D. predicting formula; it proved to be the case according to the results of previous investigators. The Figs. 32 and 33 show the importance of the group $(1 + 1/AFR)$ on S.M.D., because although it was allowed to vary only a few percent, the inverse proportionality law between S.M.D. and V_r no longer holds even if it deviates slightly from it.

The situation which arises when using a smaller air nozzle (12.7 mm = $\frac{1}{2}$ ") is illustrated in Figs. 34 and 35. The tests were carried out with water and kerosine as usual and by decreasing the relative air velocity of the atomizing airstream down to values less than 100 m/s at constant liquid flow rate: values of A.F.R. as low as 4 were obtained. This situation has markedly enhanced the impact of the group $(1 + 1/AFR)$ on the original inverse proportionality law between S.M.D. and V_r and this law now certainly no longer holds.

5.3 - Atomizer Scale Effect

The linear scale effect on droplet size due to different fuel orifice diameters is illustrated in Figs. 36 and 37 for tests run with water and kerosine and in Fig. 38 for high viscosity liquids (36×10^{-3} Kg/ms). All tests were run with the 6.85 mm air nozzle and with all the plain-jet orifices available, namely: 0.397, 0.794, 1.191 and 1.588 mm diameters. The water, kerosine and high liquid viscosity tests results were obtained for liquid flow rates ranging only from 0.5 to 1 gr/s in order to prevent liquid jet velocities from exceeding 5 m/s when testing the smallest orifice.

Kerosine and water tests were run with relative air velocity as the variable parameter although A.F.R. also was varying due to the fact that only one air nozzle was used throughout the tests. Anyhow, the important feature about the curves of Fig. 36 & 37 is that the data points obtained for the different atomizers and for similar flow situations, all lie along a unique curve (at least within the experimental error) and this seems to suggest that the effect of scale for the atomizers tested with water and kerosine is very small. To validate this conclusion reference should be made to Figs. 32, 33, 34 and 35, which describe some tests also carried out for the purpose of showing the scale effect by obtaining data points with more than one fuel orifice in similar flow situations. It will be seen that the points obtained with different fuel orifices experience only a very negligible scatter for similar situations.

Different conclusions are drawn if one examines the curves in Fig. 38. They show the effect of liquid orifice diameters for high viscosity liquids. In this situation the atomizer linear scale effect has to be taken into account in that the larger is the atomizer liquid orifice diameter the bigger are the droplet sizes, all other parameters being constant.

5.4 - Effect of Liquid Flow Rate

It was found (Figs. 39 and 40) that the liquid flow rate alone has an effect on S.M.D. In order to separate this effect from all the others, use was made once again of the different air nozzles; by this arrangement it was possible to run the tests for kerosine and water at constant A.F.R., constant velocity ($V_r = 100$ m/s) and variable liquid flow rate. As was expected, W_1 has an influence on S.M.D., the effect being that increase W_1 in liquid flow rate produces larger droplets. This effect was noticeable for a range of A.F.R.'s extending from 2.5 to 8 for the water tests and from 2 to 8 for the kerosine tests. All the available atomizers were used in order to cover as wide a range of liquid flow rates as possible (from a minimum of 0.38gr/s up to a maximum of 3.9 gr/s). The tests also demonstrated the beneficial effect of an increase in A.F.R. in reducing S.M.D.

5.5 - Effect of Liquid Viscosity

Figs. 41 and 42 confirm the well established fact that viscosity forces tend to oppose the disintegration of ligaments into drops and to resist the further shattering of drops. The figures illustrate the sharp increase in S.M.D. values when the absolute liquid viscosity is increased at constant air velocity (Fig. 42) and at constant liquid flow rate (Fig. 41). In both cases it is perhaps worth stressing again that an increase in A.F.R. is beneficial in reducing droplet sizes as also is an increase in relative air velocity. In the two series of tests, the same air nozzle was used (6.86 mm). The range of liquid viscosity investigated was between 1.29×10^{-3} Kg/ms and 76×10^{-3} Kg/ms. As was observed for low viscosity liquids, at large A.F.R.'s an increase in air mass flow rate does not appreciably affect the mean droplet diameter. This point is well illustrated for a high viscosity liquid in Fig. 45. For this particular test a maximum A.F.R. of 53 was employed.

5.6 - Effect of Liquid Surface Tension

Surface tension also tends to oppose the shattering action of the atomizing air stream. This effect is shown in Figs. 46 and 47 where mean droplet sizes increase with increasing surface tension. Two tests were conducted, both of them at constant A.F.R.; the first (Fig. 46) at constant relative air velocity (100 m/s) and variable liquid flow rate, the second (Fig. 47) at constant liquid flow rate and variable relative air velocity.

5.7 - Effect of Liquid Density

The data shown in Figs. 48 and 49 give evidence that the higher is the liquid density the smaller the liquid droplet sizes tend to be. Again, tests were carried out at constant relative air velocity (100 m/s) and constant liquid flow rate (2 gr/s). Results seem to indicate that for high atomizing air velocities and small liquid flow rates, S.M.D. became less sensitive to any variation of liquid density. It should be emphasized nevertheless that the combination of liquids used to obtain the variation in liquid density from 0.81 gr/cc to 2.18 gr/cc (namely pure methylated spirit and pure dibromo-ethane) did not provide constant liquid surface tension value which varied from 26.17×10^{-3} to 42.05×10^{-3} N/m (26 dyn/cm to 42.05 dyn/cm). It was then not possible to separate out completely the effect of surface tension which became more important when using higher concentrations of dibromo-ethane in the mixture of the two liquids used. The opposing effects that surface tension and liquid density have on the atomization

of liquids may have accounted for the tendency shown in Figs. 48 and 49 for S.M.D. to flatten out at the high liquid density values. It appears then likely that, had the surface tension been maintained reasonably constant throughout the tests, the S.M.D. would have decreased uniformly.

CHAPTER 6

ANALYSIS OF DATA RESULTS

CHAPTER 6

ANALYSIS OF DATA RESULTS

From the experimental results obtained so far, and described in the previous chapter, it is possible to draw some general conclusions concerning the effect that liquid physical properties and atomizing air velocity have on the S.M.D. of air-atomized sprays.

It was natural to expect that the higher the atomizing air velocity, the finer would be the spray. The effect of increased ^{viscosity} velocity in increasing drop size is also to be expected because when the viscosity is high more energy is required to overcome the viscous forces. In regard to liquid surface tension, again one's expectations are satisfied in that the higher is the surface tension the more difficult it becomes to disintegrate the liquid. The effect of liquid density is less easy to visualize, but the results obtained are consistent with those of other investigators, in that the higher the density the finer is the spray. It was also found that the air/liquid mass ratio exerts an influence on S.M.D. The larger is the amount of air taking part in the process of atomization the more finely is the liquid jet atomized, again as one would expect. It was also apparent from the results obtained over a wide test range, that liquid viscosity played an independent and separate role from that of air velocity. This suggested a form of empirical equation in which S.M.D. is expressed as the sum of two terms, the first term being dominated by air velocity and the second by liquid viscosity.

Fig. 26 gives a 3-D impression of airblast atomization performance for a particular liquid at different liquid flow rates. Its purpose is simply to convey a "visual feeling" of S.M.D. variation with air/liquid mass ratio and air velocity, for plain-jet atomizers.

6.1 - Empirical Results

It is desirable to express the experimental data quantitatively by assigning a numerical value to the exponent of each variable in equation (23),

$$\text{S.M.D.} = f (V_r^a, W_l^b, W_l/W_a^c, \rho_l^d, \sigma_l^e, \eta_l^f, D^g) \quad (23)$$

Apart from the inverse proportionality law between S.M.D. and relative air velocity, which is evident from examination of Figs. 30 and 31, all the other exponents have been derived by the usual method of plotting the experimental results on logarithmic paper. This is illustrated in Figs. 50 to 56.

6.1.1 - The Effects of the Atomizer Linear Dimensions on Spray Atomization

The effect of atomizer size, or scale, on spray quality has been investigated with low viscosity and high viscosity liquids using four separate plain-orifice atomizers and the results are illustrated in Figs. 36, 37 and 38.

The low viscosity tests suggest that no variation in the fineness of atomization can be attributed to the difference in the orifice diameters used. Reynolds No. higher than the critical one (around 2000), may have triggered a turbulent situation in the liquid jet, with the onset of radial velocities which assist and favour the atomization processes. This may have overshadowed the scale effect, if any, associated with different size atomizers. For higher viscosity liquids this is less likely to happen: in the present work the flow tended to be less turbulent because of liquid jet Reynolds No. less than critical in most cases and S.M.D. was then more sensitive to the effect of orifice size. A proof that this may be the case is given by Fig. 38 which illustrates the results of tests at high liquid viscosity. In this situation a scale effect is very noticeable and the exponent of an orifice diameter power law was found by log-plot analysis (Fig. 54) to be 0.53. In this case, the fuel orifice size effect seems to have been isolated and brought to play a separate effect on S.M.D.

With high viscosity liquids the spray cone angle did not vary appreciably with change in orifice diameter, thus suggesting that coalescence phenomena, if any, played the same role throughout the tests. Different results were obtained with low viscosity liquids. In most cases it was observed that the larger the atomizer diameter, the larger the spray cone angle appeared to be. As a consequence a better atomization followed because the greater exposure of liquid to a larger amount of atomizing air produced a finer spray. This could possibly be another explanation for justifying the fact that, when using plain-jet atomizers with larger diameters, S.M.D.'s do not seem to increase as might otherwise be expected.

Plates 9 and 10 show the difference between atomizing 1 gr/s of kerosine at 100 m/s with a 0.794 mm plain-orifice atomizer (Plate 9) compared with a 1.588mm plain-orifice (Plate 10). Although the cone angle of the spray does not seem to increase very much, nevertheless a more disrupted jet

is noticeable with the larger atomizer, so that coalescence of droplets may have taken place to a lesser extent combined to a greater exposure of liquid to the atomizing air.

Comparing Plates 11, 12 and 13, it is interesting to note the different spray disruption pattern when using convergent air-nozzles of different diameters, namely: 5.83, 6.85 and 12.70 mm. The tests were run with kerosine at an atomizing air-velocity of 100 m/s, a liquid flow rate of 2 gr/s and A.F.R.'s of 1.5, 2.10 and 7 respectively. As one would expect in these circumstances, the thicker the layer of atomizing air surrounding the liquid jet, the lower is the possibility of the disintegrating jet spreading outwards, resulting in a more concentrated form of jet.

Plates 14, 15 and 16 show the effect of air velocity (70, 100 and 140 m/s respectively) on the atomization of kerosine at a flow rate of 2 gr/s, using a 1.191 mm diameter plain-jet orifice in conjunction with a 6.85 mm convergent air nozzle. It may be noticed that the process of liquid disintegration, as indicated by the radial spreading of the liquid, starts more readily when using higher air velocities as shown in Plate 16, compared with Plates 14 and 15. In fact, at the air nozzle exit plane the liquid jet at 140 m/s has already spread outwards, whereas in the other two situations of lower air velocity the process of disintegration is retarded.

An illustration of good atomization, obtained at an air velocity of 120 m/s, is shown in Plate 6 where the process of droplet shattering is seen to start at two to three nozzle diameters downstream of the liquid exit plane.

6.1.2 - The Effect of Other Variables on S.M.D.

The plots in Figs. 50 to 56 do not call for any particular comment. From the results shown in these figures, S.M.D. may be expressed as:

$$S.M.D. = 904 \frac{\sigma_1^{0.32} W_1^{0.135}}{\rho_1^{0.37} V_r} \left(1 + \frac{1}{AFR}\right)^{1.70} + 11 \frac{\eta_1^{0.72} D^{0.53}}{(\sigma_1 \rho_1)^{0.5}} \left(1 + \frac{1}{AFR}\right)^{1.80}$$

(24)

where:	ρ_1	:	Liquid density	gr/cm ³
	σ_1	:	Liquid surface tension	dyn/cm
	η_1	:	Liquid absolute viscosity	centipoise
	V_r	:	Atomizing air velocity	m/s
	D	:	Plain-jet atomizer diameter	mm
	A.F.R.	:	W_a/W_l	
	W_a	:	Air flow rate	gr/s
	W_l	:	Liquid flow rate	gr/s
	S.M.D.	:	Sauter Mean Diameter	microns

Converting into strict S.I. units, equation (24) becomes:

$$\begin{aligned}
 \text{S.M.D.} = & 0.270 \frac{\sigma_1^{0.32} W_l^{0.135}}{\rho_1^{0.37} V_r} \left(1 + \frac{1}{\text{AFR}}\right)^{1.70} + \\
 & + 0.06186 \frac{\eta_1^{0.72} D^{0.53}}{(\sigma_1 \rho_1)^{0.5}} \left(1 + \frac{1}{\text{AFR}}\right)^{1.80} \quad (25)
 \end{aligned}$$

where:	ρ_1	:	liquid density	Kg/m ³ (= 10 ⁻³ gr/cm ³)
	σ_1	:	liquid surface tension	N/m (= 10 ³ dyn/cm)
	η_1	:	liquid absolute viscosity	Kg/ms (= 10 ³ centipoise)

W_1	:	liquid flow rate	Kg/s (= 10^3 gr/s)
D	:	plain-jet atomizer diameter	m (= 10^3 mm)
A.F.R.	:	W_a/W_1	
W_a	:	air flow rate	Kg/s (= 10^3 gr/s)
V_r	:	relative air velocity	m/s
S.M.D.	:	Sauter Mean Diameter	m (10^6 microns)

Although the formula predicts reasonably well the mean drop size, it is not dimensionally correct.

6.2 - Dimensional Analysis

In order to obtain a dimensionally correct prediction formula, i.e. a formula such as equation (24), (or (25)), but with the first and second terms having the dimensions of length, a dimensional analysis was then applied to the functional relationship (23).

It was possible to express a list of the variables affecting the mechanism of atomization, in terms of the three fundamental units, mass M, length L and time T, as follows:

Quantity	Symbol	Dimensions
Mean droplet diameter	S.M.D.	L
Orifice diameter	D	L
Atomizing air velocity	V_r	LT^{-1}
Liquid density	ρ_l	ML^{-3}
Absolute liquid viscosity	η_l	$ML^{-1}T^{-1}$
Liquid surface tension	σ_l	MT^{-2}
Air density	ρ_a	ML^{-3}
Liquid mass flow rate	W_l	MT^{-1}
Air mass flow rate	W_a	MT^{-1}

As S.M.D. must be the sum of two terms, both of which must have the dimension of length, the following equation for S.M.D. was derived:

$$S.M.D. = \frac{772}{V_r} \frac{(\sigma_l W_l)^{0.33}}{\rho_l^{0.37} \rho_a^{0.30}} \left(1 + \frac{1}{AFR}\right)^{1.70} + 4 \eta_l \left(\frac{D}{\rho_l \sigma_l}\right)^{0.5} \left(1 + \frac{1}{AFR}\right)^{1.80} \quad (26)$$

where the units are the same as the ones used in Eq. 24 with the air density expressed in Kg/m^3 .

This equation takes into account the air density ρ_a and one can observe that, apart from the value of the index, the higher is the pressure the finer is the spray, in agreement with Rizkalla and Lefebvre's results (Ref. 45). The reason why the air density arises in equation (26) is because without it any dimensionally correct formula would have been in disagreement with the experimental results. For example, the S.M.D. would have been independent of liquid density which the experimental data show is not true.

In strict S.I. units, equation (26) becomes:

$$\text{S.M.D.} = 0.950 \frac{(\sigma_1 W_1)^{0.33}}{v_r \rho_1^{0.37} \rho_a^{0.30}} \left(1 + \frac{1}{\text{AFR}}\right)^{1.70} + 0.127 \cdot \eta_1 \left(\frac{D}{\sigma_1 \rho_1}\right)^{0.5} \left(1 + \frac{1}{\text{AFR}}\right)^{1.80} \quad (27)$$

where S.M.D. is expressed in meters.

Using either equation (26) or (27) it appears that for liquids of low viscosity (such as water and kerosine), the first term predominates and S.M.D. will increase with liquid surface tension, liquid flow rate and will decrease with increasing atomizing air velocity, liquid density and air pressure (i.e. ρ_a). For liquids of higher viscosity, the second term assumes importance.

A reasonable prediction of spray S.M.D. may still be obtained if the two mass flow ratio factors, affecting the first and second term of equation (27), are combined into one of average index in the following somewhat simpler expression:

$$\text{S.M.D.} = \left[\frac{0.950}{v_r} \left(\frac{\sigma_1 W_1}{\rho_1 \rho_a}\right)^{0.35} + 0.127 \eta_1 \left(\frac{D}{\sigma_1 \rho_1}\right)^{0.5} \right] \left(1 + \frac{1}{\text{AFR}}\right)^{1.75} \quad (28)$$

which is easier to handle for general purposes.

6.3 - Analysis of Drop-Size Data

Under conditions of near-zero liquid viscosity the main factors governing drop size are: the mass flow ratio and the Weber No. The latter is taken into consideration because it describes the breakup of liquid drops by inertia forces to overcome surface tension. The mass flow ratio is considered to be a factor having an influence on S.M.D., not only because this has been found experimentally, but on account of the following considerations which also permits mass flow rate to be presented in the correct form. In fact, following Giffen and Muraszew (Ref. 12), as well as Marshall (Ref. 32) (see also Appendix A), the power ξ required to overcome the surface tension force σ_l by creating the liquid surface area 'S' per unit time is:

$$\xi = \sigma_l S \quad (29)$$

Following Wigg (Ref. 52), if we assume that the loss of kinetic energy of the air-stream is used to overcome the surface tension force and if we assume also that the air and liquid droplets in the spray have the same velocity V_s , the loss of kinetic energy is proportional to:

$$W_a V_a^2 + W_l V_l^2 - (W_a + W_l) V_s^2$$

Assuming no loss of momentum

$$W_a V_a + W_l V_l = (W_a + W_l) V_s$$

Substituting for V_s gives the loss of kinetic energy as:

$$\xi \propto \frac{W_a W_l (V_a - V_l)^2}{W_a + W_l} = \frac{W_l V_r^2}{1 + \frac{1}{AFR}} \quad (30)$$

Combining with equation (29) gives:

$$S \sigma_1 \left(1 + \frac{1}{AFR}\right) \propto W_1 V_r^2 \quad (31)$$

If 'n' is the number of droplets of uniform diameter created per unit time then:

$$S = \pi n (\text{S.M.D.})^2 \quad (32)$$

The volumetric liquid flow rate 'Q₁' is obtained from:

$$Q_1 = \frac{4}{3} n \pi \frac{(\text{S.M.D.})^3}{8}$$

which, if combined with equation (32), yields:

$$S = 6 \frac{Q_1}{(\text{S.M.D.})} = 6 \frac{W_1}{(\text{S.M.D.}) \rho_1} \quad (33)$$

From equations (31) and (33) one obtains:

$$\text{S.M.D.} \propto \frac{\sigma_1}{V_r^2 \rho_1} \left(1 + \frac{1}{AFR}\right) \quad (34)$$

and this expression, obtained from spray energy considerations, presents the mass flow ratio in the same form as obtained from experiment, apart from the exponent which from the tests appeared to be equal to 1.7.

From earlier considerations, and by replacing S.M.D. with d_1 to indicate the Sauter Mean Diameter relative to the first term of S.M.D. prediction equation, it follows:-

$$\frac{d_1}{D} \propto W_e^a \left(1 + \frac{1}{AFR}\right)^b$$

where:

$$W_e = \frac{\rho_1 V_r D}{\sigma_1} \quad (\text{Weber No. based on liquid properties})$$

D = fuel orifice diameter

A.F.R. = air/liquid mass ratio.

In order to obtain some agreement with the experimental data the following values for 'a' and 'b' must be assigned:

$a = -0.5$ and $b = 1.7$, therefore:

$$d_1 \propto \frac{\sigma_1^{0.5} D^{0.5}}{\rho_1^{0.5} V_r} \left(1 + \frac{1}{AFR}\right)^{1.7} \quad (35)$$

which is also the first term of equation (24) where the experiment has shown that the exponent affecting the liquid jet nozzle diameter is very small indeed, such that $D^{0.5} \rightarrow 1$, and that an extra term appears in the form $W_1^{0.135}$.

For viscous liquids an additional factor must be taken into account which is the Reynolds No. and again it must be combined with Weber No. because the latter describes the breakup of liquids drops by inertia forces to overcome surface tension. In a similar procedure to that followed earlier to describe the first term of equation (24), we may write (with the convention that S.M.D. is now d_2):

$$\frac{d_2}{D} \propto W_e^a R_e^b \left(1 + \frac{1}{AFR}\right)^c \quad (36)$$

and in order to obtain agreement with the experimental data the following values for 'a', 'b' and 'c', must be assigned: a = 0.5, b = -1.0 and c = 1.80.

It follows that:

$$d_2 \propto \frac{\eta_1 D^{0.5}}{\sigma_1^{0.5} \rho_1^{0.5}} \left(1 + \frac{1}{AFR}\right)^{1.8} \quad (37)$$

which is also the second term of equation (24), or better, of equation (26).

For real liquids, i.e. liquids of finite viscosity, the S.M.D. is given as the sum of $d_1 + d_2$ obtained from equations 35 and 37. These equations tell us that the drop size cannot fall below a certain minimum value, no matter how high the atomizing air velocity may be. This minimum size is equal to d_2 and it implies that the minimum drop size obtainable under any conditions is a function of fuel properties only.

6.4 - Comparison between Experimental Data-Points and Equation (24)

Figures 57 to 60 show the ability of equation (24) to predict the experimental results obtained with a "plain-jet" airblast atomizer of the type illustrated in Fig. 1, over a wide range of liquid properties at atmospheric pressure.

The ability to predict experimental data for low viscosity liquids (e.g. kerosine and water) as in Fig. 57, is very good for liquid flow rates from 0.5 to 3 gr/s and air velocities up to 180 m/s, at least for S.M.D. values less than 120 microns. The same comment can be made for liquids of high viscosity up to 76×10^{-3} Kg/ms (=76 centipoise), but some scatter is evident above 120 microns as shown in Fig. 58. The correlation between theoretical and experimental data is less satisfactory for values of surface tension between 24 and 73×10^{-3} N/m (24 to 73 dyn/cm). This is illustrated in Fig. 59, where the scatter increases regularly from 60 to 100 microns but nevertheless good correlation still exists for low surface tension liquids which is the case for most fuels. The equation gives remarkably good correlation with experimental data in predicting the effect of changes in liquid density on S.M.D., as illustrated in Fig. 60.

6.5 - Comparison with Rizkalla-Lefebvre's Measured Results

Experimental data from the two separate investigations are compared in Figs. 61 to 65. From a first inspection of the graphs it appears that for otherwise similar situations (i.e. the same atomizing air velocity and A.F.R.) the 'plain-jet' airblast atomizer performs less satisfactorily than a 'thin-sheet' airblast atomizer.

In Fig. 61, where a comparison is made for kerosine, it appears that for the plain-jet atomizer the situation deteriorates at low air/fuel mass ratios (e.g. below $3 \frac{1}{2}$ 4). In order to have comparable performance with 'thin-sheet' airblast atomization it is necessary to run at atomizing air velocities in excess of 100 m/s for A.F.R.'s above 3, unless fuel flow rates of less than 3 gr/s are involved. In Fig. 62, where a comparison has been presented for high viscosity liquids, the graphs obtained of S.M.D. versus A.F.R. are very similar, but S.M.D.'s in the present study are somewhat higher. The similarity of the two sets of curves is due mainly to the fact that the viscosity term in both the Rizkalla-Lefebvre's and the present predicting formula, is affected by a mass flow ratio term which has a comparable exponent in both cases.

The comparative results for kerosine and high viscosity liquids, with atomizing air velocity as the variable parameter, are presented in Figs. 63 and 64. Apart from the usual diversity in atomizer performance, it may be appreciated how adverse is the effect of operation at low air velocity for a 'plain-jet' airblast atomizer. This effect, at high liquid viscosity, is less apparent when compared to a 'thin-sheet' airblast atomizer because the performance is bad anyway for both atomizers.

Fig. 65 represents the atomizing ability of the 'plain-jet' airblast atomizer and the 'thin-sheet' airblast atomizer when compared against the Weber No. Both curves tend to converge at high Weber No., i.e. for the high inertia forces obtained at high air velocities, but for the fuels and atomizing air velocities normally encountered, the 'plain-jet' atomizer does not produce such small droplets as the 'thin-sheet' airblast atomizer.

6.6 - Comparison with Nukiyama and Tanasawa's Calculated Results (Ref. 39)

Fig. 66 shows the experimental data obtained in the presented investigation for water and kerosine plotted against corresponding values calculated from the prediction formula of Nukiyama and Tanasawa. It is remarkable how the data points obtained experimentally from the present study cluster very closely to a straight line when plotted against predictions based on Nukiyama

and Tanasawa's formula. A deviation from a perfect correlation with Nukiyama and Tanasawa's formula exists because higher S.M.D. values have been obtained in most cases in the present experimental research programme. A reason for this difference may be found in the way the experiments were conducted in both cases. In the present study most tests were run at atomizing air velocities less than 140 m/s (apart from some tests with water up to 180 m/s), whereas Nukiyama and Tanasawa tested their liquids at air velocities over 100 m/s and up to 300 m/s and even higher. Naturally the S.M.D.s obtained in most of their tests are considerably smaller than those obtained in the present study. This is probably the reason why correlations made against the Japanese formula deviates for situations of low velocity and low A.F.R. where the mass ratio term becomes important, and this is a feature found to exist both in Rizkalla-Lefebvre's work and in the present research. All this becomes apparent from the graph when it is observed that at the low S.M.D. range (up to about 50 microns) a very good correlation does exist.

6.7 - Comparison with Wigg's (Ref. 52) Calculated Results

The experimental values of S.M.D. for water and kerosine sprays at atmospheric pressure obtained in the present work are compared with the predictions of Wigg (equation 7) in Fig. 67. The correlation seems to give satisfactory agreement apart from a tendency of Wigg's formula to predict larger droplets. It must be pointed out that Wigg used large prefilm-airblast atomizers; whereas in the present study 'plain-jet' atomizers have been used; the droplets probably did not tend to coalesce very much and this is probably a consequence of their small concentrations for a given volume due to the low liquid flow rates used throughout the tests.

CHAPTER 7

CONCLUSIONS

CHAPTER 7

CONCLUSIONS

Recent studies on airblast atomization have been mainly confined to systems in which the fuel is first spread into a thin conical sheet and then subjected on both sides to the atomizing action of high velocity air. However, some aircraft gas turbines employ a different type of airblast atomizer in which the fuel is not transformed into a thin sheet but instead is injected into the high velocity airstream in the form of discrete jets. Since both types of fuel injection are in general use, an accurate knowledge of their relative merits is clearly desirable and it was in order to obtain the information needed for this comparison that the present investigation was undertaken. Since a considerable body of data already existed (Refs. 43, 45, 51 and 52) to describe the characteristics of 'thin sheet' atomizers, the study essentially resolved into a detailed experimental exploration of the spray characteristics of 'plain jet' airblast atomizers.

Measurements of S.M.D. (Sauter Mean Diameter) were obtained using the well-established light scattering technique. Specially prepared liquids were employed to distinguish between the separate effects on S.M.D. of viscosity, surface tension and density. Atomizing air velocities of up to 180 m/s were used in order to cover the range of interest for the gas turbine. The effect of scale on S.M.D. was studied using several different fuel injectors varying in orifice diameter between 0.39 and 1.58 mm.

From the test data collected on the performance of 'plain-jet' airblast atomizers, where single jets of liquids are atomized by a high velocity airstream, certain conclusions can be drawn.

- (a) Results obtained at atmospheric pressure with different liquids atomized under otherwise identical conditions show that at high A.F.R. the spray fineness depends on the liquid properties of density, viscosity and surface tension. The mean size of the liquid spray increases with increases in liquid viscosity and surface tension and decreases with increase in liquid density. The effect

of liquid flow rate alone has been successfully isolated and it appears that the higher the fuel flow rate the larger are the S.M.D.'s obtained.

- (b) The air/liquid mass flow ratio plays a significant role especially at low air velocities where a decrease of atomizing air flow, compared to the same liquid flow rate, has the effect of increasing the Sauter Mean Diameter of the spray quite significantly. The effect is only slight at high A.F.R.'s where a variation in A.F.R. has only limited effect on S.M.D.
- (c) For low liquid viscosities the atomizer linear dimension has virtually no effect on droplet size, but the effect of scale is very significant for liquids of high viscosity.
- (d) The effect of increasing atomizing air velocity is to produce finer sprays and it has been ascertained once again that for liquids of low viscosity an inverse proportionality law exists between S.M.D. and V_r .
- (e) This 'natural' airblast atomization mechanism can be conveniently used to atomize fuels of high viscosity provided high atomizing air velocities are used at A.F.R.'s exceeding about 5.
- (f) As a result of tests carried out over the following range of conditions:

Liquid viscosity	-	1.0 to 76×10^{-3}	Kg/ms
Liquid surface tension	-	26 to 73×10^{-3}	N/m
Liquid density	-	794 to 2180	Kg/m^3
Air velocity	-	70 to 180	m/s
Air/liquid mass ratio	-	1 to 36	

the following dimensionally correct formula was derived:

$$\text{S.M.D.} = 950 \times 10^{-3} \frac{(\sigma_1 W_1)^{0.33}}{V_r \rho_1^{0.37} \rho_a^{0.30}} \left(1 + \frac{1}{\text{AFR}}\right)^{1.7} + 127 \times 10^{-3} \eta_1 \left(\frac{D}{\rho_1 \sigma_1}\right)^{0.5} \left(1 + \frac{1}{\text{AFR}}\right)^{1.8}$$

which predicts reasonably well the Sauter Mean Diameter of the spray in microns.

- (g) Comparison with Rizkalla and Lefebvre's work (Ref. 45) and Figs. 61 to 65 shows broad agreement except for:
 - 1) the effect of liquid density which the present work has shown to be beneficial to spray quality if increased,
 - and 2) the effect of air/liquid mass ratio which, in the present study, has a greater effect on the first term of the S.M.D. prediction equation than in Lefebvre's formula.
 In general terms the performance of a 'plain-jet' airblast atomizer is inferior to a 'thin-sheet' airblast atomizer in that coarser sprays are usually obtained especially at low air atomizing velocities and low A.F.R.'s.
- (h) Comparison with Nukiyama and Tanasawa's work (Ref. 39) and Fig. 66 reveals good agreement only at high air velocities, i.e. for low S.M.D. values, because their experimental results were obtained mainly at high atomizing air velocities and this is reflected in their prediction formula.
- (i) A comparison with Wigg's work (Ref. 52) and Fig. 67 shows a better correlation even for low air velocities and low air/liquid mass ratios. Slightly higher droplet sizes are predicted by Wigg and this is believed to be due to the fact that in the present study coalescence of droplets did not take place to any great extent.

7.1 - SUGGESTIONS FOR FUTURE WORK

- (a) Further research on 'plain-jet' airblast atomization should be continued with the aim of improving spray quality by better atomizer geometry and by studying the effect of the axial position of the liquid nozzle in relation to the convergent air nozzle.
- (b) Research should also be carried out to assess the effect of air pressure on 'plain-jet' airblast atomization and also to provide an experimental value for the air density index in the prediction formula.
- (c) It is felt that some attention should be given in future work to the quality of the spray produced on the light of such factors as accuracy of orifice surface finish and l/D ratio.

X

REFERENCES

REFERENCES

1. PB-CHEMICALS INTERNATIONAL LTD. "Hyvis Polybutenes", Technical Booklet No. HB/102/2.
2. BRIFFA, F.E.J.; and DOMBROWSKI, N. "Entrainment of Air into a Liquid Spray", A.I.Ch.E. Journal, Vol. 12, No. 4, July, 1966, pp. 708 - 717.
3. BRYAN, R.H. "An Experimental Study of an Airblast Atomizer", Cranfield M.Sc. Thesis, Department of Aircraft Propulsion, Oct. 1967.
4. CASTLEMAN, R.A. "The Mechanism of Atomization of Liquids", National Bureau of Standards Journal of Research (U.S. Dept. of Commerce), Vol. 6, No. 281, 1931, p. 369.
5. CLARE, H.; and RADCLIFFE, A. "An Airblast Atomizer for Use with Viscous Fuels", Journal of Institute of Fuels, Vol. 27, Oct. 1954, p. 510.
6. COHEN, N.; and WEBB, M.J. "Evaluation of Swirl Atomizer Spray Characteristics by a Light Scattering Technique", Princeton University Aeronautical Engineering Laboratory Report, No. 597, Feb. 1962.
7. COLLINS, R.D.; MAYER, G.M.; and NEWBY, M.P. "The Efficiency of Momentum Production by Fluid-Atomizing Burners", Journal of Institute of Fuels, Vol. 26, No. 5th Oct. 1953, pp. 203 - 208.
8. DICKERSON, R.A.; and SCHUMAN, M.D. "Rate of Aerodynamic Atomization of Droplets". Journal of Spacecraft and Rockets, Vol. 2, No. 1, Jan. - Feb. 1965, pp. 99 - 100.

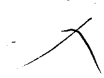
X


9. DOBBINS, R.A.;
CROCCO, L.; and
GLASSMAN, J. "Measurement of Mean Particle Sizes of
Spray from Diffractively Scattered
Light", A.I.A.A. Journal, Vol. 1,
No. 8, Aug. 1963, pp. 1882 - 1886.
10. ENGEL, O.G. "Fragmentation of Water Drops
in the Zone Behind an Air Shock",
National Bureau of Standards
Journal of Research, Vol. 60,
No. 3, March 1958.
11. FRASER, R.P. "Liquid Fuel Atomization",
6th Symposium on Combustion
(International), 1957.
12. GIFFEN, E.; and
MURASZEW, A. "The Atomization of Liquid
Fuels", Chapman and Hall Ltd.,
1953.
13. GODBOLE, P.S. "The Effect of Ambient Pressure
on Airblast Atomizer Performance",
Cranfield Thesis, Department of
Aircraft Propulsion, Sept. 1968.
14. GODFREY, D. "An Assessment of a Light
Scattering Technique for Drop
Size Measurement", Cranfield
Thesis, Department of Aircraft
Propulsion, Sept. 1969.
15. GOLITZINE, N.;
SHARP, R.; and
BADHAM, L.G. "Spray Nozzles for the Simulation
of Cloud Conditions in Icing
Tests of Jet Engines", N.A.E.
Canada, Report 14, 1951.
16. GREEN, H.L. "Problems in the Atomization of
Liquids", Conference on Fluid
Flow, Institute of Physics,
1951, pp. 75 - 86.
17. GRETZINGER, J.; and
MARSHALL, Jr., W.R. "Characteristics of Pneumatic
Atomization", Journal of the
American Institute of Chemical
Engineering, Vol. 7, No. 2,
June 1961, pp. 312- 318.

X

18. HANSON, A.R.;
DOMICH, E.G.; and
ADAMS, H.S. "An Experimental Investigation
of Impact and Shock Wave Break-up
of Liquid Drops", Research Report
125, Jan. 1956, Rosemount Aeronautical
Laboratory, Minneapolis, Minn.
19. HINZE, J.O. "Fundamentals of the Hydrodynamic
Mechanism of Splitting in Dispersion
Processes", Journal of the American
Institute of Chemical Engineering, Vol. 1,
No. 3, Sept. 1955, pp. 289 - 295.
20. INGEBO, R.D.; and
FOSTER, H.H. "Drop-size Distribution for Cross-
current Break-up of Liquid Jets in
Air Streams", N.A.C.A. TN 4087,
Oct. 1957.
21. JOYCE, J.R. "Fuel Atomizers for the Gas Turbine",
Shell Thornton Research Centre,
Miscellaneous 396, 1948.
22. JOYCE, J.R. "The Atomization of Liquid Fuels
for Combustion", Journal of
Institute of Fuel, Feb. 1949,
pp. 150 - 156.
23. LANE, W.R. "Shatter of Drops in Streams of Air",
Industrial and Engineering Chemistry,
Vol. 43, No. 6, June 1951, pp. 1312 -
1316.
24. LAWRENCE, O.N. "Gas Turbine Accessory Systems",
Journal of Royal Aeronautical Society,
1948, p. 151.
25. LEE, D.W.; and
SPENCER, R.C. "Photomicrographic Studies of Fuel
Sprays", N.A.C.A. Report No. 454, 1933,
pp. 215 - 239.
26. LEFEBVRE, A.H. "A Proposed Airspray Atomizer for
Aircraft Combustion Chambers",
Unpublished College of Aeronautics
Memorandum, March, 1964.

X

27. LEFEBVRE, A.H. "Progress and Problems in Gas Turbine Combustion", 10th Symposium on Combustion, 1965, pp. 1129 - 1137.
28. LEFEBVRE, A.H. "Design Considerations in Advanced Gas Turbine Combustion Chambers," Cranfield International Symposium Series, Vol. 10, Edited by E.I. Smith, Pergamon Press, 1968, pp. 3 - 19.
29. LEFEBVRE, A.H.; and MILLER, D. "The Development of an Airblast Atomizer for Gas Turbine Application", Cranfield College of Aeronautics, Report Aero No. 193, June 1966.
30. LEFEBVRE, A.H.; and NORSTER, E.R. "A proposed 'Double Swirler' Atomizer for Gas Turbine Fuel Injection", Cranfield SME Report No. 1, June 1972.
31. LEWIS, H.C.; EDWARDS, D.G.; GOGLIA, M.J.; RICE, R.I.; and SMITH, L.W. "Atomization of Liquids in High Velocity Gas Streams", Industrial and Engineering Chemistry, Vol. 40, No. 1, Jan. 1948, pp. 67 - 74.
32. MARSHALL, W.R. Jr. "Atomization and Spray Drying", Chemical Engineering Programme Monograph Series, No. 2, Vol. 5, 1954.
33. MAYER, E. "Theory of Liquid Atomization in High Velocity Gas Streams", A.R.S. Journal, Vol. 31, 1961, pp. 1783 - 1785.
34. MOCK, F.C.; and GANGER, D.R. "Practical Conclusions on Gas Turbine Spray Nozzles", S.A.E. Transactions, Vol. 4, No. 3, July, 1950, pp. 357 - 367.
35. MUGELE, R.A.; and EVANS, H.D. "Droplet Size Distribution in Sprays", Journal of Industrial and Engineering Chemistry, Vol. 43, No. 6, June, 1951, pp. 1317 - 1324.
- 

36. NEYA, K. "Measuring Methods for the Spray Characteristics of a Fuel Atomizer at Various Conditions of the Ambient Gas", Paper of Ship Research Institute, Tokyo, Japan, No. 23, Sept. 1967.
37. NEYA, K.; and SATO, S. "Effect of Ambient Air Pressure on the Spray Characteristics of Swirl Atomizers", Paper of Ship Research Institute, Tokyo, Japan, No. 7, Feb. 1968.
38. NORSTER, E.R.; and LEFEBVRE, A.H. "Effects of Fuel Injection Methods on Gas Turbine Combustor Emissions", Symposium on Emissions from Continuous Combustion Systems, General Motors Research Laboratories, Michigan, U.S.A., 1971.
39. NUKIYAMA, S.; and TANASAWA, Y. "Experiments on the Atomization of Liquid by means of an Air Stream", Transactions of the Society of Mechanical Engineers (Japan), Reports 1 - 6, Vols. 4 - 6, 1938 - 1940.
40. POPOV, M. "Model Experiments on Atomization of Liquids", N.A.S.A. T.T. F. 65, July 1961.
41. RADCLIFFE, A.; and CLARE, H. "A Correlation of the Performance of Two Airblast Atomizers with Mixing Sections of Different Size", N.G.T.E. Report No. 144, Oct. 1953.
42. RANGER, A.A.; and NICHOLLS, J.A. "Aerodynamic Shattering of Liquid Drops", A.I.A.A. Journal, Vol. 7, No. 2, Feb. 1969, pp. 285 - 290.
43. RIZKALLA, A.A.; and LEFEBVRE, A.H. "Influence of Liquid Properties on Airblast Atomizer Spray Characteristics", A.S.M.E. Gas Turbine Conference, Zurich, April, 1974, Journal of Engineering for Power, April, 1975 (pp. 173 - 179).
- 

44. RIZKALLA, A.A. "The Influence of Air and Liquid Properties on Airblast Atomization", Cranfield Institute of Technology, S.M.E. Ph.D. Thesis, 1974.
45. RIZKALLA, A.A.; and LEFEBVRE, A.H. "The Influence of Air and Liquid Properties on Airblast Atomization", Journal of Fluids Engineering, Transactions of the A.S.M.E., Sept. 1975, pp. 316 - 320.
46. ROBERTS, J.H.; and WEBB "The Use of the Upper Limit Distribution Function in Light Scattering Theory as Applied to Droplet Diameter Measurement", Princeton University Aeronautical Engineering Laboratory Report No. 650, 1963.
47. ROBERTS, J.H.; and WEBB, M.J. "Measurement of Droplet Size for Wide Range Particle Distributions", A.I.A.A. Journal, Vol. 2, No. 3, March, 1964, pp. 583 - 585.
48. VAN DE HULST, H.C. "Light Scattering by Small Particles", Wiley, New York, 1956.
49. WEISS, M.A.; and WORSHAM, C.H. "Atomization in High Velocity Air Streams", Applied Science Research, Vol. 29, No. 4, April 1959, or: Journal of the American Rocket Society (1959) Vol. 29, p. 252.
50. WELCH, C. "Design of an Optical System for Counting and Sizing Airborne Particles", National Symposium on Instrumental Methods of Analysis, 8th Proceedings, 1962, pp. 173 - 178.
51. WIGG, L.D. "The Effect of Scale on Fine Sprays Produced by Large Airblast Atomizers", N.G.T.E. Report No. 236, July 1959.

X

52. WIGG, L.D. "Drop-Size Prediction for Twin-Fluid Atomizers", Journal of the Institute of Fuel, Vol. 27, No. 286, Nov. 1964, pp. 500 - 505.
53. WOLFE, H.; and ANDERSEN, W. "Aerodynamic Break-up of Liquid Drops", Paper SP 70, (American Physical Society), April 1965.
54. WOOD, R. "Spray Characteristics of Nene Atomizers: Results with Four Atomizers Used in the R.A.E. Nene Altitude Tests", Shell Thornton Research Centre, Report No. K. 112, Sept. 1953.
55. WOOD, R. "The Rolls-Royce Airspray Atomizer: Spray Characteristics", Shell Thornton Research Centre, Report No. K 123, July, 1954.
56. YORK, J.L.; and STUBBS, H.E. "Photographic Analysis of Sprays", Transactions of A.S.M.E., Oct. 1952, pp. 1157 - 1162.
57. YORK, J.L.; STUBBS, H.E.; and TEK, M.R. "The Mechanism of Disintegration of Liquid Sheets," A.S.M.E. Paper No. 53-S-40, 1953.
58. WETZELL, R.H.; and MARSHALL, W.R. Washington, D.C., National Meeting American Society Mechanical Engineers, 1954.
59. RAYLEIGH, LORD. Proc. Lond. Math. Soc. 1879-10-4.

X

APPENDICES

APPENDIX A

ATOMIZATION EFFICIENCY

The theoretical energy requirement for atomization is most simply calculated from an estimate of the surface area S produced and the liquid surface tension forces involved σ_1 . As shown in Refs. (12) and (32), the energy \mathcal{E} required is:

$$\mathcal{E} = (\text{surface tension}) \times (\text{surface area}) = \left[\text{N/m} \times \text{m}^2 \right]$$

or:
$$\mathcal{E} = \sigma_1 S \quad (I)$$

Due to the atomization process, a volume of liquid of surface area A_1 will be shattered into a very large number of droplets of total surface area A_2 . As an example, consider a plain-jet orifice of diameter $D = 1 \text{ mm}$ (10^{-3} m) delivering a jet of fuel of density $\rho_1 = 0.8 \text{ gr/cm}^3$ at a mass flow rate $W_1 = 1 \text{ gr/s}$. Initially the liquid emerges in the form of a column which, if allowed to form without disruption, would travel 1.59 m in one second.

In fact:

$$Q_1 = \frac{W_1}{\rho_1} = \frac{1}{0.8} = 1.25 \text{ cm}^3/\text{s} \quad \begin{array}{l} 1 \text{ mm} = \text{m} \times 10^{-3} \\ 1 \text{ cm} = \text{m} \times 10^{-2} \end{array}$$

therefore:

$$V_1 = \frac{Q_1}{\pi \frac{D^2}{4}} = \frac{4 \times 1.25 \times 10^{-6}}{\pi} = \frac{4 \times 1.25 \times 10^{-6}}{\pi \times 10^{-6}} = 1.59 \text{ m/s}$$

The surface area of this initial column of liquid created in one second, and whose purpose is only to stand as a model for ease of calculations, is:

$$A_1 = \pi D V_1 = 3.14 \times 10^{-3} \times 1.59 = 5 \times 10^{-3} \text{ m}^2/\text{s}$$

X

If we think of the spray created by the disruptive action of the atomizing air on this liquid column as consisting of droplets of uniform size, it is possible to write an expression for the number of droplets 'n' created in one second as:

$$n = \frac{Q_1}{\frac{4}{3} \pi \left(\frac{\text{S.M.D.}}{2} \right)^3} = \frac{3 \times 1.25 \times 10^{-6}}{4 \times 3.14 \times (15 \times 10^{-6})^3} = 8.84 \times 10^7$$

where S.M.D. = 30 μ has been chosen as a representative droplet size. At this point it is possible to calculate the total surface area A_2 , after break-up of the liquid into small droplets, in the following way:-

$$A_2 = \pi (\text{S.M.D.})^2 n = 3.14 \times 8.84 \times 10^7 \times (30 \times 10^{-6})^2 = 0.250 \text{ m}^2$$

and by the mechanism of atomization, the liquid surface area has been increased by:-

$$A_2/A_1 = \frac{0.250}{0.005} = 50 \text{ times}$$

If 'S' is the increase in surface area, it follows then from equation (I):

$$\xi = \sigma_1 (A_2 - A_1) = \sigma_1 S$$

In this particular case, assuming $\sigma_1 = 30 \times 10^{-3}$ N/m, the power required for atomization is:

$$\xi = 30 \times 10^{-3} (0.250 - 0.005) = 7.35 \times 10^{-3} \text{ W} \quad \text{Nm}$$

Assume that this fineness of atomization has been achieved using the present experimental set up with an atomizing air flow rate $W_a = 4 \times 10^{-3}$ Kg/s delivered at 100 m/s. Assuming also adiabatic expansion through the air nozzle at a pressure ratio $\frac{p_1}{p_2} = 1.061$, we can say that the total power available

in form of kinetic energy can be expressed as:

$$E = W_a RT_1 \left[1 - \left(\frac{P_2}{P_1} \right)^{\gamma-1/\gamma} \right]$$

$$E = 4 \times 10^{-3} \times 287 \times 300 \left[1 - \left(\frac{1}{1.061} \right) \right] \frac{0.4}{1.4} = 5.68 \text{ W}$$

where: R (gas constant) = $287 \frac{\text{J}}{\text{Kg K}}$

T_1 (upstream air temperature) = 300 °K

The fraction of energy applied which is utilized in the creation of new surface is expressed as:

$$\mathcal{E}/E = (7.35 \times 10^{-3} / 5.68) \times 10^2 = 0.13\%$$

and this result shows how low is the atomization efficiency encountered with this mechanism of drop shattering.

APPENDIX B

CALIBRATION AND OPERATING PROCEDURE

OF THE LOGARITHMIC AMPLIFIER

Calibration of the X-Y plotter is necessary after installation and should be repeated subsequently each time before use or when it is re-installed in a different axis or recorder main frame. The calibration and operating procedure is done in the following way:

- a) With the function switch in the OdB position switch on the recorder and allow 15 minutes warm-up period.
- b) Place a sheet of Log 5 cycles x mm paper on the recorder and check that it is held in position by the vacuum.
- c) By means of the Pen Offset Control move the pen to half scale.
- d) Turn the Range Control to its calibrated position i.e. fully anti-clockwise and switch to Internal Reference.
- e) Switch the Internal Reference switch to 100 mV and adjust the sub-panel SET OdB potentiometer with a small screwdriver so that the pen returns to the OdB-line.
- f) Switch to 10 V and adjust the CAL potentiometer to give 10 cm deflection corresponding to 2 decades (2 log cycles) i.e. to 40 dB.
- g) Switch to 0.316 mV and adjust the CAL 0.316 mV potentiometer to give a deflection of - 12.5 cm corresponding to - 2.5 decades.
- h) When calibration is performed, repeated use of the Pen Offset Control is necessary to ensure that the pen does not exceed full scale deflection in either direction.

- i) Check the full range of Internal Reference sources from 0.316 mV to 10 V. The Log Amplifier will now be calibrated with a scale factor of 4 dB/cm over the full dynamic range from 0.316 mV to 10 V.
- j) After the required 15 minutes warm-up period the Log Amplifier is ready for use. The Log x mm paper is useful for the indication of the actual magnitude of the compressed input signal.
- k) Switch to OdB. The input from the photomultiplier is now disconnected from the Log Amplifier and the pen will have taken up a position corresponding to OdB.
- l) Move the pen by means of the Pen Offset Control to the maximum desired pen deflection e.g. full scale deflection. This will be the OdB position.
- m) Switch to Internal Reference and switch the Internal Reference switch to the level desired for OdB (in this case the highest voltage to be measured).
- n) Switch the highest voltage to be measured and rotate the range control until the pen position coincides with the desired lines on the paper for this voltage e.g. zero scale deflection.
- o) Switch the Input to plot the input function i.e. the photomultiplier output against the traverse distance.
- p) After use switch to either OdB or Internal Reference and disconnect the input signal line from the input terminals before switching off the recorder.

TABLE (1)

Solutions of the synthetic hydrocarbon polymer, Hyvis Polybutene No. 05 in kerosine to obtain a wide range of viscosity:

Solution	η_L	σ_L	ρ_L
Pure kerosine	1.293	27.67	0.784
30% Hyvis 05	2.868	28.67	0.800
40% Hyvis 05	4.286	28.78	0.809
50% Hyvis 05	6.042	28.87	0.812
60% Hyvis 05	9.789	29.17	0.819
70% Hyvis 05	17.014	30.08	0.823
80% Hyvis 05	33.802	30.16	0.828
85% Hyvis 05	44.104	30.27	0.830
90% Hyvis 05	76.541	30.46	0.833
95% Hyvis 05	123.921	30.70	0.838
Pure Hyvis 05	218.562	30.96	0.840

TABLE (2)

Mixtures of sec-Butyl Alcohol (Butan - 2 ol) with water to obtain different values of surface tension:

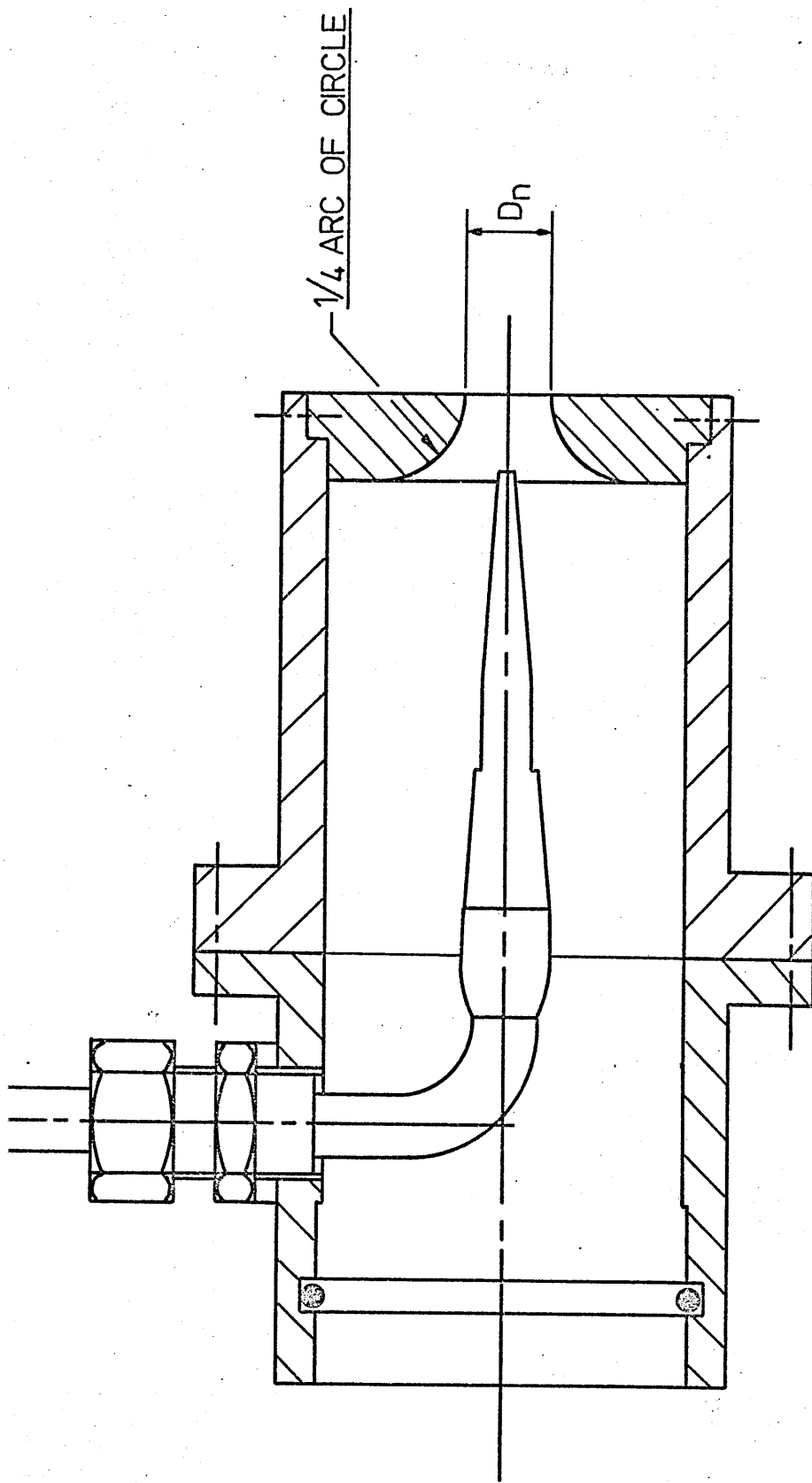
Solution	η_l	σ_l	ρ_l
Pure Water	0.998	73.45	0.998
1.48 % Butan-2-ol	1.127	55.94	0.990
2.44 % Butan-2-ol	1.131	51.89	0.988
3.85 % Butan-2-ol	1.150	46.45	0.986
6.98 % Butan-2-ol	1.274	39.45	0.983
11.11 % Butan-2-ol	1.404	33.96	0.980
16.67 % Butan-2-ol	1.712	29.07	0.978
25.93 % Butan-2-ol	2.342	26.77	0.968
Pure Butan-2-ol	3.468	24.16	0.807

TABLE (3)

Dibromo-ethane (ethylene dibromide) diluted with methylated spirit to obtain a wide range of density:

Solution	η_L	σ_L	ρ_L
Pure methylated spirit	1.530	26.17	0.812
9.09 % Dibromo-ethane	1.537	29.86	0.933
13.04 % Dibromo-ethane	1.545	30.29	0.978
16.67 % Dibromo-ethane	1.552	30.71	1.031
23.08 % Dibromo-ethane	1.559	31.14	1.123
28.47 % Dibromo-ethane	1.566	31.56	1.213
37.50 % Dibromo-ethane	1.574	31.99	1.315
44.44 % Dibromo-ethane	1.581	32.42	1.430
50.00 % Dibromo-ethane	1.588	32.84	1.503
54.00 % Dibromo-ethane	1.597	33.27	1.634
60.00 % Dibromo-ethane	1.603	33.70	1.830
Pure Dibromo-ethane	1.727	42.05	2.180

FIGURES



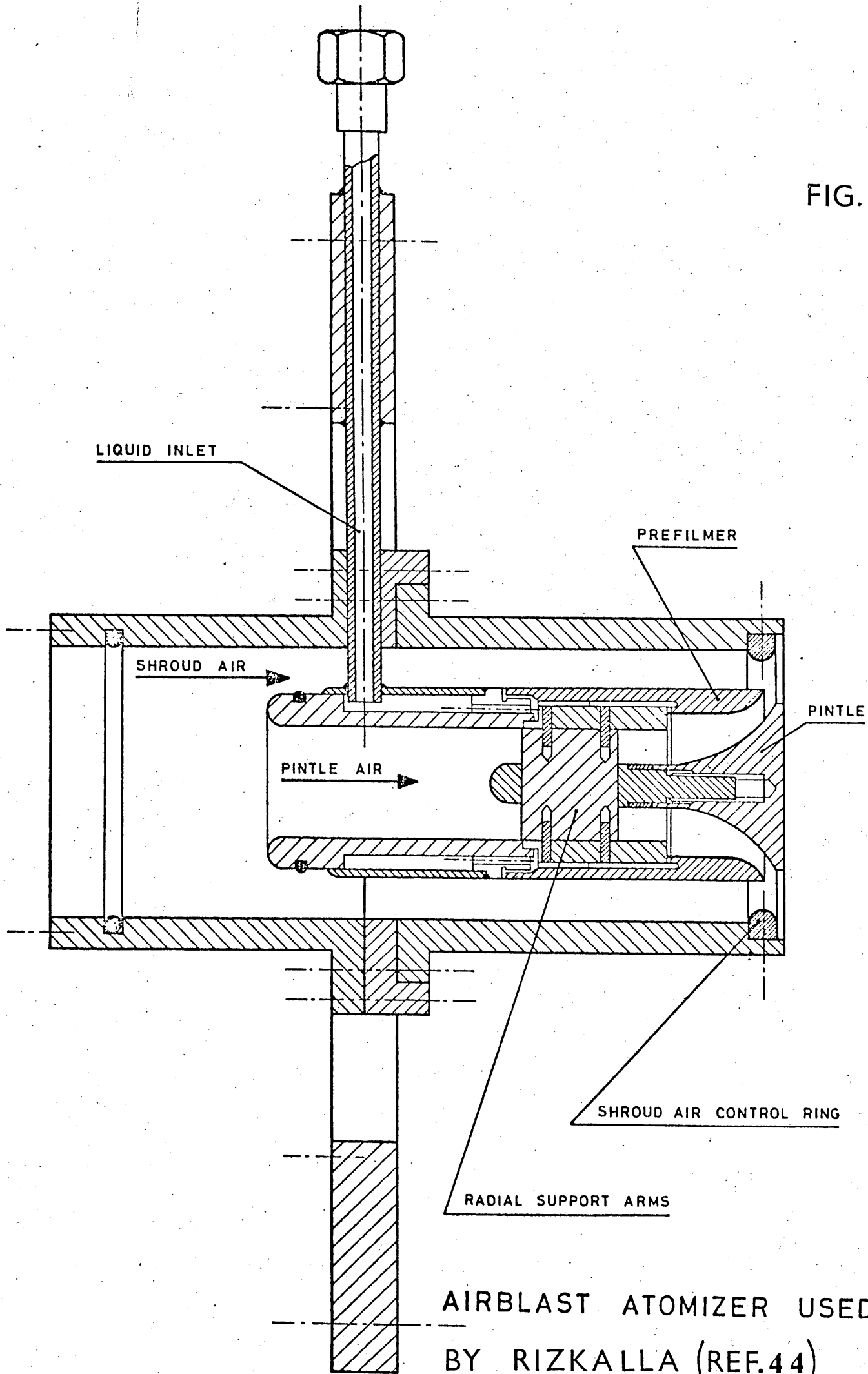
SCALE 1:1

AIRBLAST ATOMIZER USED IN PRESENT STUDY

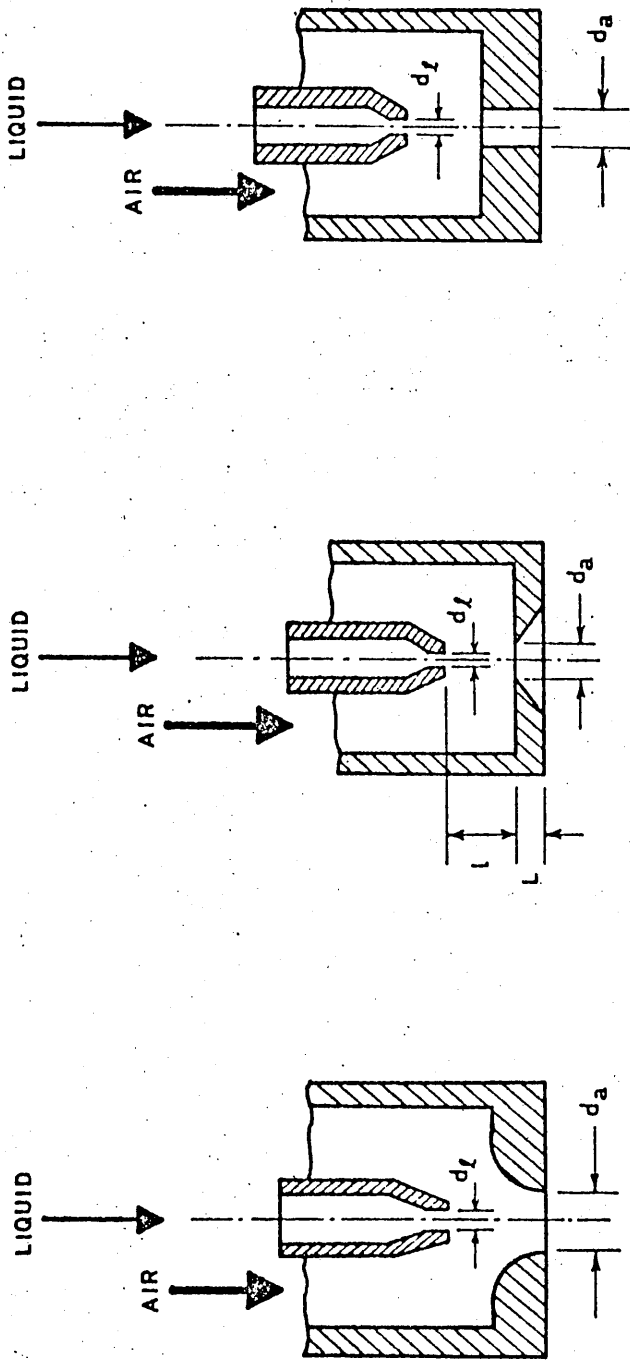
FIG. 1

7

FIG. 2



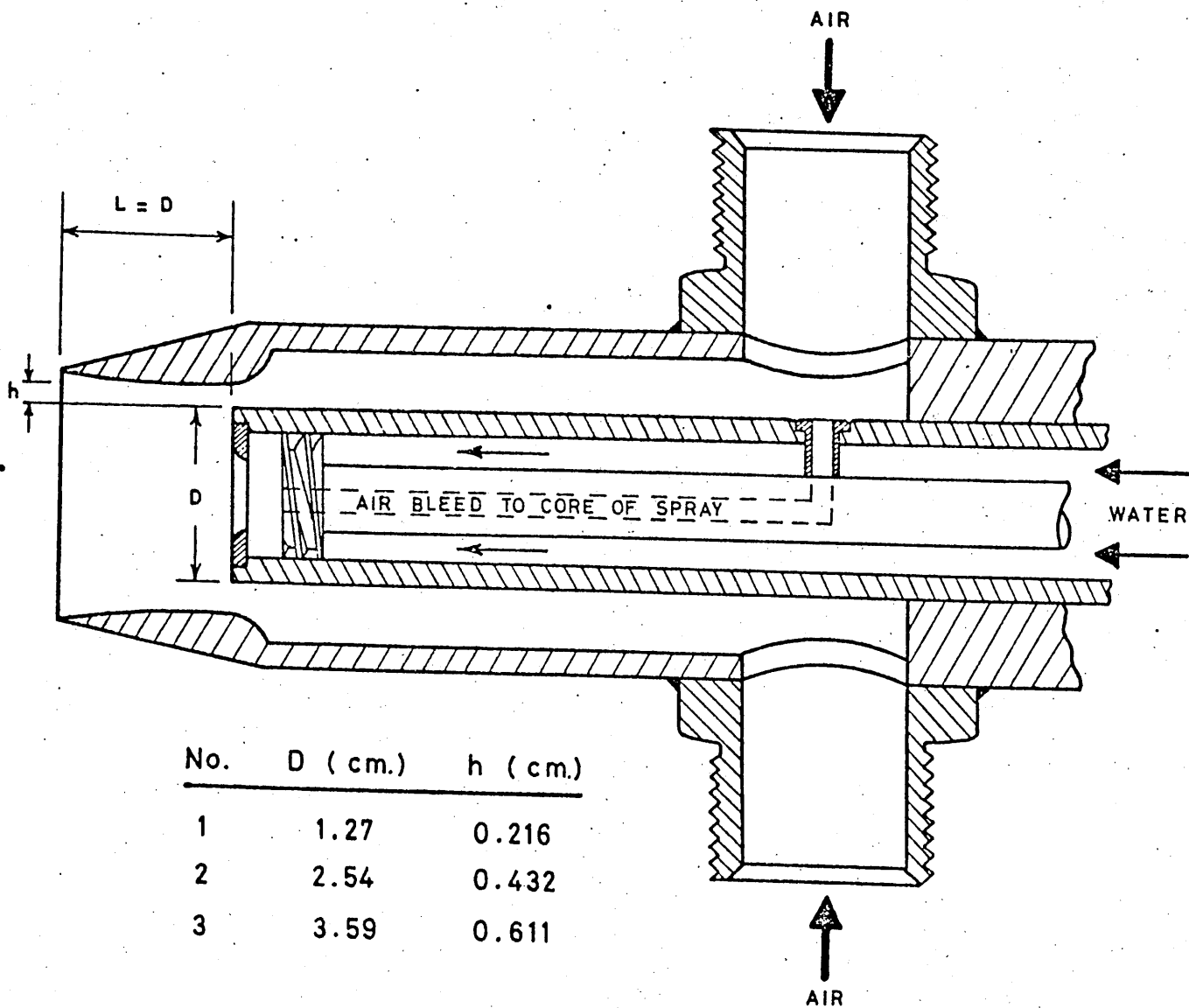
AIRBLAST ATOMIZER USED BY RIZKALLA (REF.44)



(a) Convergent Air Nozzle (b) 120° Sharp-Edged Orifice (c) Cylindrical Air Nozzle

Orifice

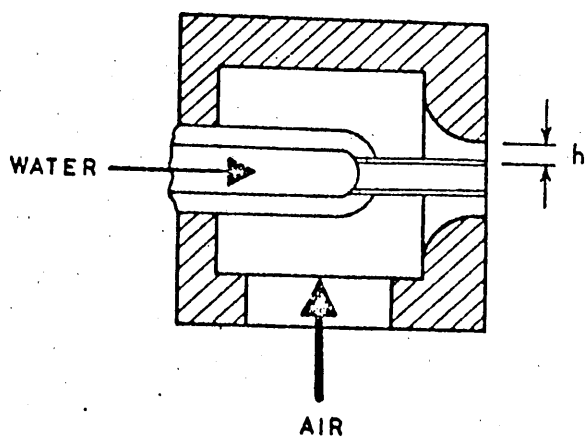
NUKIYAMA AND TANASAWA ATOMIZERS



No.	D (cm.)	h (cm.)
1	1.27	0.216
2	2.54	0.432
3	3.59	0.611

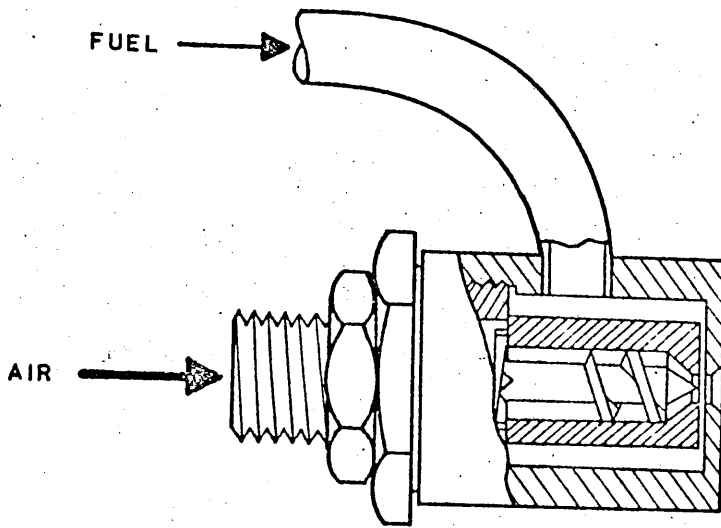
N.G.T.E. AIRBLAST ATOMIZER

FIG. 4

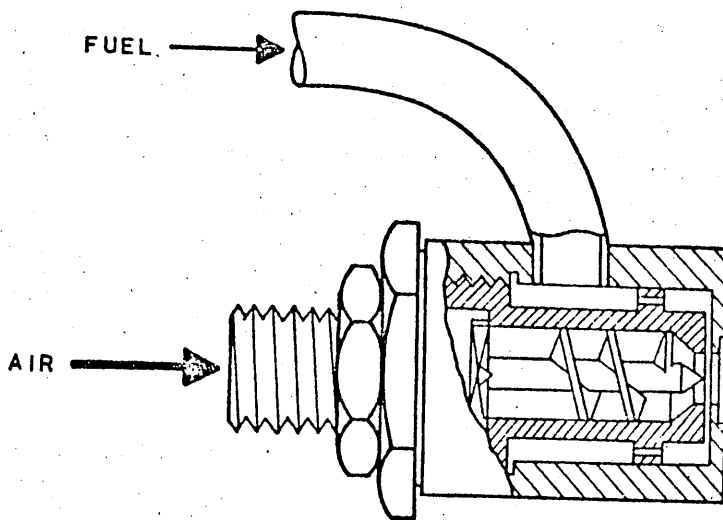


No.	h (cm.)
1	0.061
2	0.099
3	0.144

N.R.L. CANADA CONVERGENT NOZZLES FIG. 5



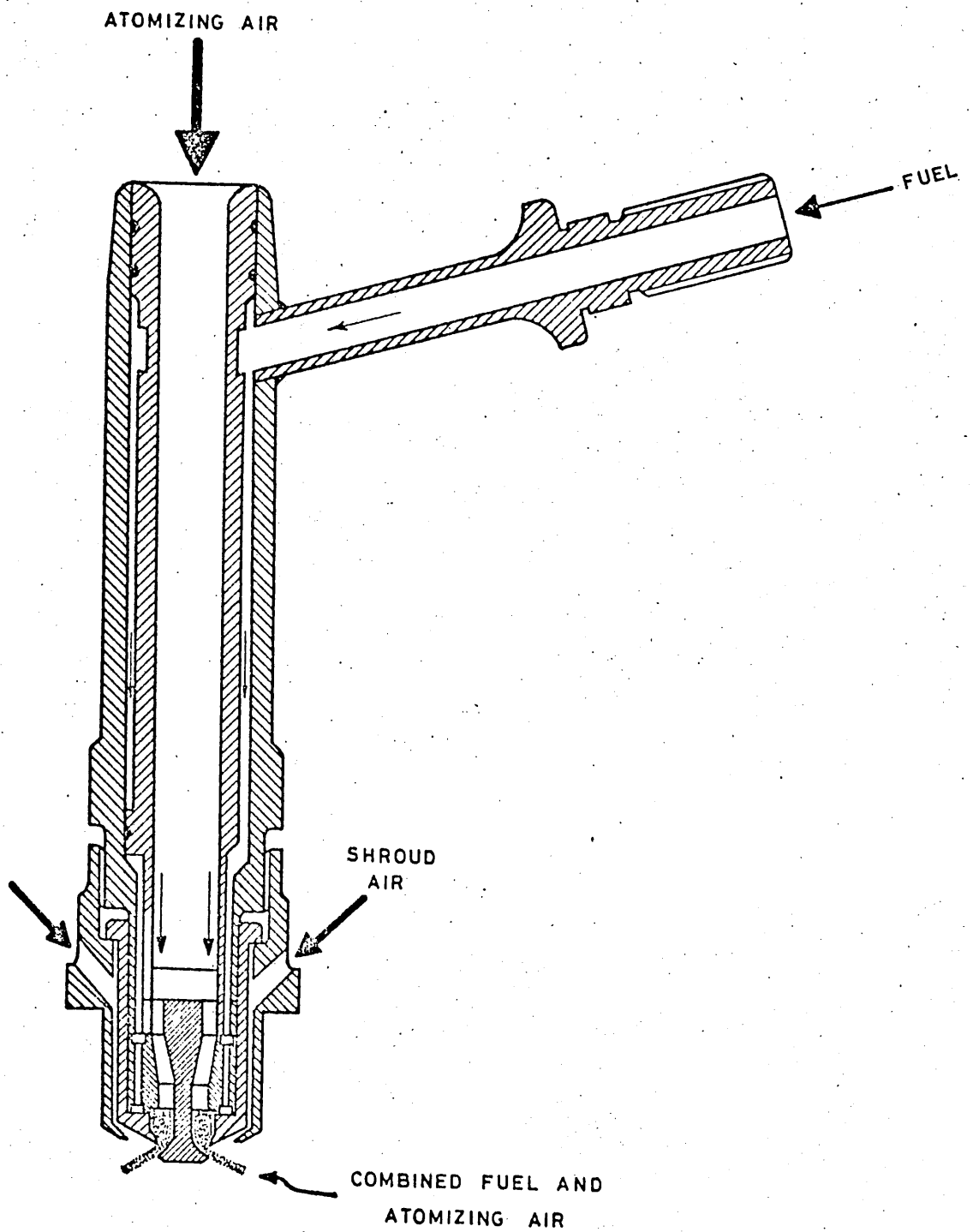
(a) 1/8 - Inch Orifice



(b) 1/4 - Inch Orifice

EARLY N.G.T.E. HIGH PRESSURE AIR ATOMIZERS

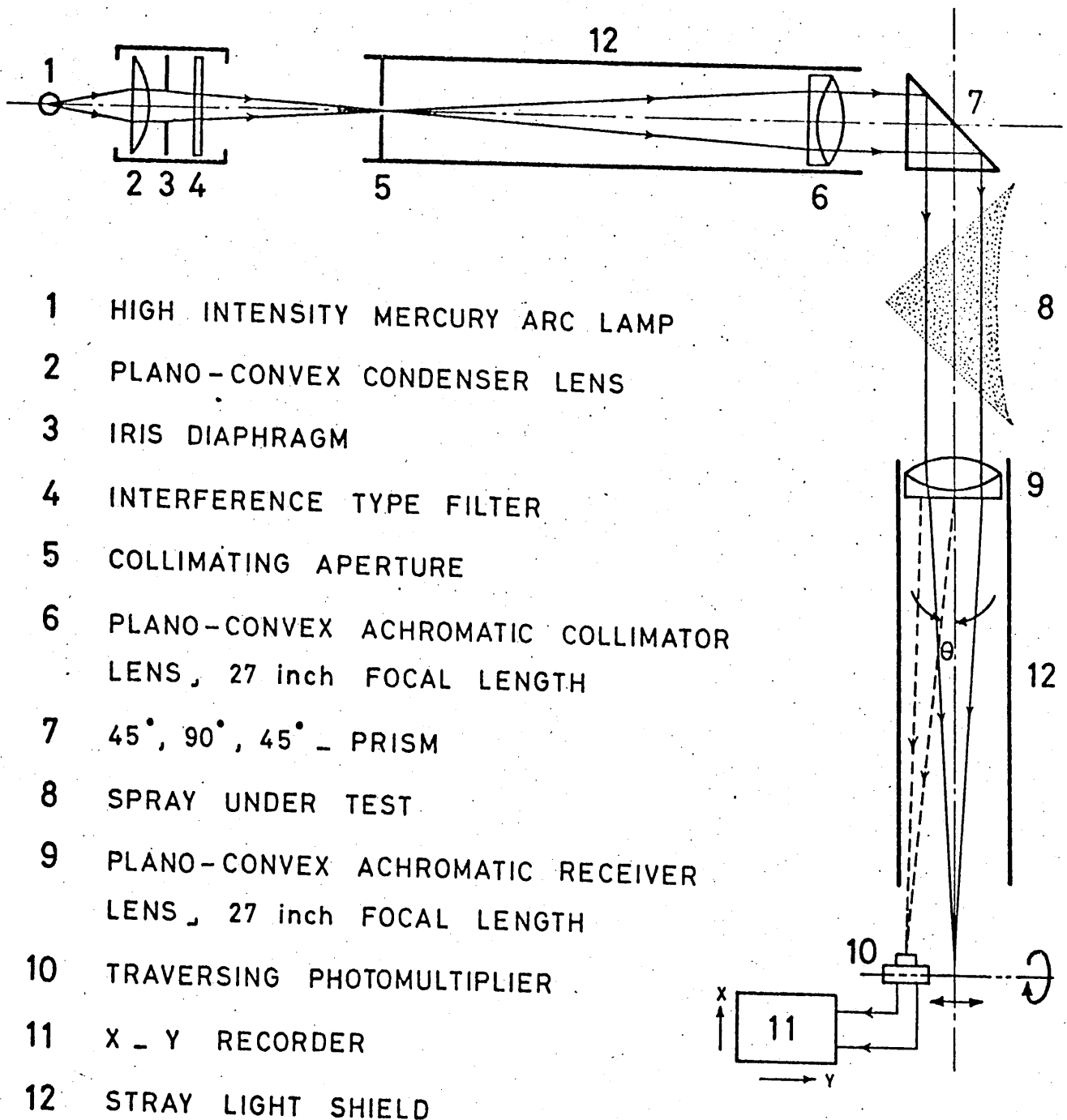
FIG. 6



ROLLS-ROYCE "DART" AIRSPRAY ATOMIZER

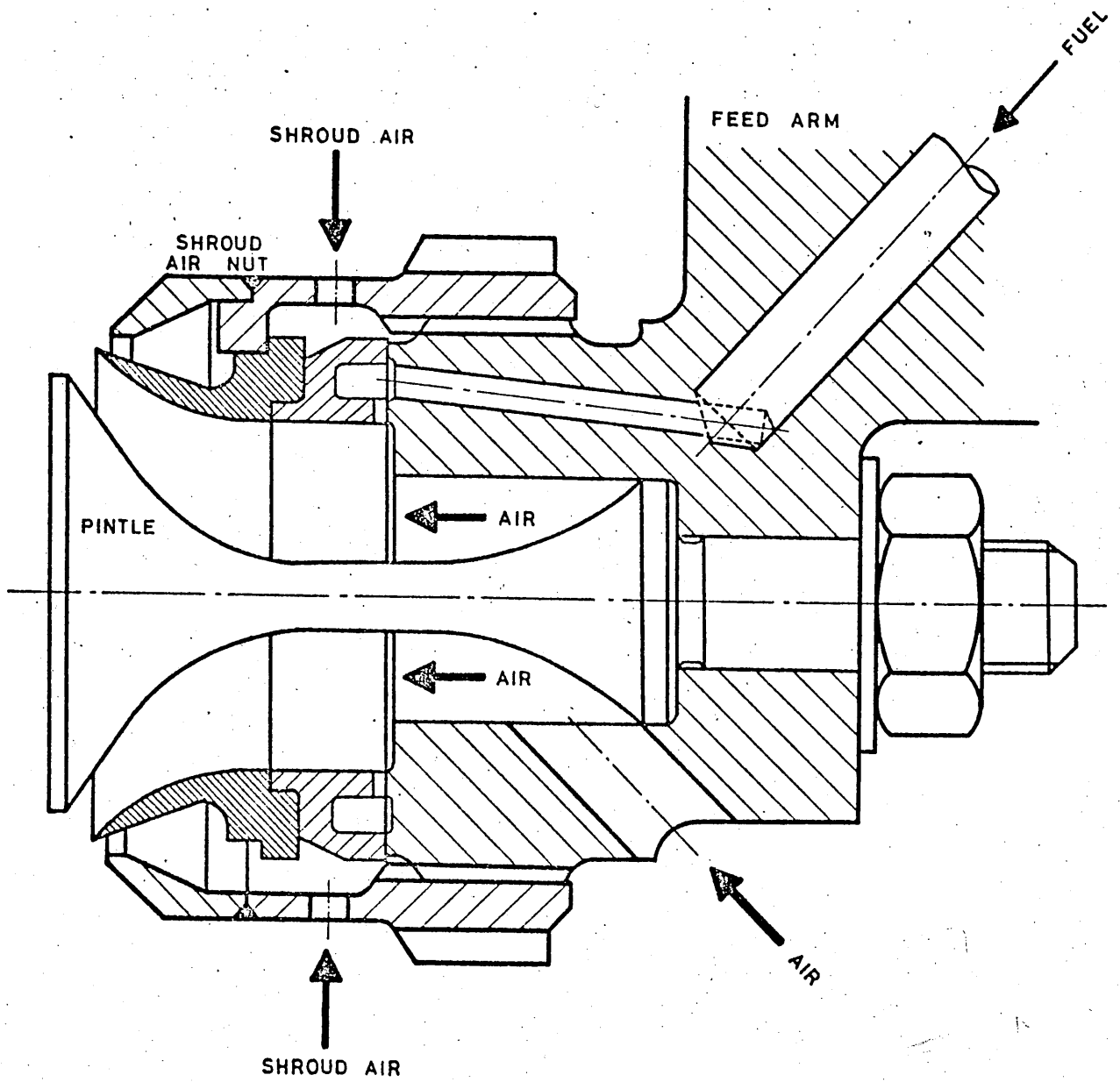
FIG. 7

7



THE OPTICAL BENCH IN DIAGRAMMATIC FORM - RIZKALLA (REF.44) -

FIG. 8



ATOMIZER NO. 3 [Ref. 13]

FIG. 9

X

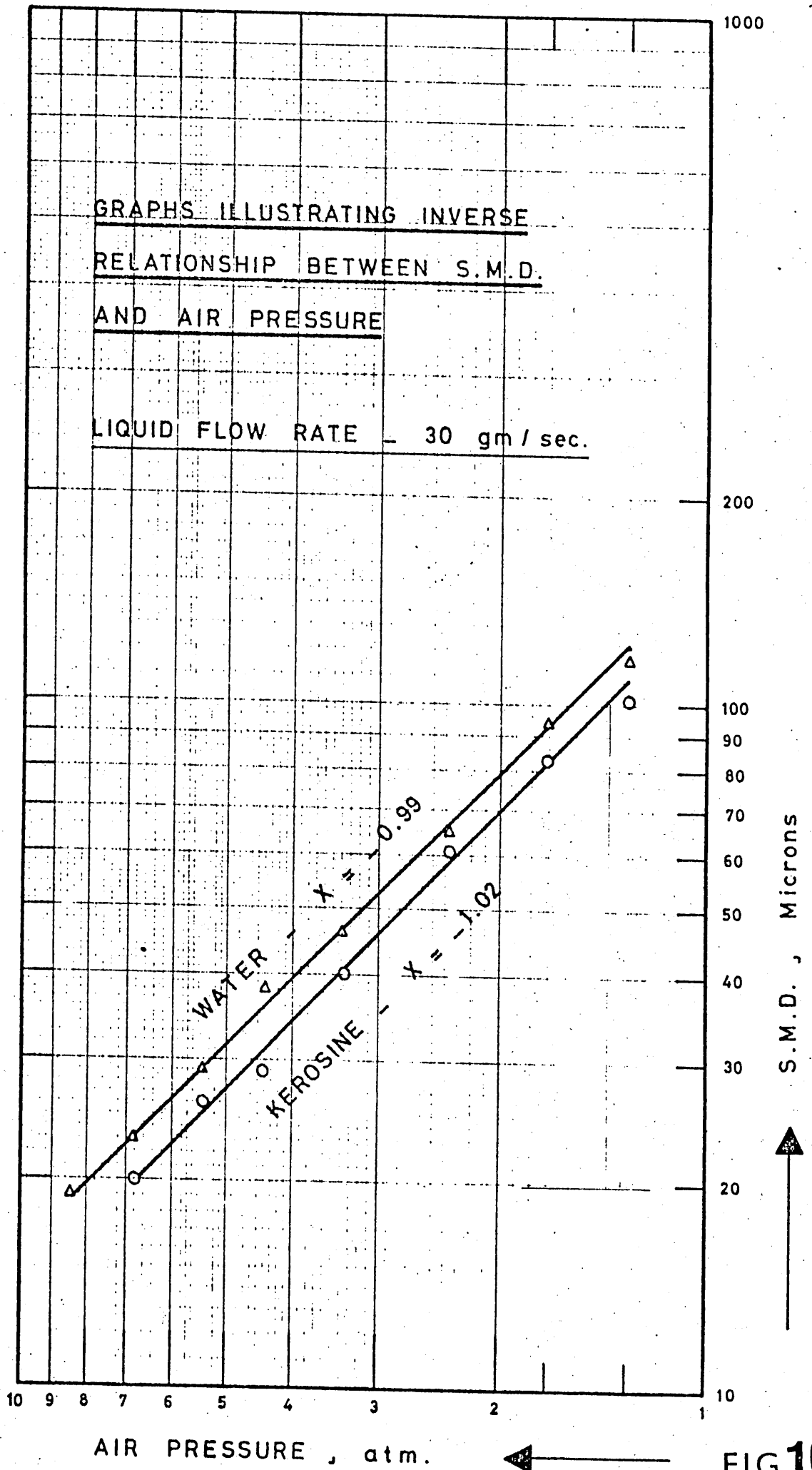
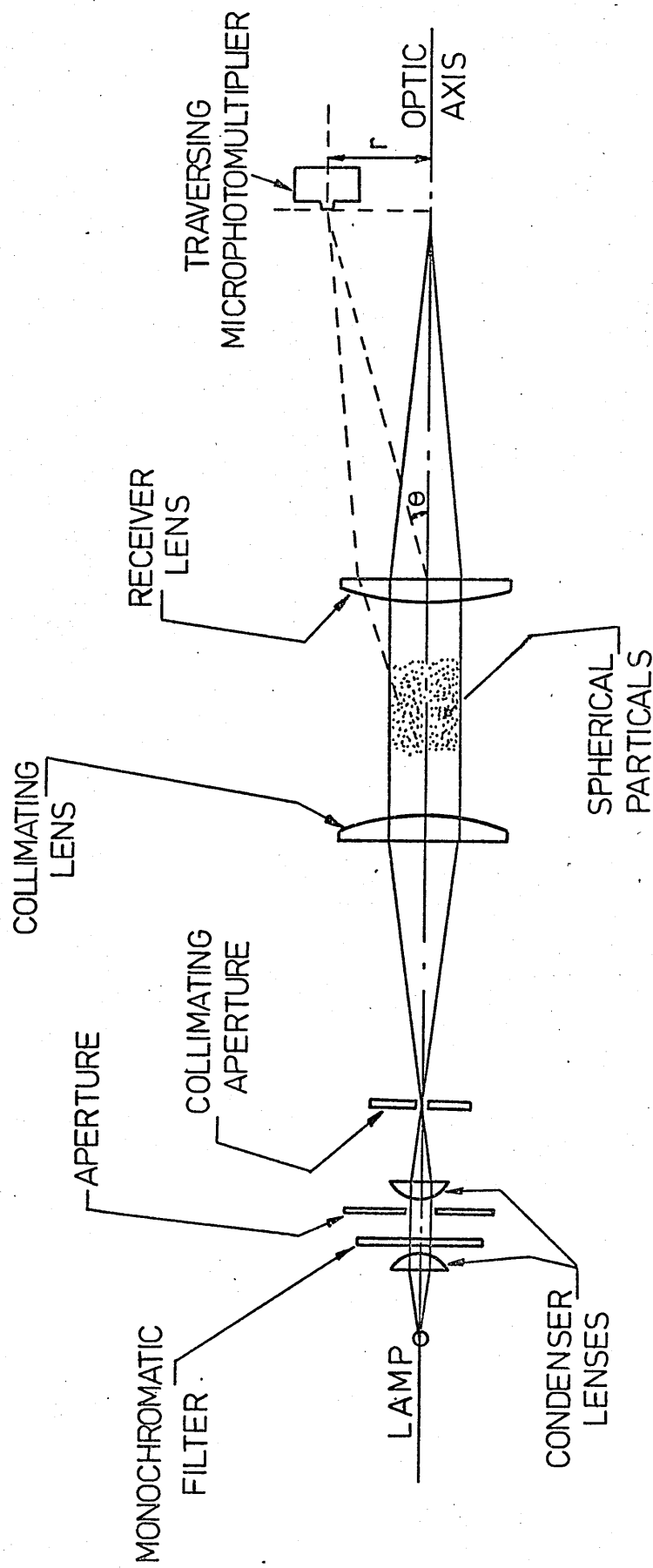


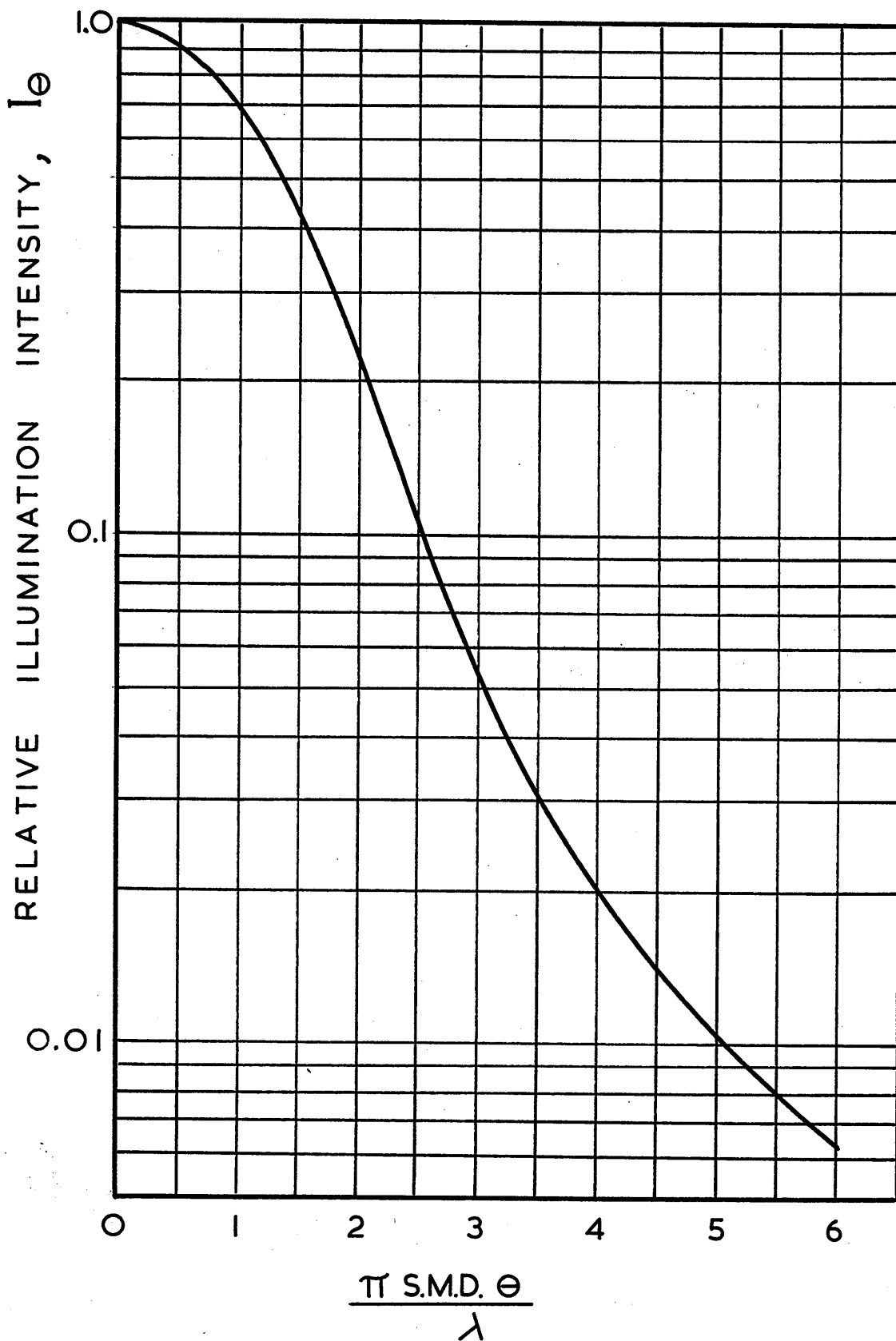
FIG.10



DOBBS OPTICAL APPARATUS

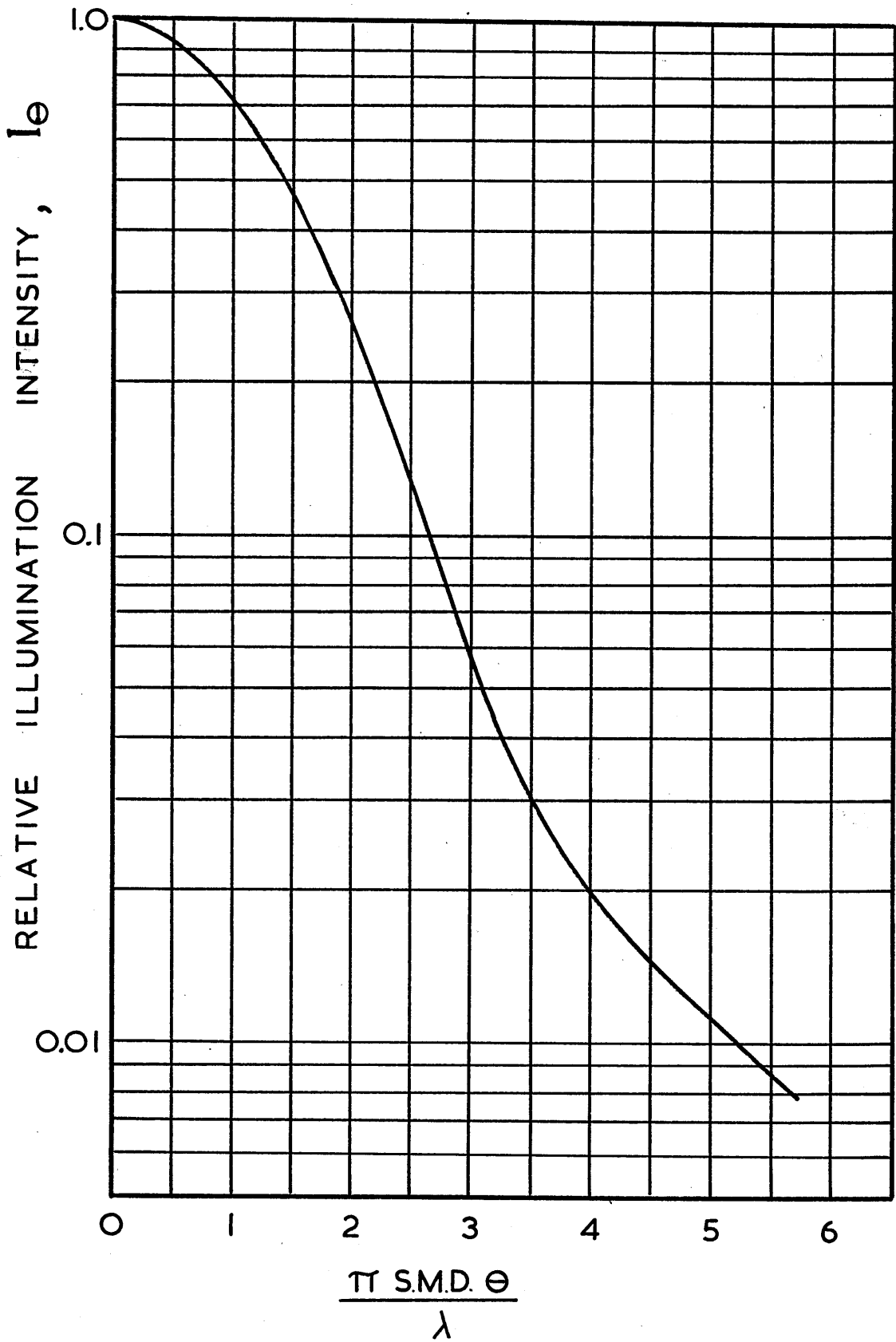
FIG. 11

X



MEAN THEORETICAL ILLUMINATION PROFILE
 (Dobbins, Crocco and Glassman)

FIG.12

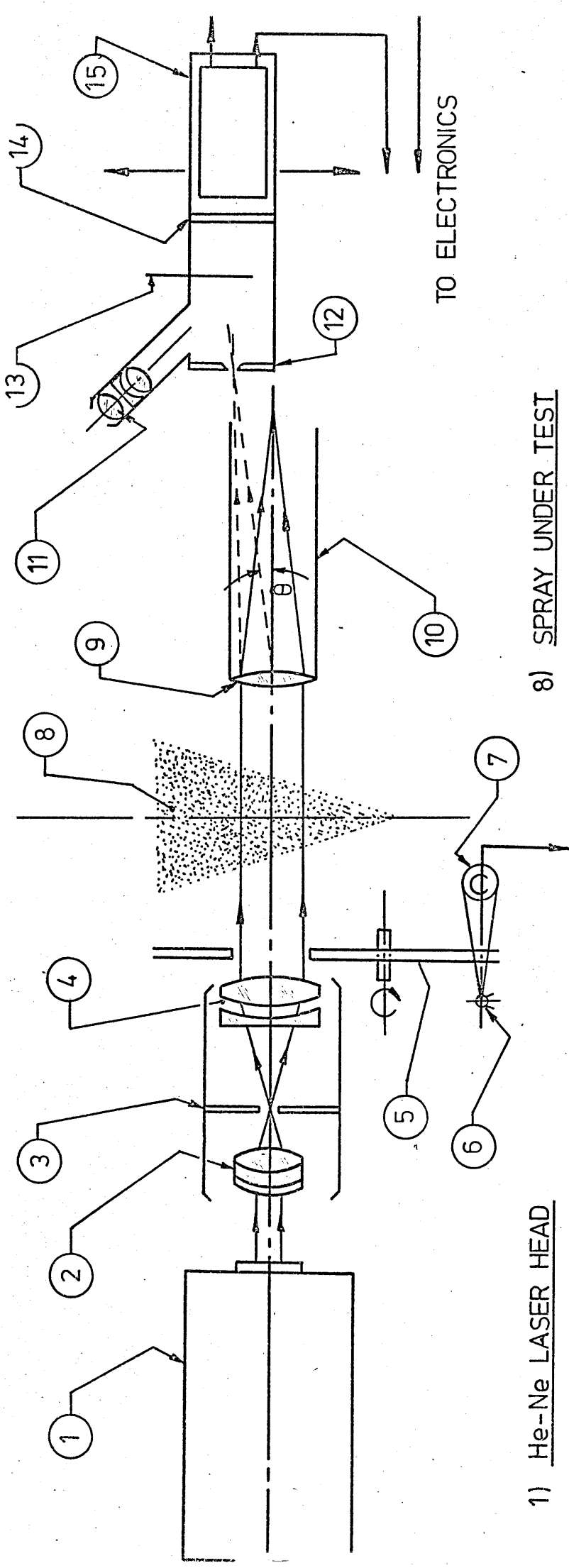


MEAN THEORETICAL ILLUMINATION PROFILE

(Roberts and Webb)

FIG.13





1) He-Ne LASER HEAD

2) CONDENSING LENS

3) SPATIAL FILTER (APERTURE)

4) TELESCOPE - COLLIMATING LENS

5) ROTATING DISC (CHOPPER)

6) SMALL LAMP

7) PHOTO CELL

TO ELECTRONICS

8) SPRAY UNDER TEST

9) RECEIVER LENS (60cm FOCAL LENGTH)

10) STRAY LIGHT SHIELD

11) EYEPIECE

12) PIN-HOLE APERTURE

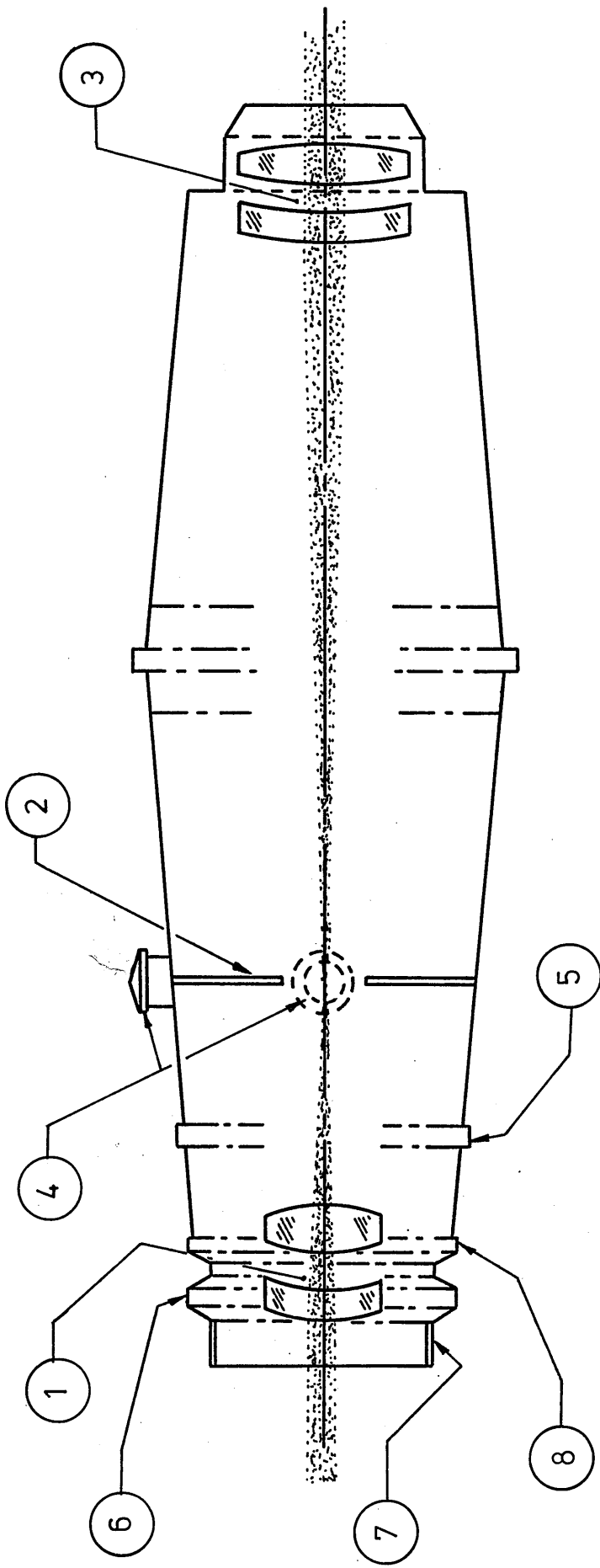
13) SHUTTER

14) NEUTRAL DENSITY FILTER

15) TRAVERSING PHOTOMULTIPLIER

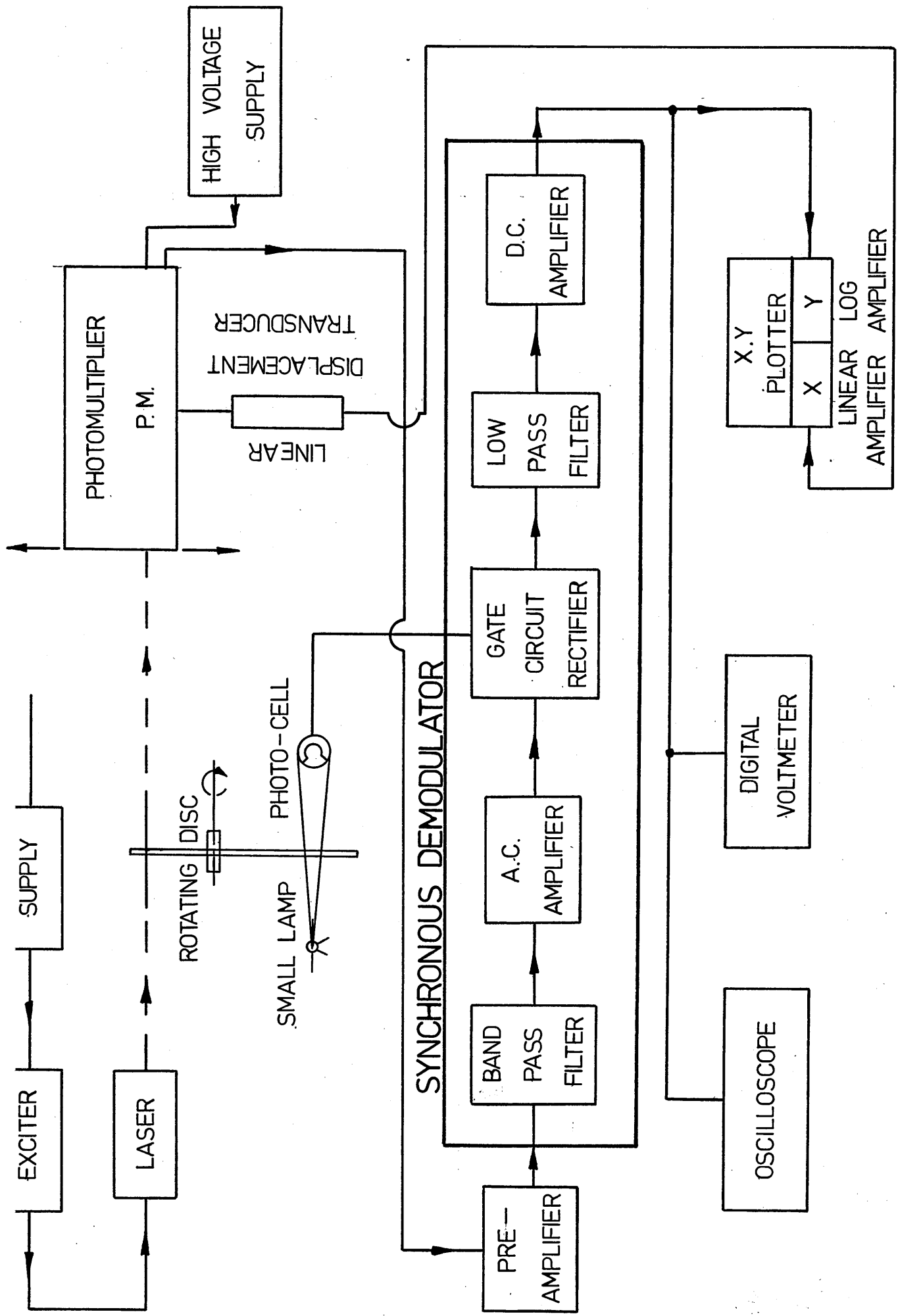
TO ELECTRONICS

THE OPTICAL BENCH IN DIAGRAMATIC FORM



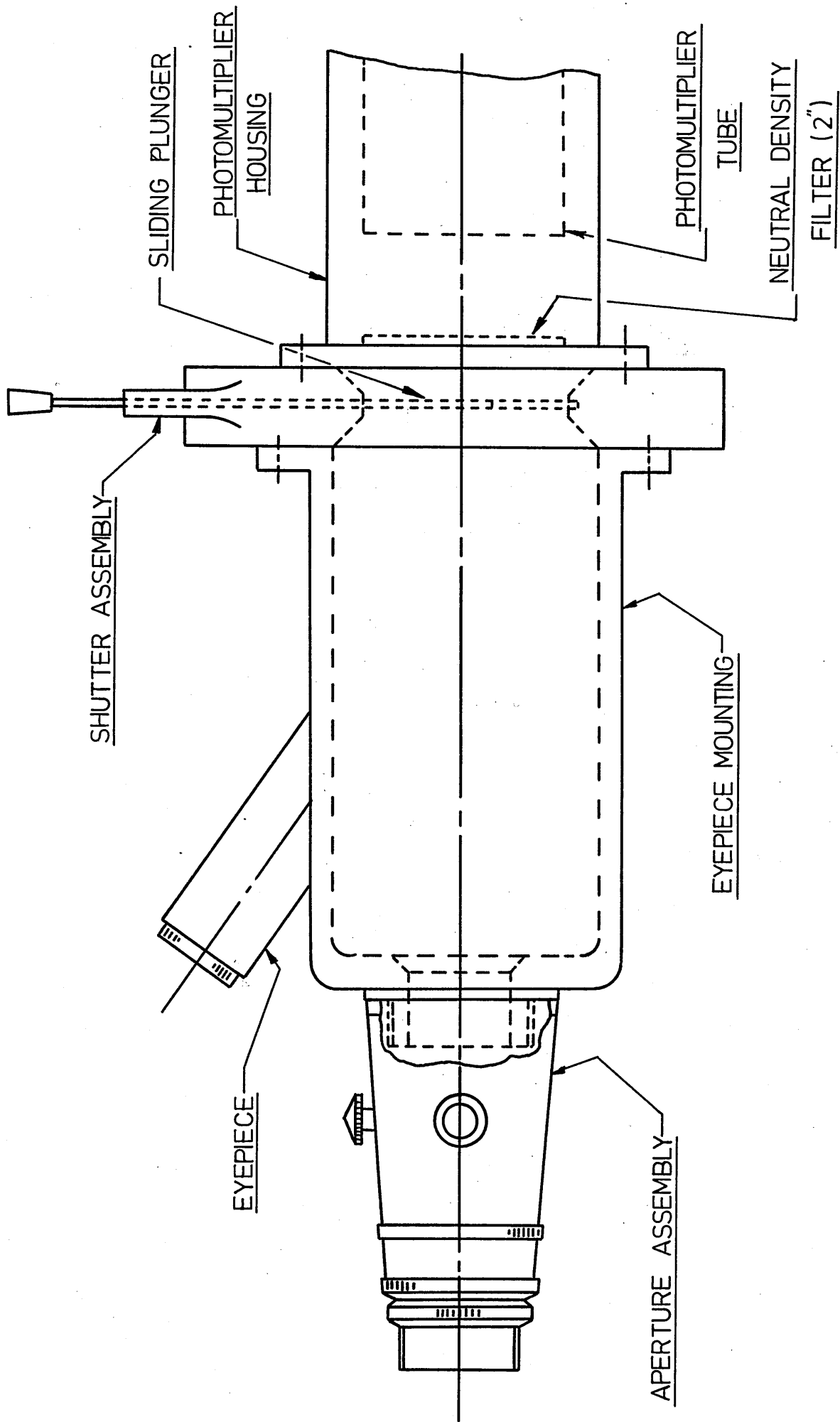
- 1) EXPANDING LENS:- EQUIVALENT FOCAL LENGTH: 12.8mm
- 2) SPATIAL FILTER:- PRECISION PIN HOLE: 22μ
- 3) TELESCOPE COLLIMATING LENS:- EQUIVALENT FOCAL LENGTH 85mm
- 4) APERTURE X&Y MOTION ADJUSTING KNOBS:-
- 5) APERTURE Z MOTION ADJUST RING:-
- 6) ROTATIONAL LOCK RING:-
- 7) 1-32 MOUNTING THREAD:-
- 8) AXIAL ALIGNMENT LOCK RING:-

BEAM EXPANDING AND COLLIMATING TELESCOPE

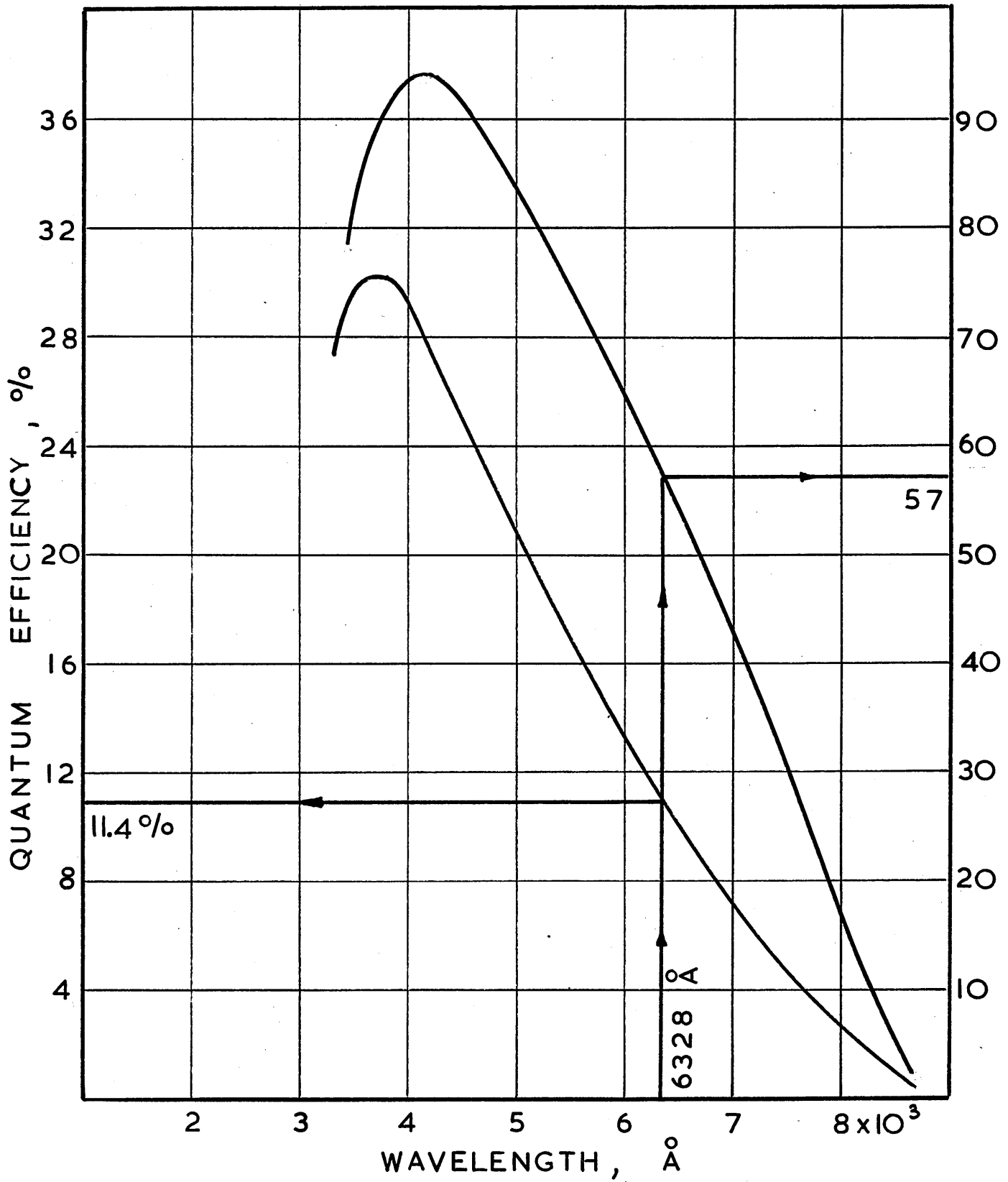


BLOCK DIAGRAM OF LIGHT SCATTERING INSTRUMENTATION

FIG.16



OPTICAL RECEIVING SYSTEM



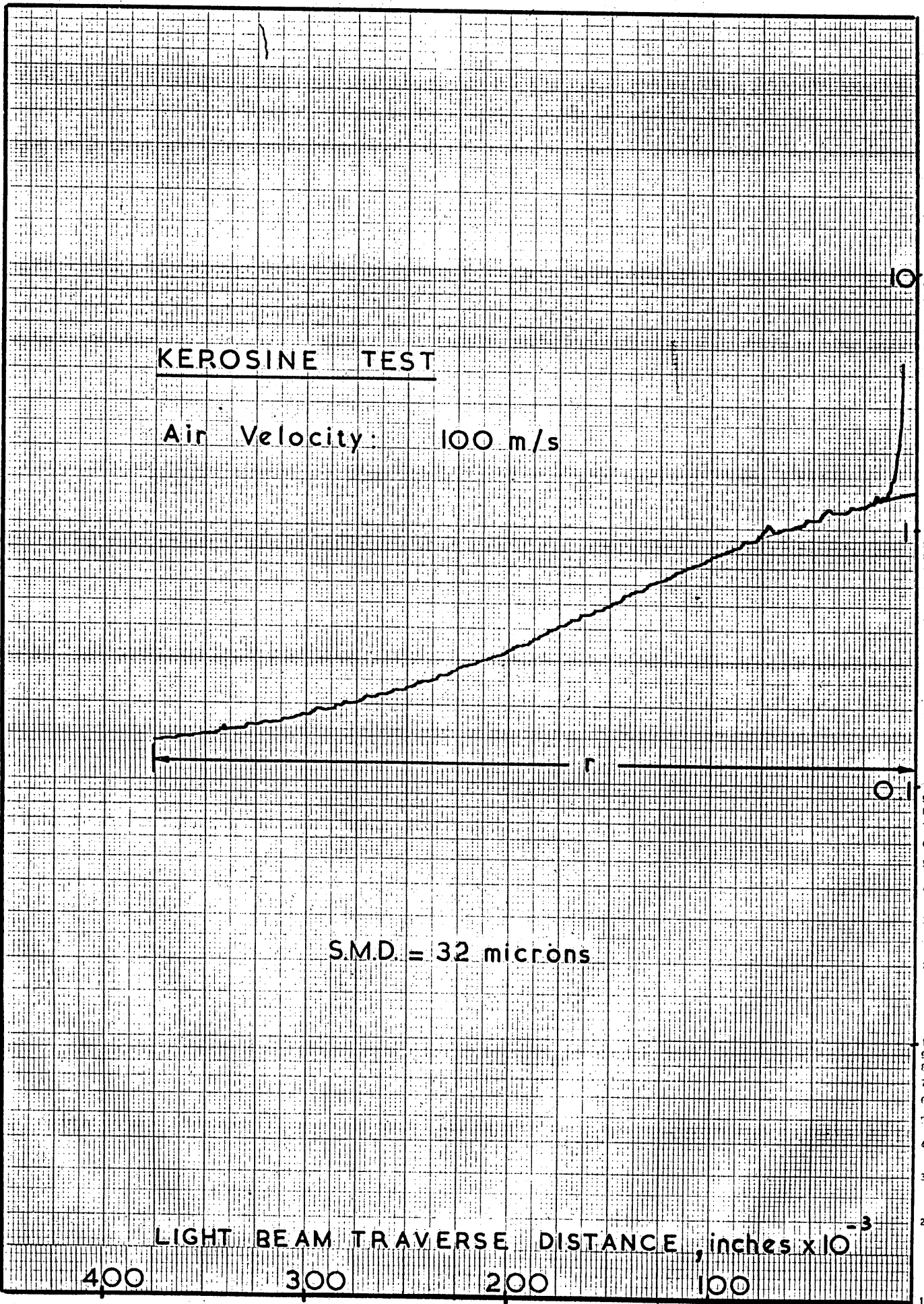
E.M.I. - 9658 MR PHOTOMULTIPLIER

SPECTRAL RESPONSE FIG. 18

X

Log 5 Cycles x mm, $\frac{1}{2}$ and 1 cm

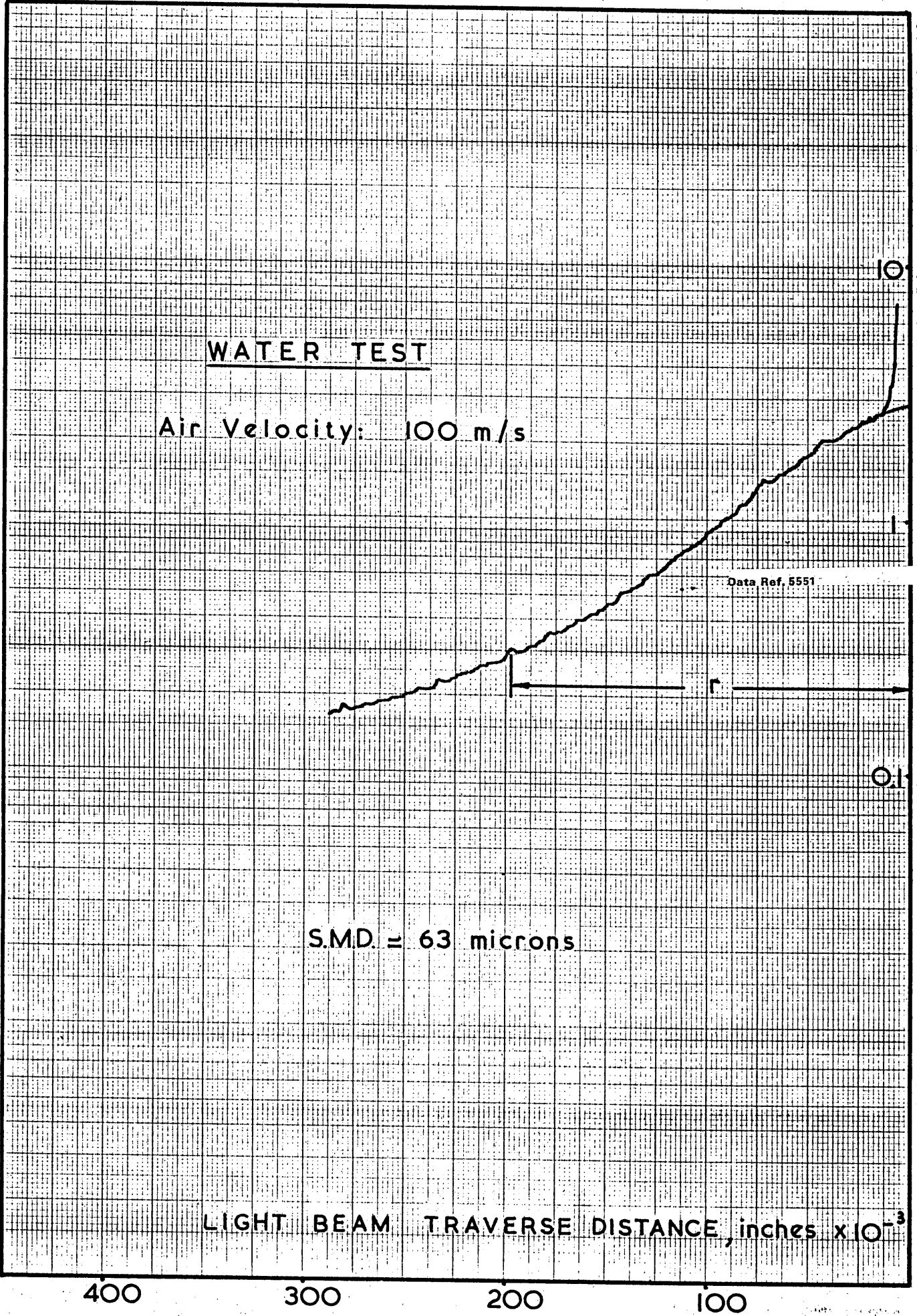
WELL Graph



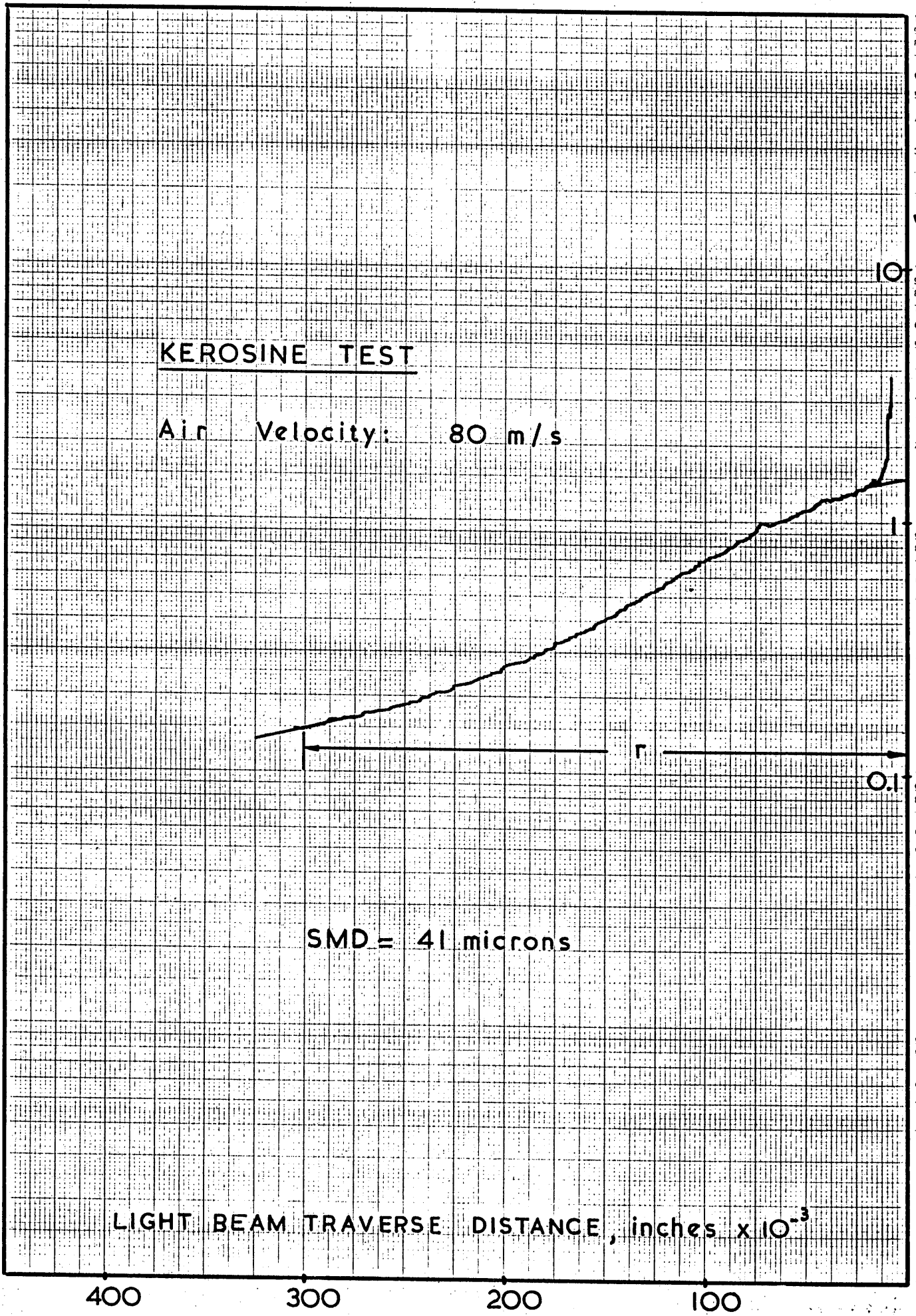
TYPICAL X-Y RECORDER PLOT FIG. 19

Log 5 Cycles. x mm, 1/2 and 1 cm

Graph Data Ref. 5551
WELL

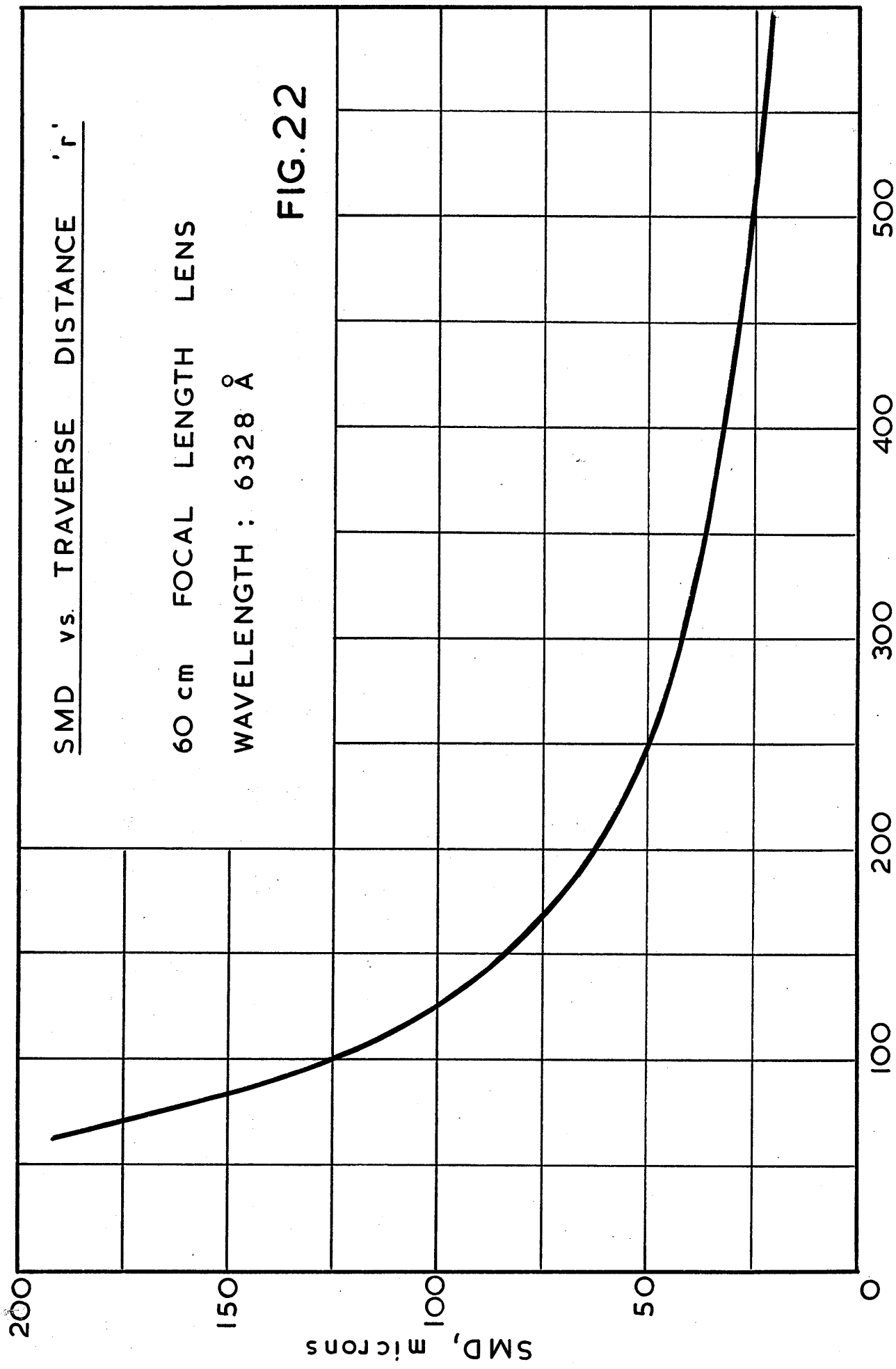


TYPICAL X-Y RECORDER PLOT FIG. 20



TYPICAL X-Y RECORDER PLOT

FIG. 21



TRAVERSE DISTANCE AT $1/10^{\text{th}}$ $I(\theta)$, r , inch $\times 10^{-3}$

X

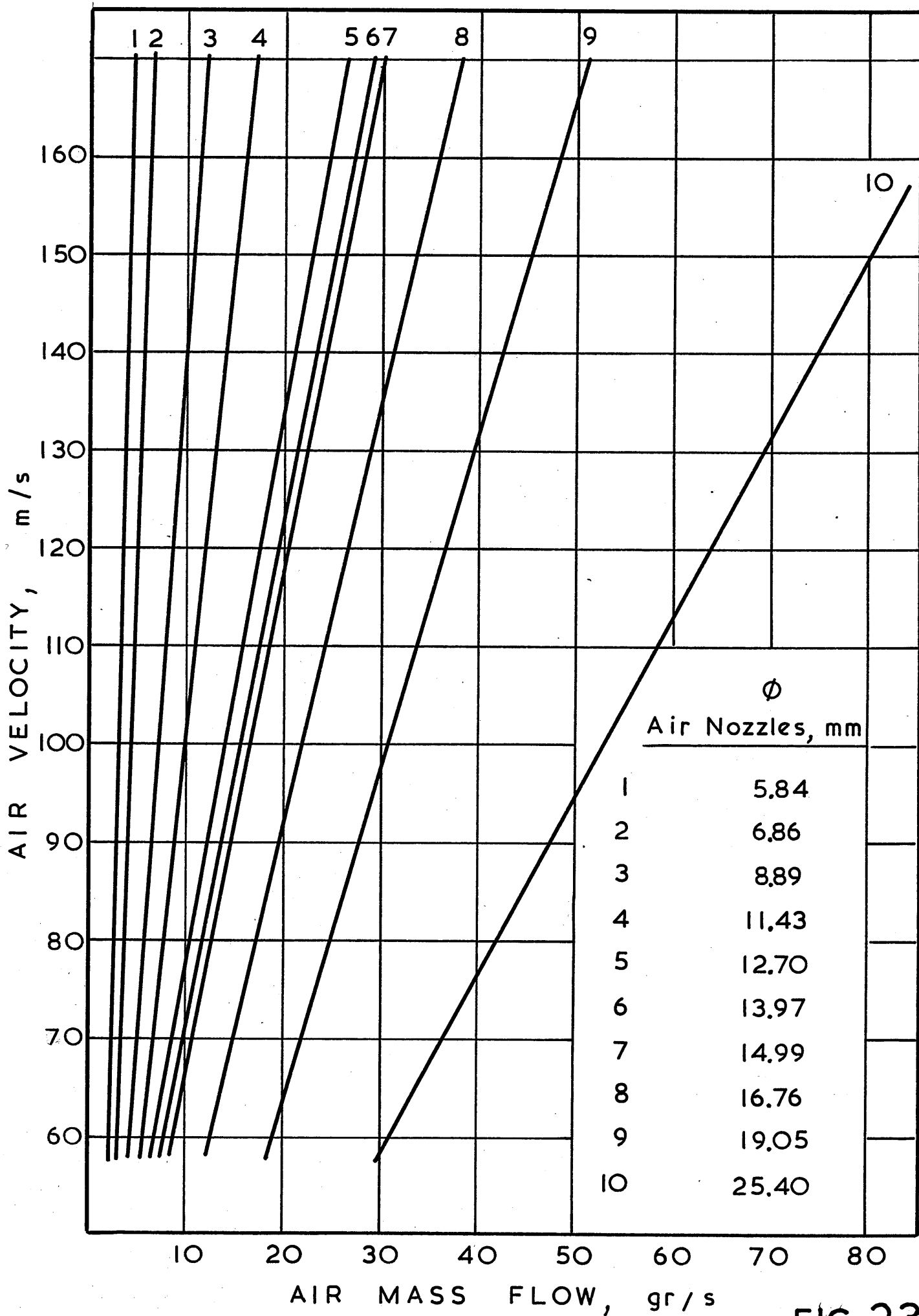
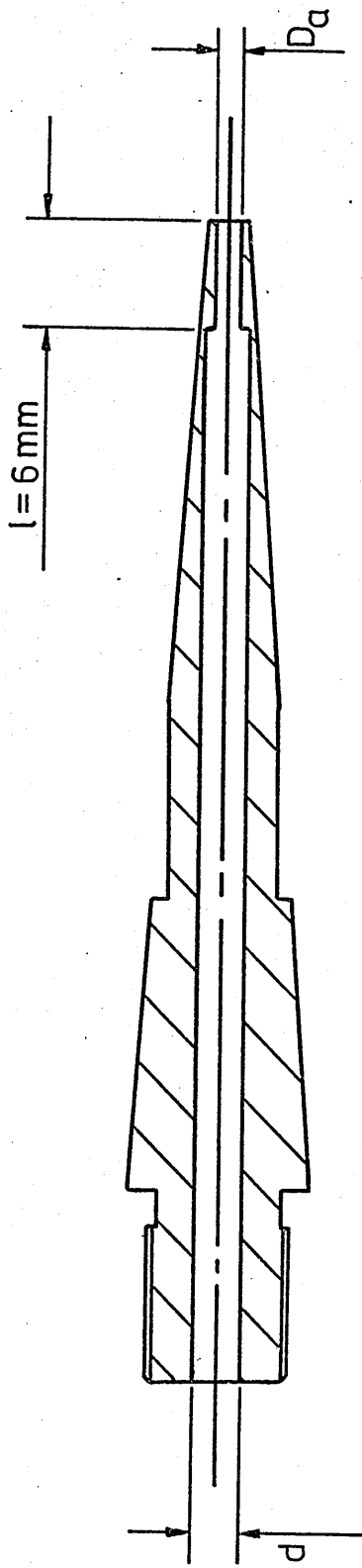


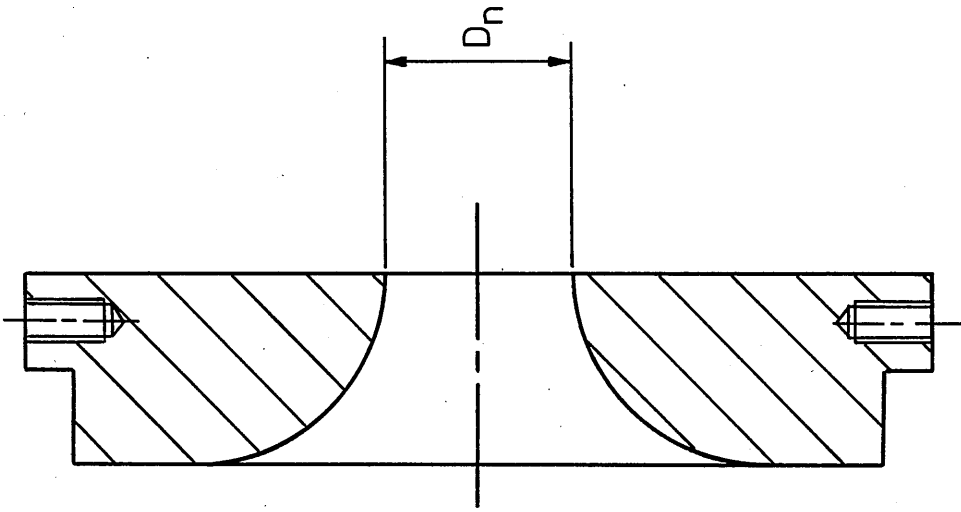
FIG. 23



SCALE 2:1

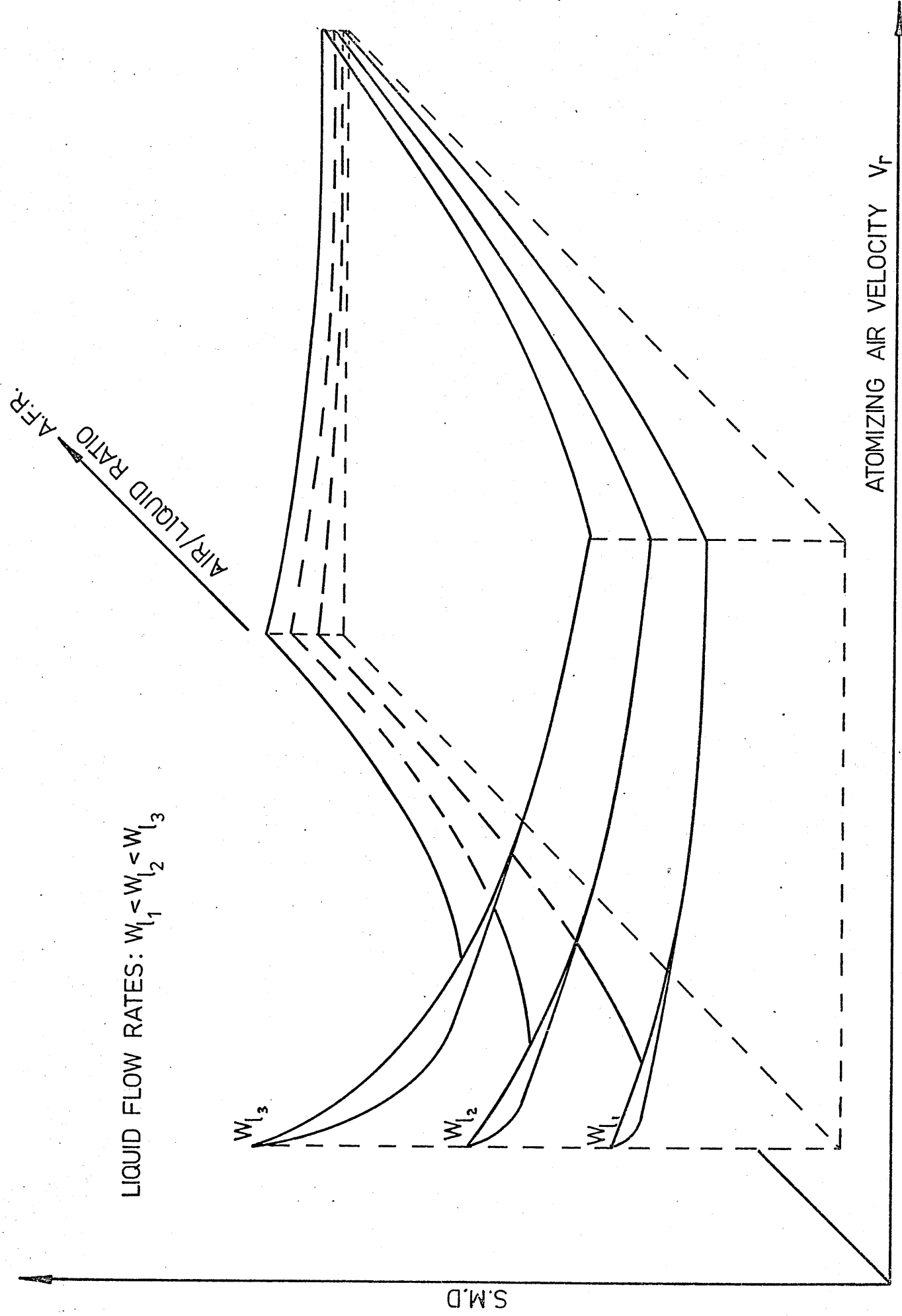
TYPICAL PLAIN JET ATOMIZER

x



SCALE 2:1

TYPICAL CONVERGENT AIR NOZZLE



LIQUID FLOW RATES: $W_{l_1} < W_{l_2} < W_{l_3}$

FIG. 26

3-D IMPRESSION OF "PLAIN-JET" ATOMIZER PERFORMANCE.

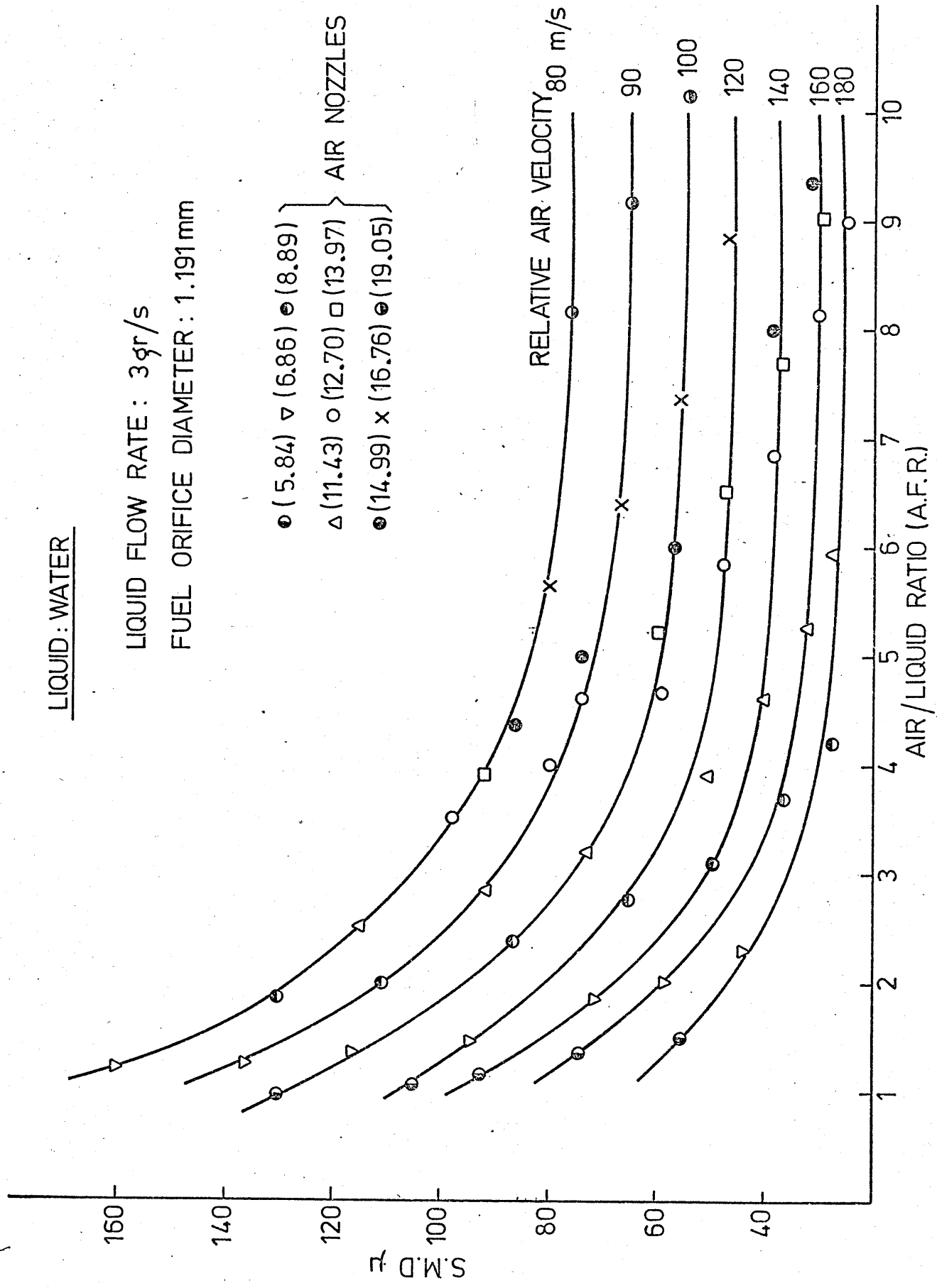
LIQUID: WATER

LIQUID FLOW RATE: 3 gr/s

FUEL ORIFICE DIAMETER: 1.191 mm

● (5.84) ▽ (6.86) ⊙ (8.89)
△ (11.43) ○ (12.70) □ (13.97) } AIR NOZZLES USED, mm
⊙ (14.99) × (16.76) ⊙ (19.05)

RELATIVE AIR VELOCITY 80 m/s



INFLUENCE OF AIR VELOCITY AND AIR / LIQUID RATIO

LIQUID: KEROSENE

LIQUID FLOW RATE: 3 gr/s

FUEL ORIFICE DIAMETER: 1.191 mm

● (5.84) ▽ (6.86) ● (8.89)

▲ (11.43) ○ (12.70) □ (13.97)

● (14.99) × (16.76) ● (19.05)

RELATIVE AIR VELOCITY:
70 m/s

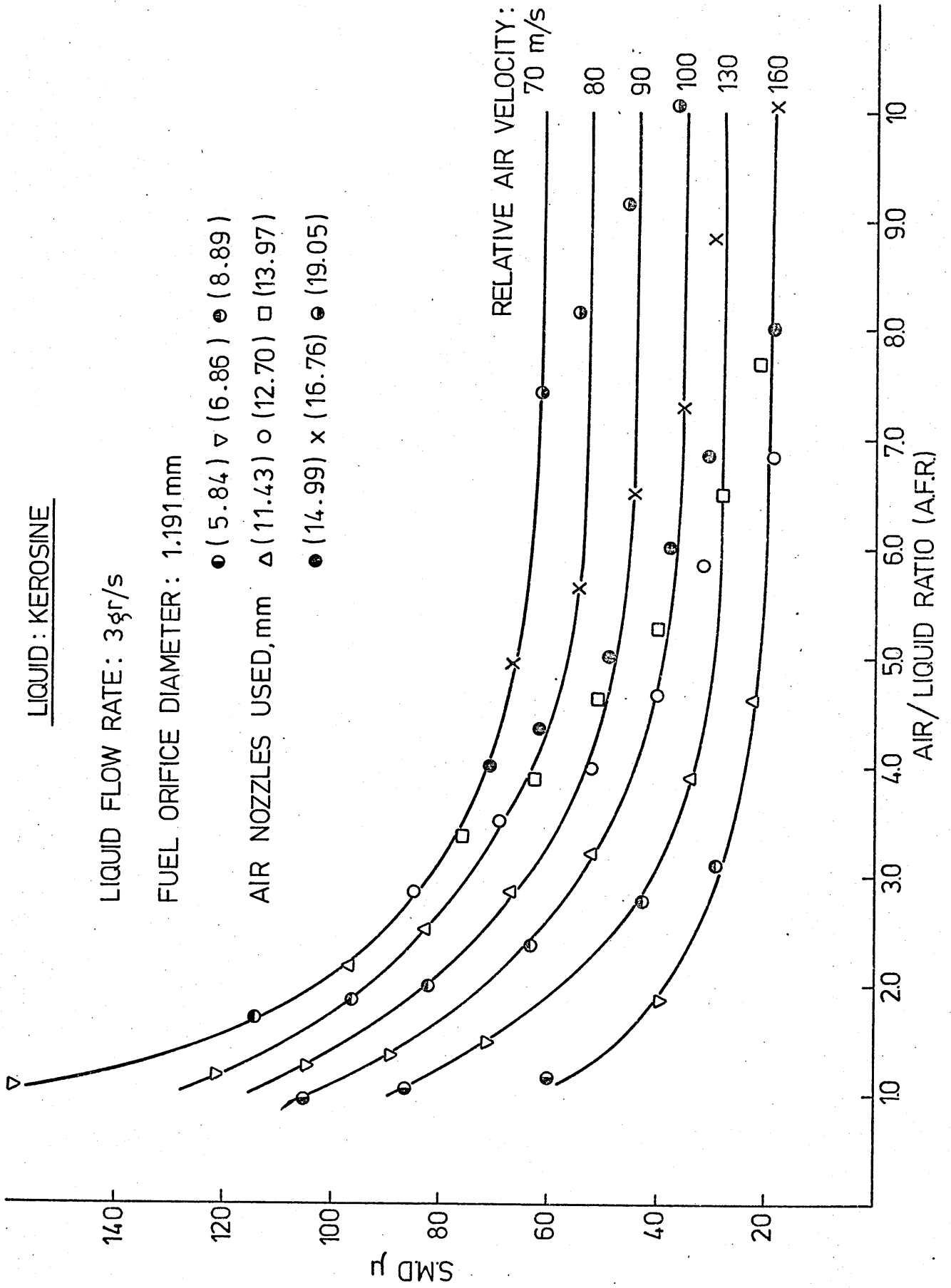
80

90

100

130

160



INFLUENCE OF AIR VELOCITY AND AIR LIQUID RATIO.

LIQUID FLOW RATE: 1.5 gr/s

RELATIVE AIR VELOCITY: 100 m/s

FUEL ORIFICE DIAMETER: 0.794 mm

● (5.84) △ (6.86) ● (8.89)

AIR NOZZLES USED, mm : △ (11.43) ○ (12.70) □ (13.97)

● (14.99) × (16.76) ● (19.05) ◇ (25.40)

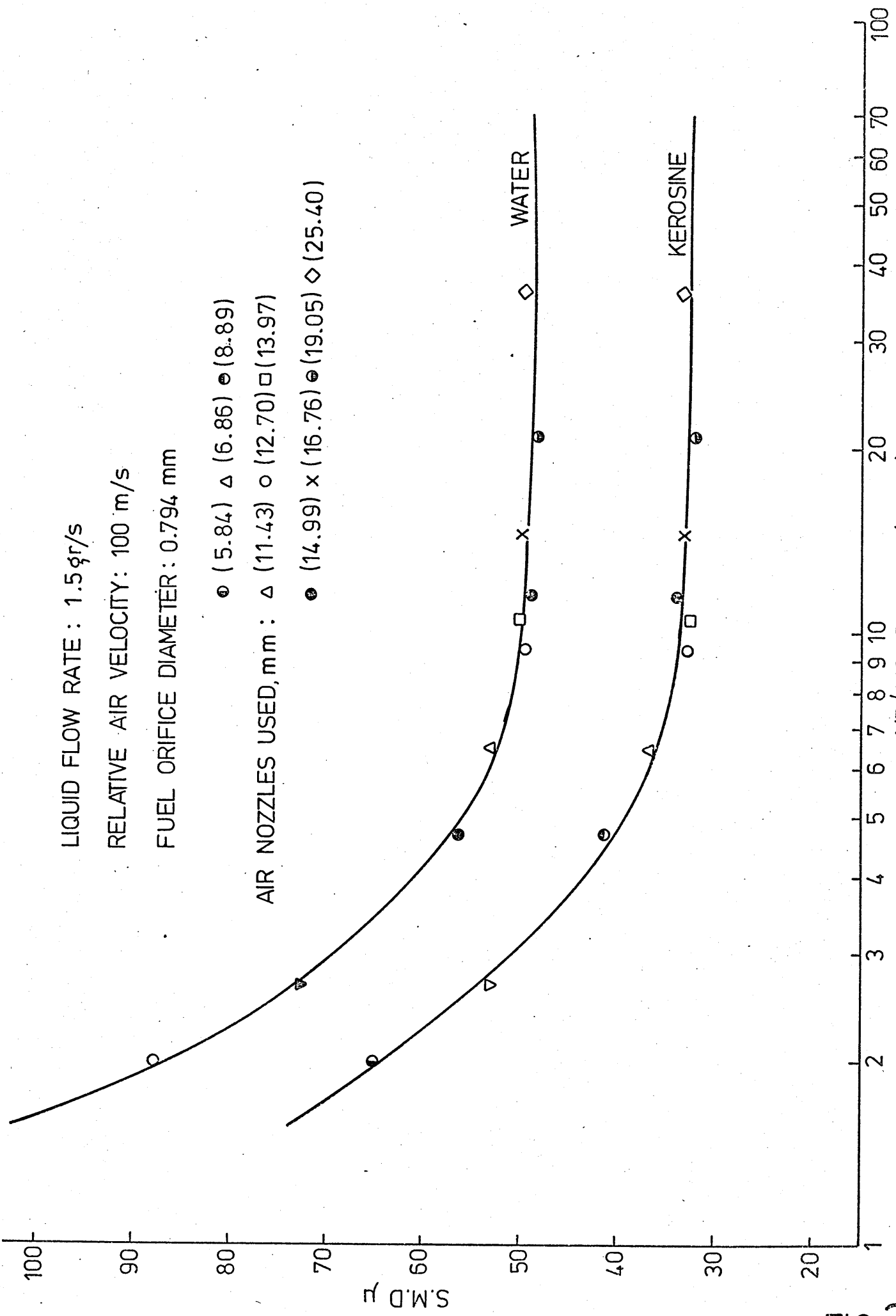


FIG. 29

LIQUID: WATER

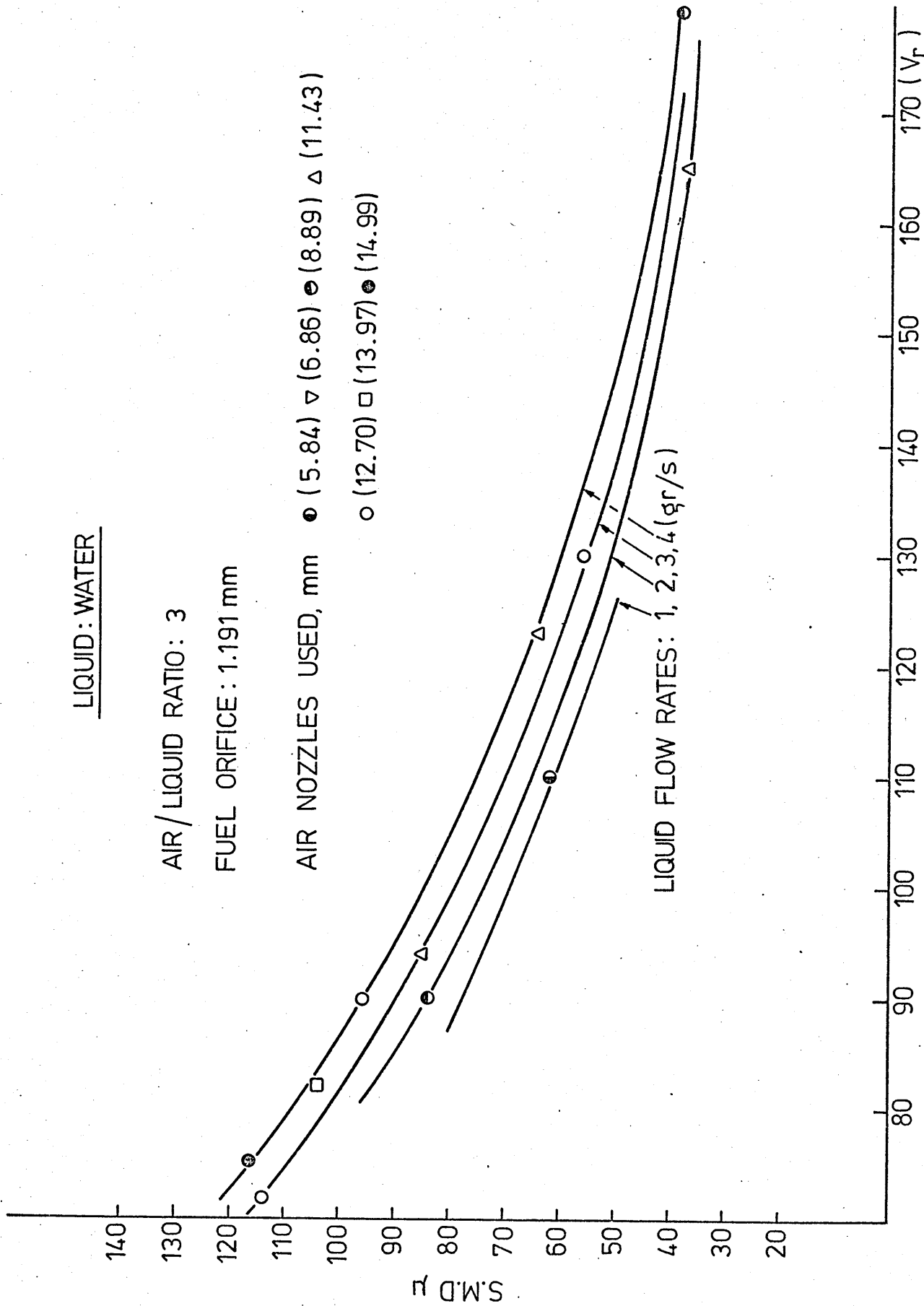
AIR/LIQUID RATIO: 3

FUEL ORIFICE: 1.191 mm

AIR NOZZLES USED, mm ● (5.84) ▽ (6.86) ○ (8.89) △ (11.43)

○ (12.70) □ (13.97) ● (14.99)

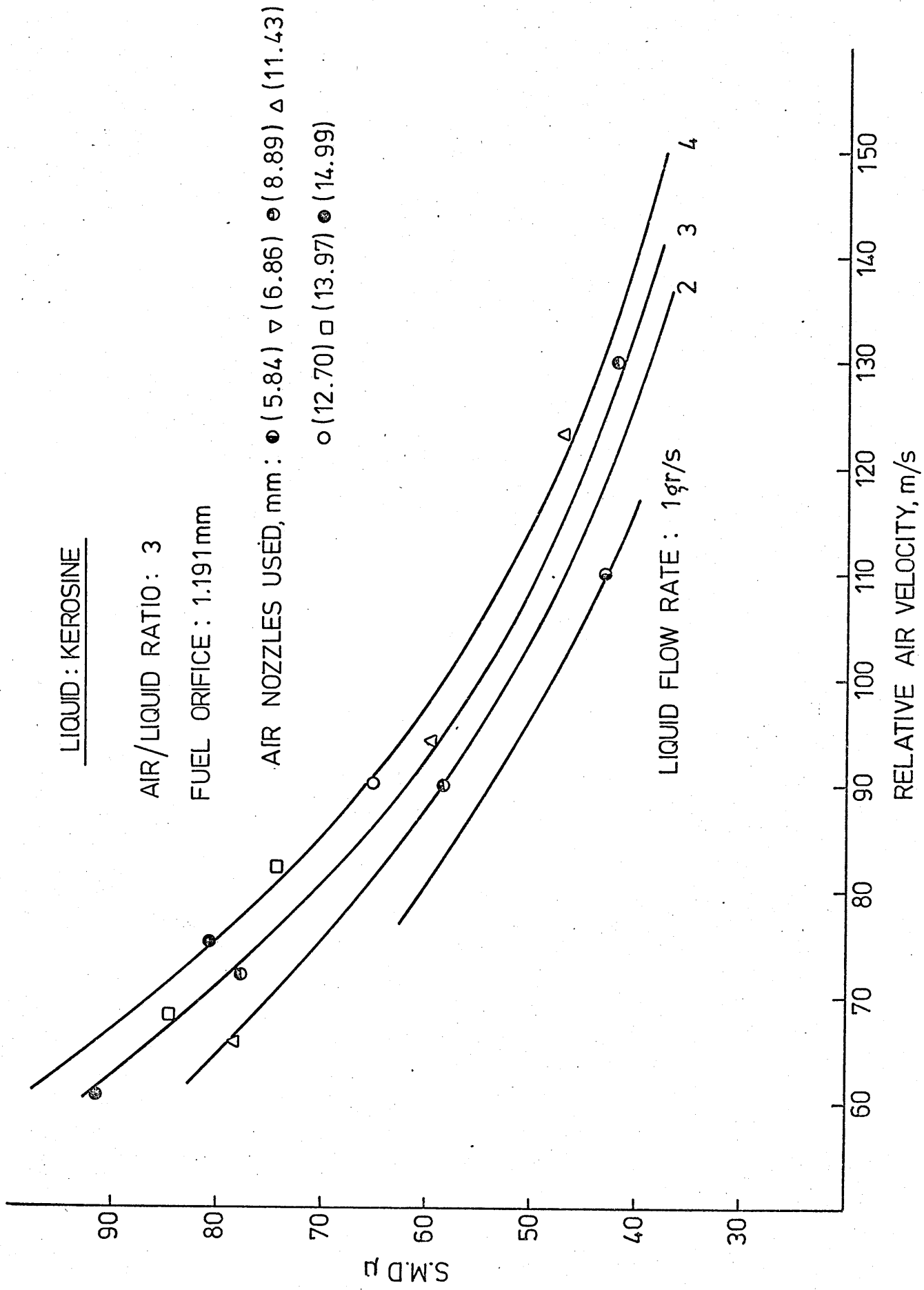
LIQUID FLOW RATES: 1, 2, 3, 4 (gr/s)



RELATIVE AIR VELOCITY, m/s

INFLUENCE OF AIR VELOCITY ALONE.

FIG. 30



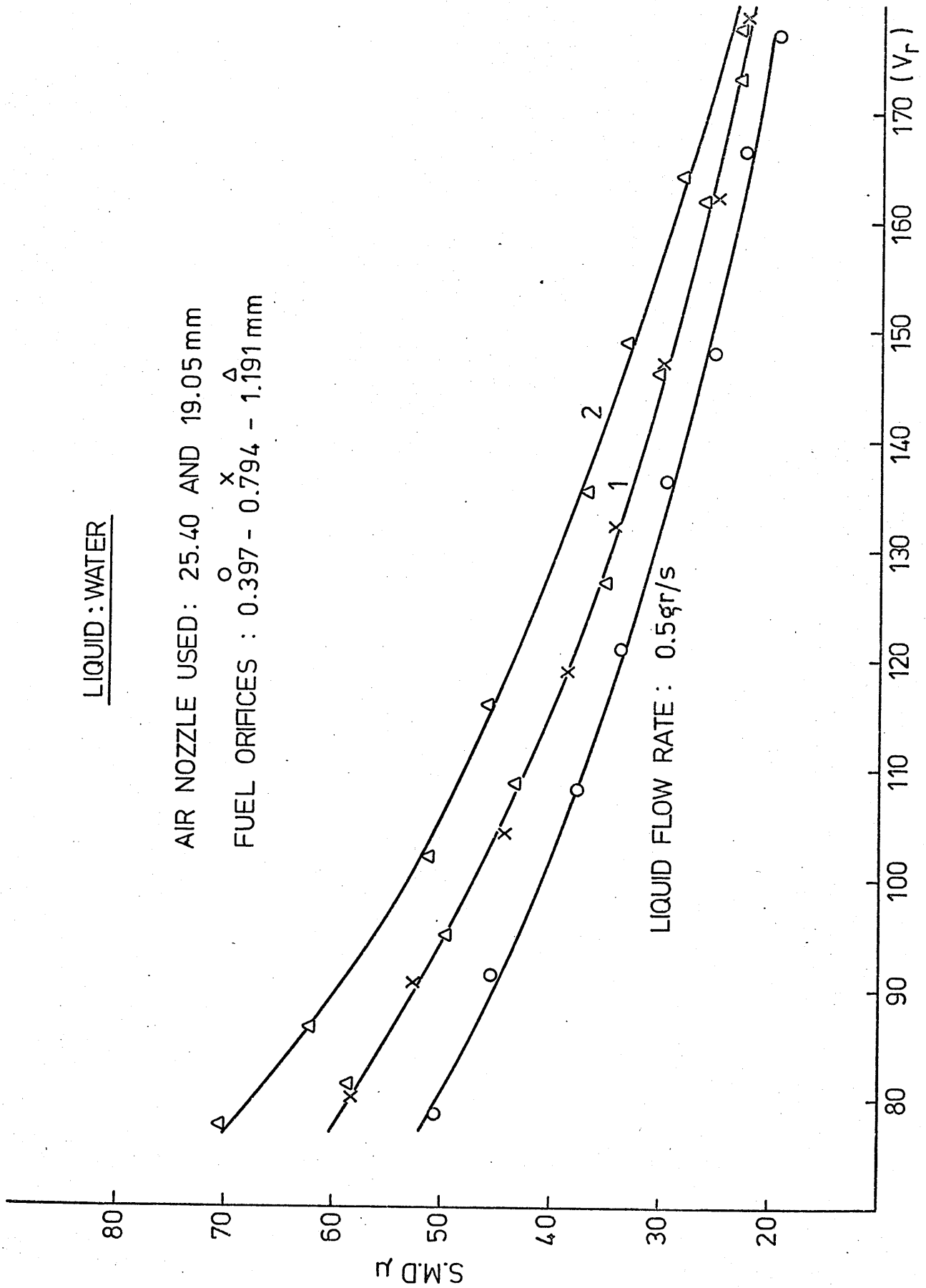
INFLUENCE OF AIR VELOCITY ALONE.

FIG.31

LIQUID : WATER

AIR NOZZLE USED: 25.40 AND 19.05 mm

FUEL ORIFICES : \circ 0.397 - \times 0.794 - Δ 1.191 mm



RELATIVE AIR VELOCITY, m/s

INFLUENCE OF AIR VELOCITY FOR LARGE A.F.R.

FIG. 32

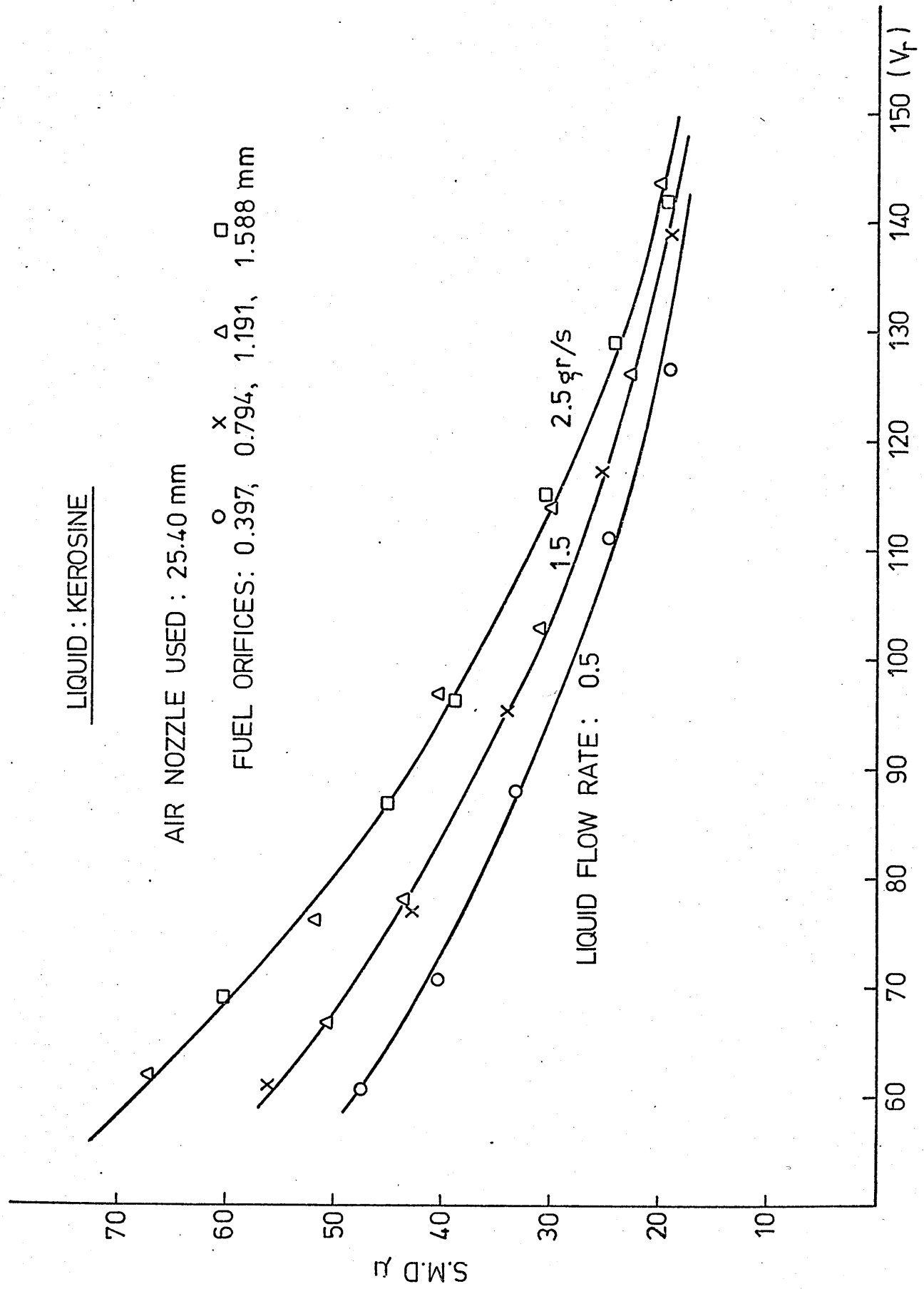
LIQUID : KEROSENE

AIR NOZZLE USED : 25.40 mm

FUEL ORIFICES: 0.397, 0.794, 1.191, 1.588 mm

LIQUID FLOW RATE: 0.5

1.5 2.5 gr/s



AIR VELOCITY, m/s

INFLUENCE OF AIR VELOCITY AT LARGE A.F.R.

FIG. 33

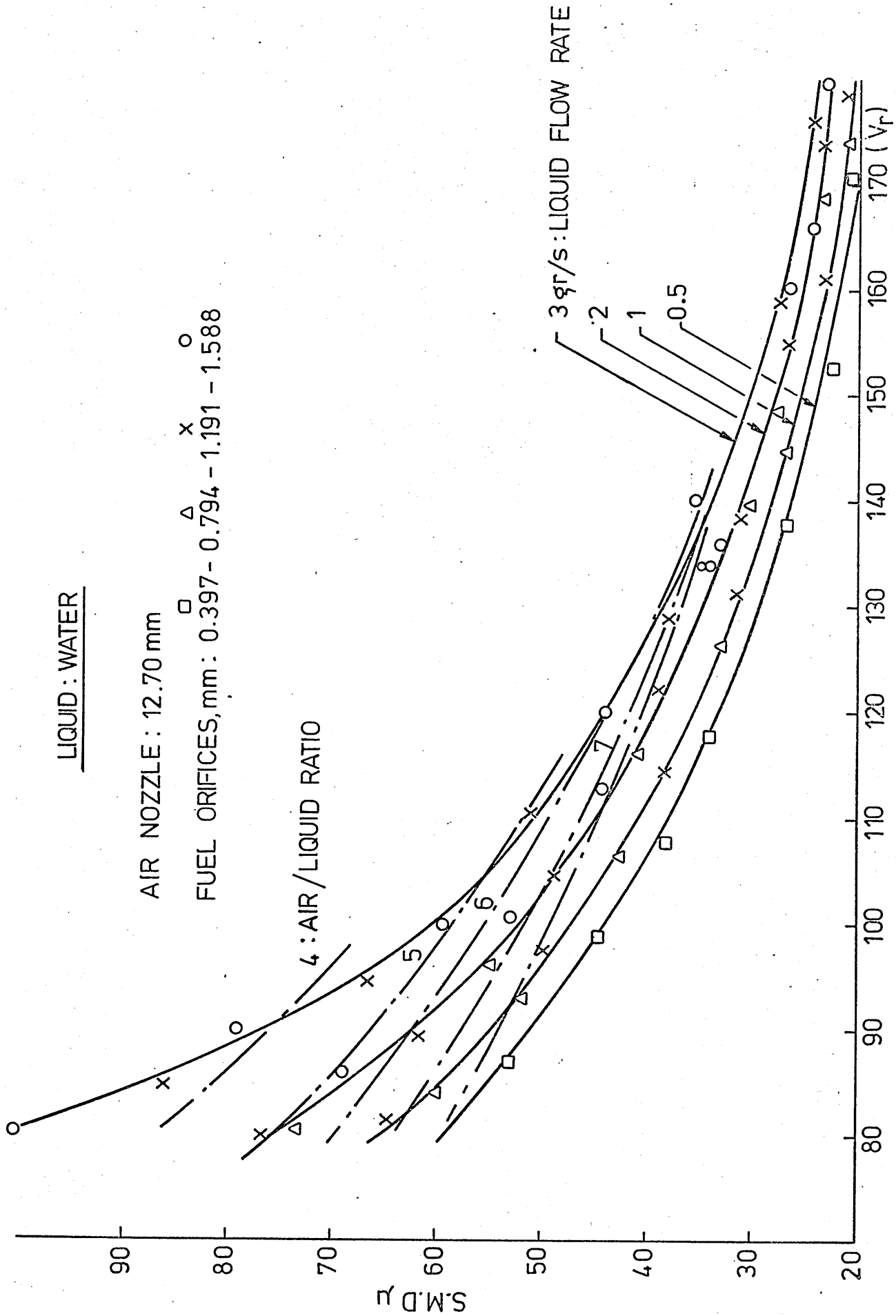
LIQUID : WATER

AIR NOZZLE : 12.70 mm

FUEL ORIFICES, mm : \square 0.397 - 0.794 - 1.191 - 1.588

4 : AIR/LIQUID RATIO

3 \dot{q} / s : LIQUID FLOW RATE



RELATIVE AIR VELOCITY, m/s
INFLUENCE OF AIR VELOCITY.

FIG. 34

LIQUID : KEROSENE

AIR NOZZLE : 12.70 mm

FUEL ORIFICES, mm 0.397 - 0.794 - 1.191

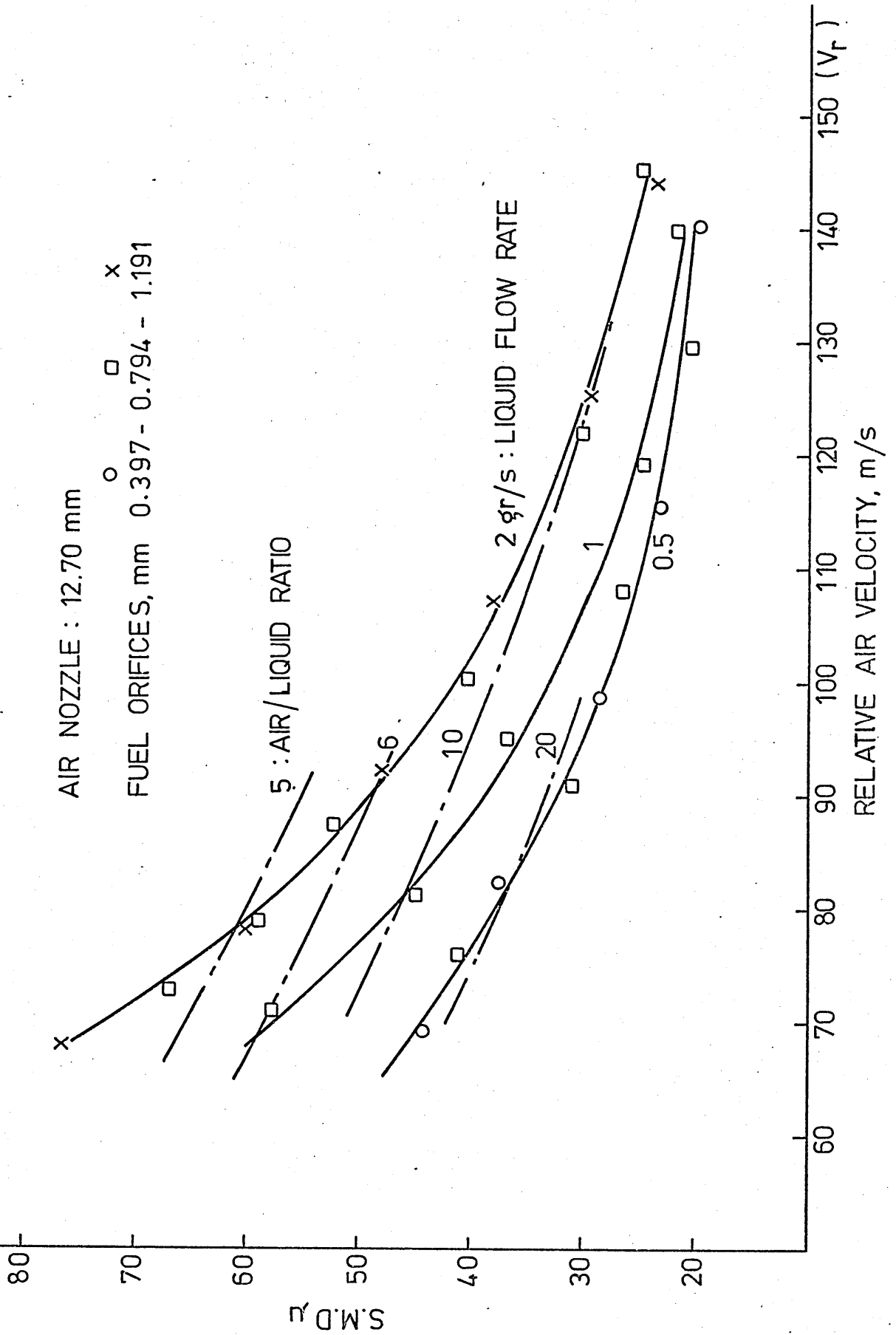


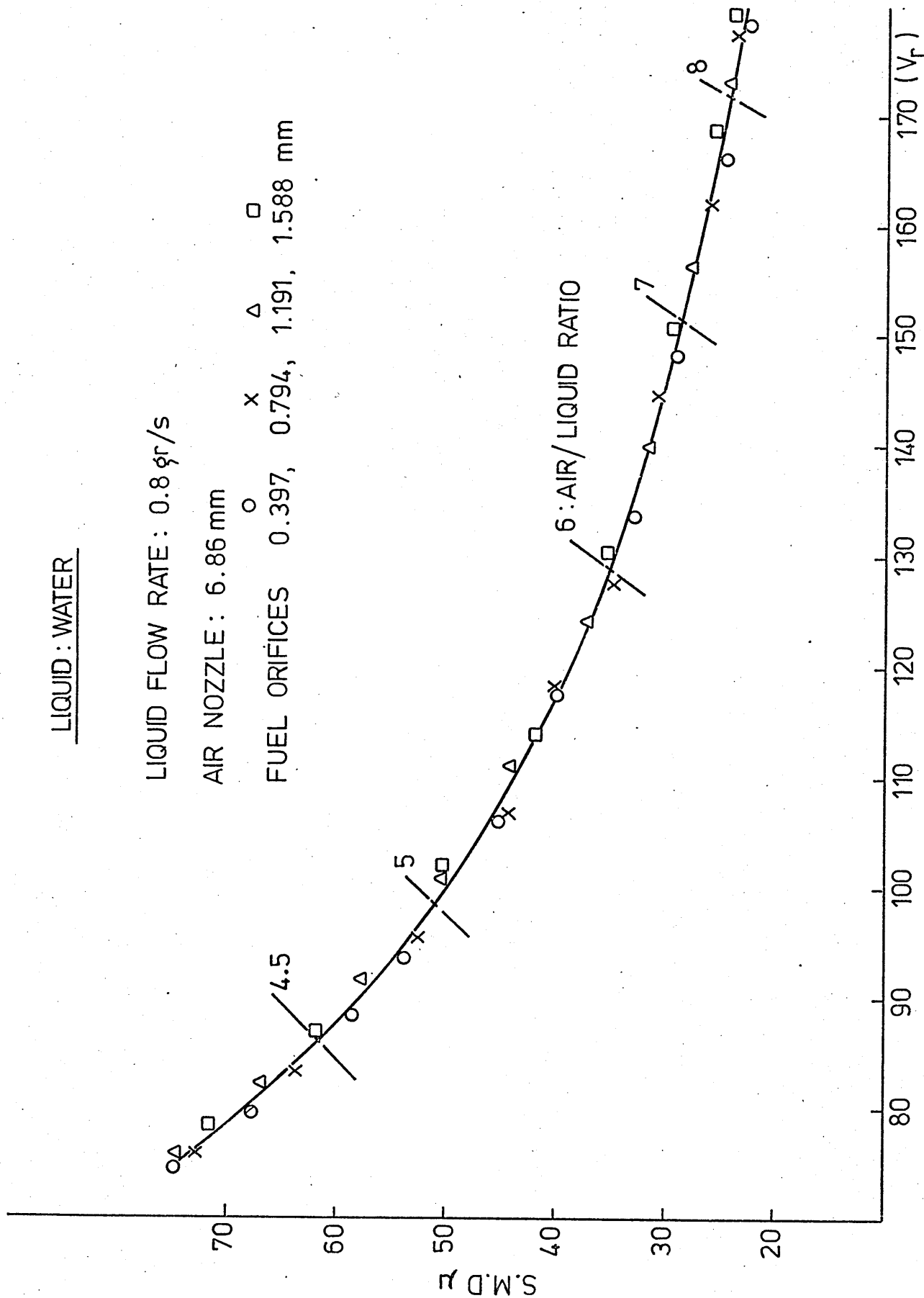
FIG. 35

LIQUID : WATER

LIQUID FLOW RATE: 0.8 gr/s

AIR NOZZLE: 6.86 mm

FUEL ORIFICES 0.397, 0.794, 1.191, 1.588 mm



RELATIVE AIR VELOCITY, m/s

INFLUENCE OF FUEL ORIFICE DIAMETER.

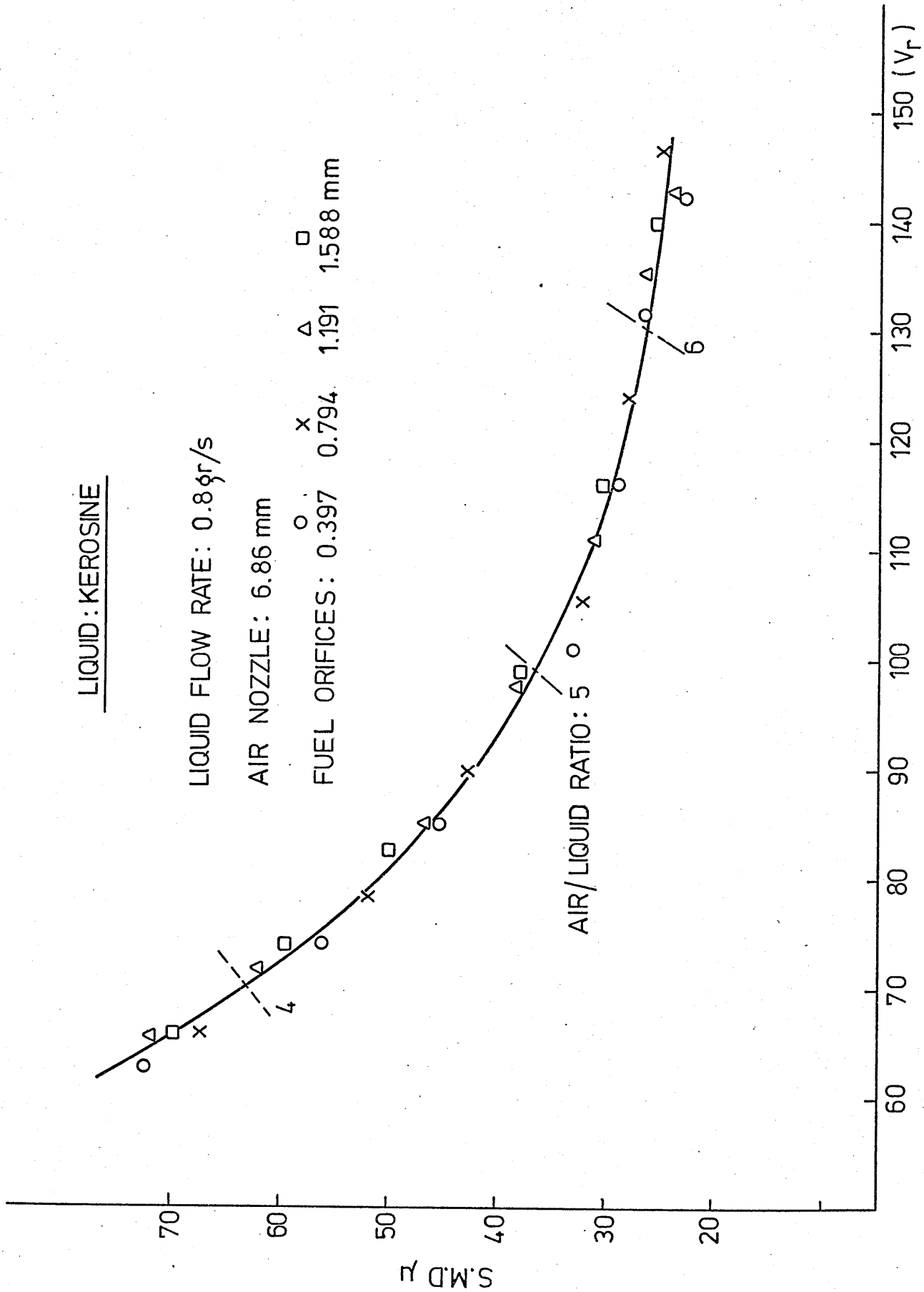
FIG. 36

LIQUID: KEROSENE

LIQUID FLOW RATE: 0.8 gr/s

AIR NOZZLE: 6.86 mm

FUEL ORIFICES: 0.397 mm 0.794 mm 1.191 mm 1.588 mm



RELATIVE AIR VELOCITY, m/s

INFLUENCE OF FUEL ORIFICE DIAMETER.

FIG. 37

HIGH VISCOSITY LIQUID

AIR NOZZLE: 6.86 mm

RELATIVE AIR VELOCITY: 100 m/s

VISCOSITY: 36×10^{-3} Kg/ms

1 gr/s

0.5 gr/s

LIQUID FLOW RATE

(4.2)

(8.4) : AIR / LIQUID RATIO

120

100

S.M.D. μ

80

60

40

0.2

0.4

0.6

0.8

1.0

1.2

1.4

1.6

1.8 (D)

FUEL ORIFICE DIAMETERS, mm

FUEL ORIFICE SCALE EFFECT AT HIGH VISCOSITY.

LIQUID: WATER

RELATIVE AIR VELOCITY: 100 m/s

AIR NOZZLES USED, mm

● (5.84) ▽ (6.86) ⊙ (8.89)

△ (11.43) ○ (12.70) □ (13.97)

⊛ (14.99) × (16.76) ⊙ (19.05)

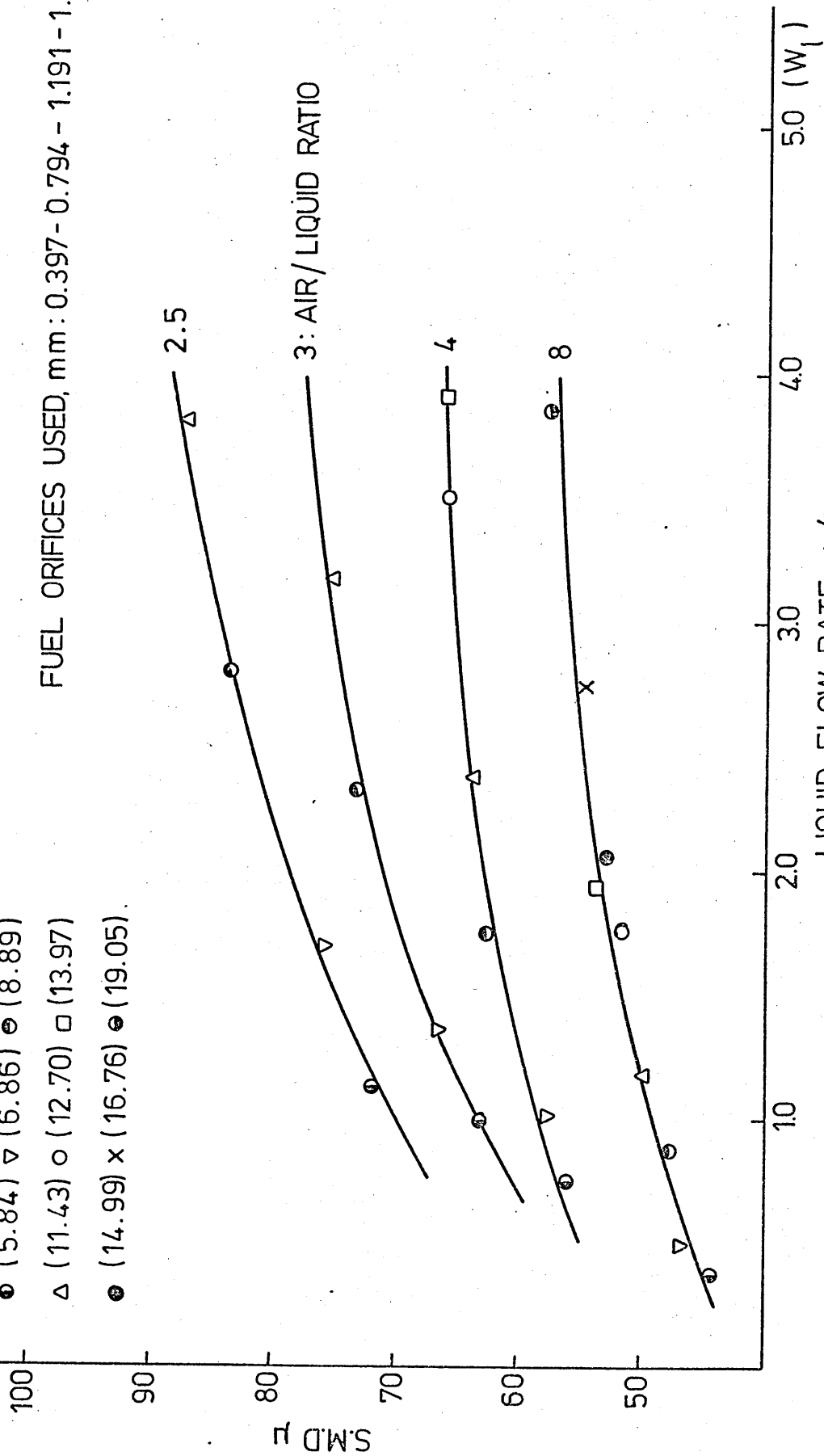
FUEL ORIFICES USED, mm: 0.397 - 0.794 - 1.191 - 1.588

2.5

3: AIR/LIQUID RATIO

4

8



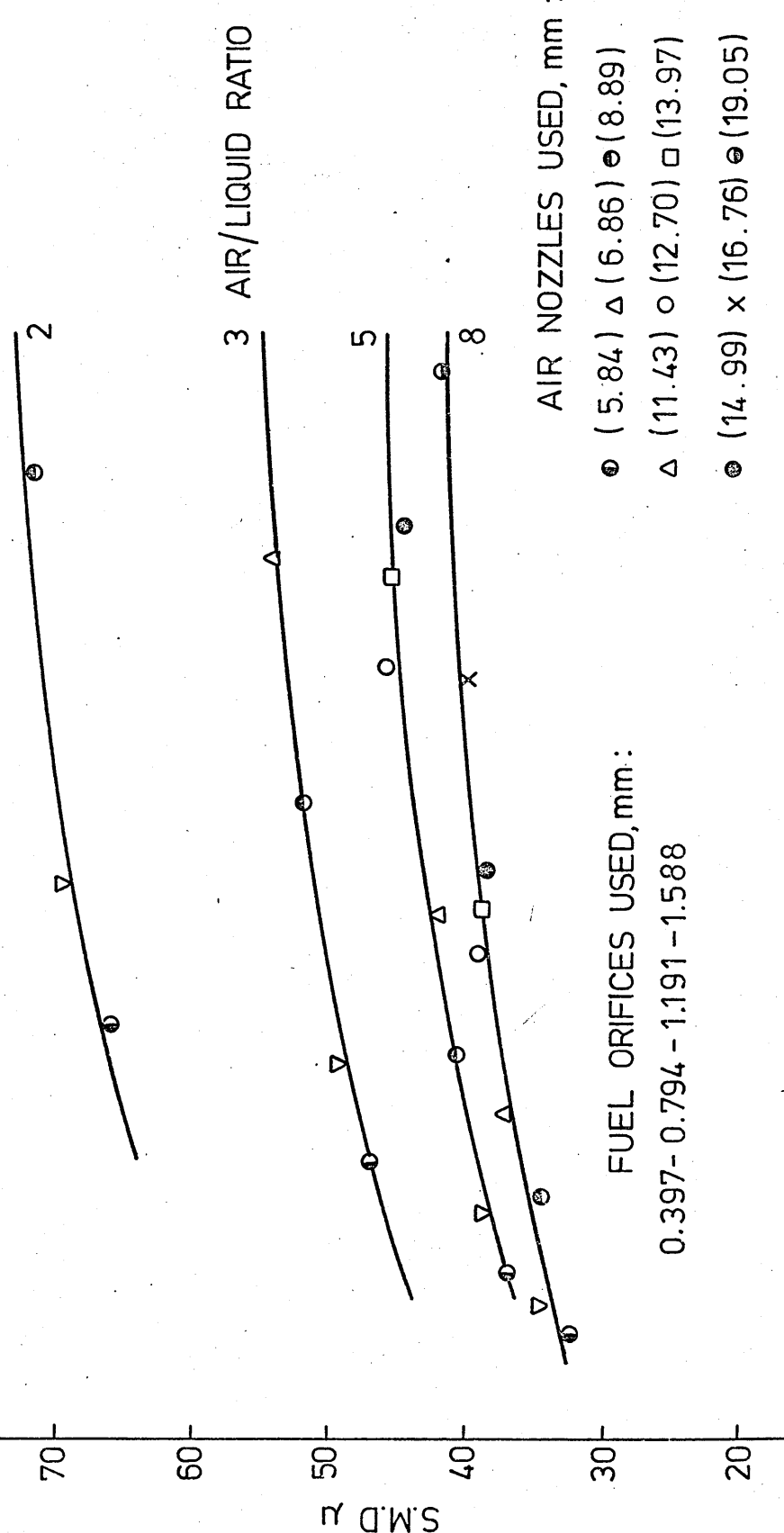
LIQUID FLOW RATE, gr/s

INFLUENCE OF LIQUID FLOW RATE.

FIG. 39

LIQUID : KEROSENE

RELATIVE AIR VELOCITY: 100 m/s



FUEL ORIFICES USED, mm :
 $0.397 - 0.794 - 1.191 - 1.588$

AIR NOZZLES USED, mm :
 ● (5.84) △ (6.86) ○ (8.89)
 △ (11.43) ○ (12.70) □ (13.97)
 ● (14.99) × (16.76) ○ (19.05)

LIQUID FLOW RATE, g/s
 1.0 2.0 3.0 4.0 5.0 (w_l)

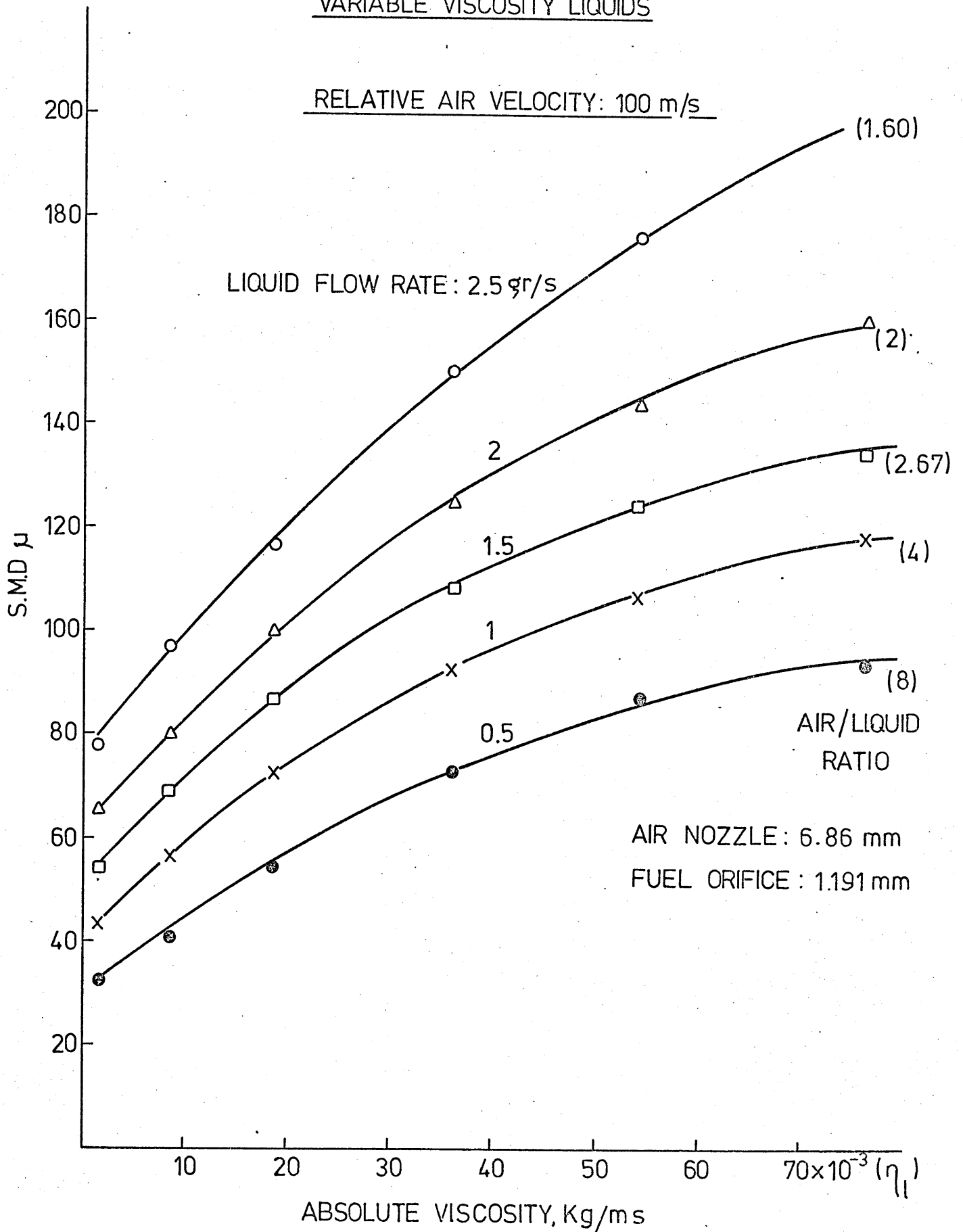
INFLUENCE OF LIQUID FLOW RATE.

FIG. 40

VARIABLE VISCOSITY LIQUIDS

RELATIVE AIR VELOCITY: 100 m/s

LIQUID FLOW RATE: 2.5 gr/s



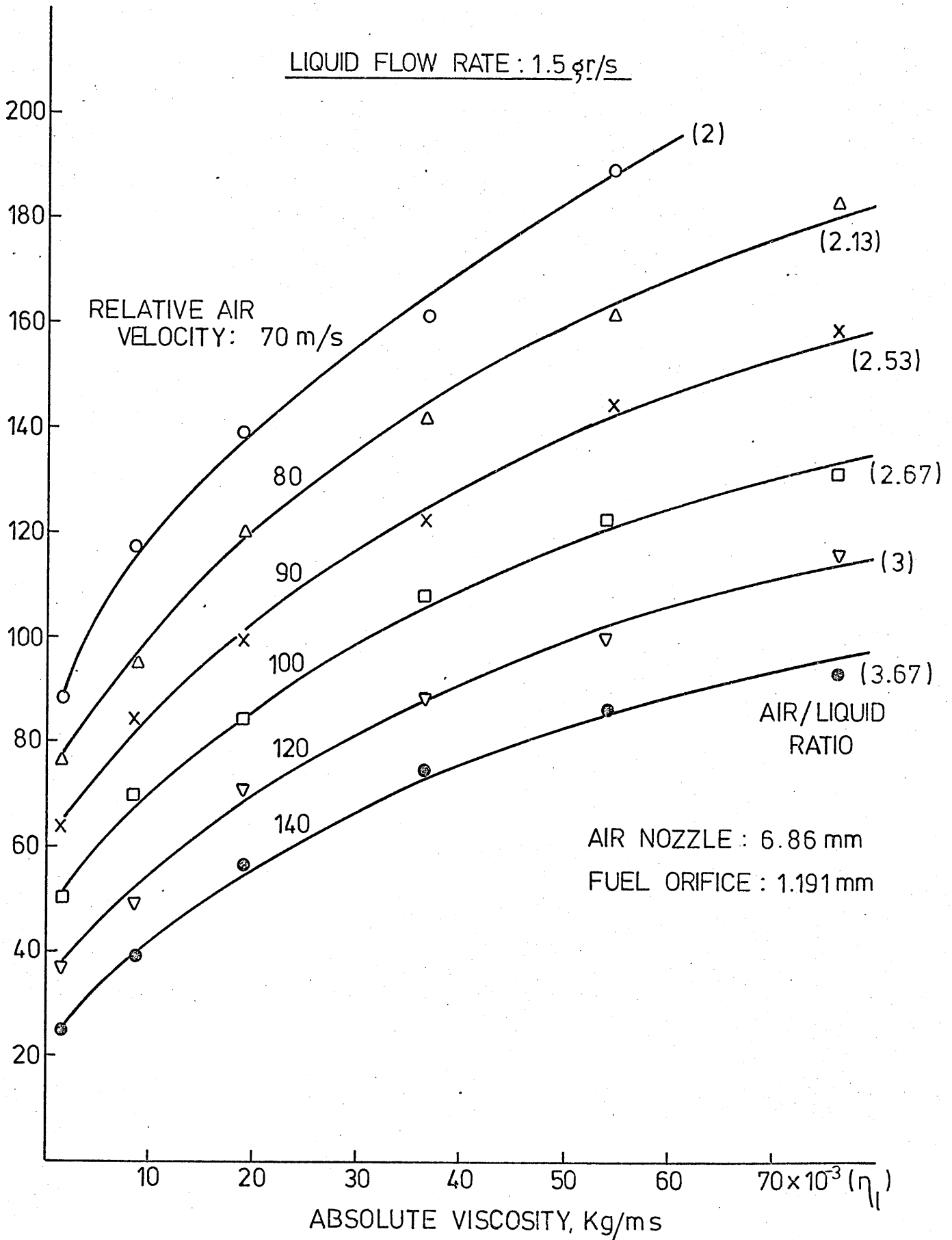
AIR NOZZLE: 6.86 mm
FUEL ORIFICE: 1.191 mm

INFLUENCE OF LIQUID VISCOSITY.

FIG. 41

VARIABLE VISCOSITY LIQUIDS

LIQUID FLOW RATE : 1.5 gr/s



INFLUENCE OF LIQUID VISCOSITY.

FIG. 42

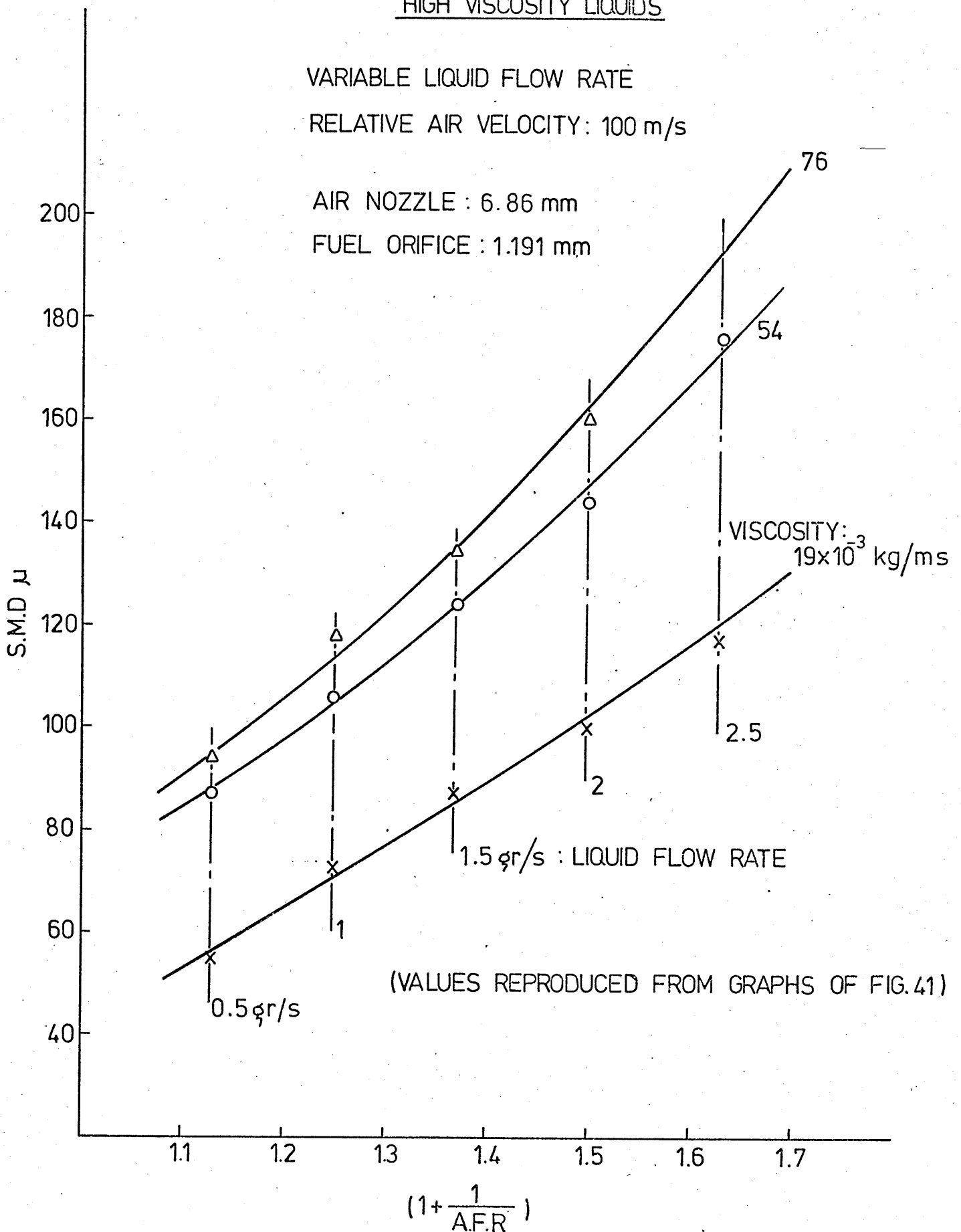
HIGH VISCOSITY LIQUIDS

VARIABLE LIQUID FLOW RATE

RELATIVE AIR VELOCITY: 100 m/s

AIR NOZZLE : 6.86 mm

FUEL ORIFICE : 1.191 mm



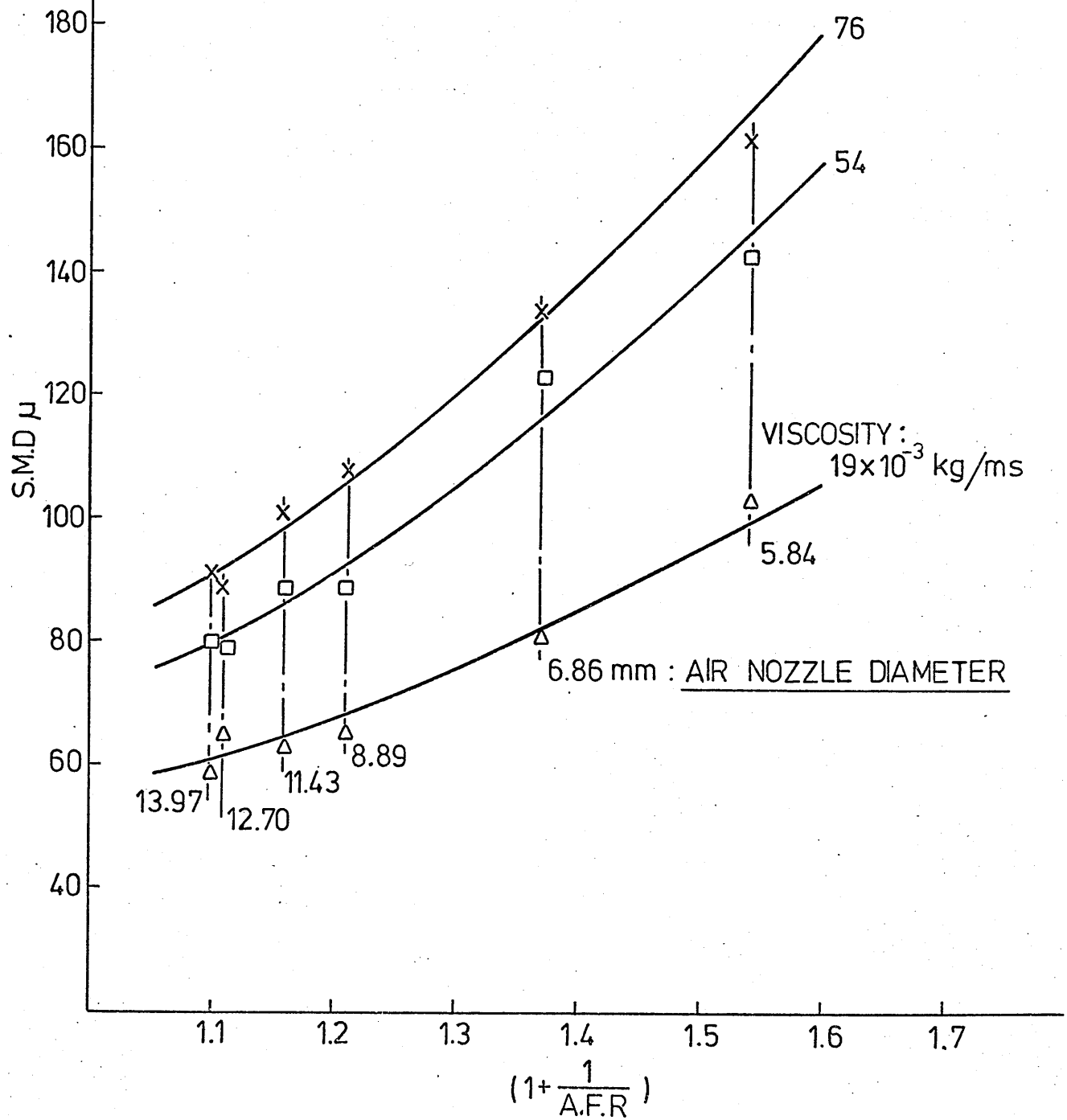
INFLUENCE OF AIR/LIQUID RATIO AT HIGH VISCOSITY.

HIGH VISCOSITY LIQUIDS

CONSTANT LIQUID FLOW RATE : 1.5 gr/s

FUEL ORIFICE : 1.191 mm

RELATIVE AIR VELOCITY : 100 m/s



INFLUENCE OF AIR/LIQUID RATIO AT HIGH VISCOSITY

HIGH VISCOSITY LIQUID: 54×10^{-3} Kg/ms

LIQUID FLOW RATES CLOSE TO 1 gr/s

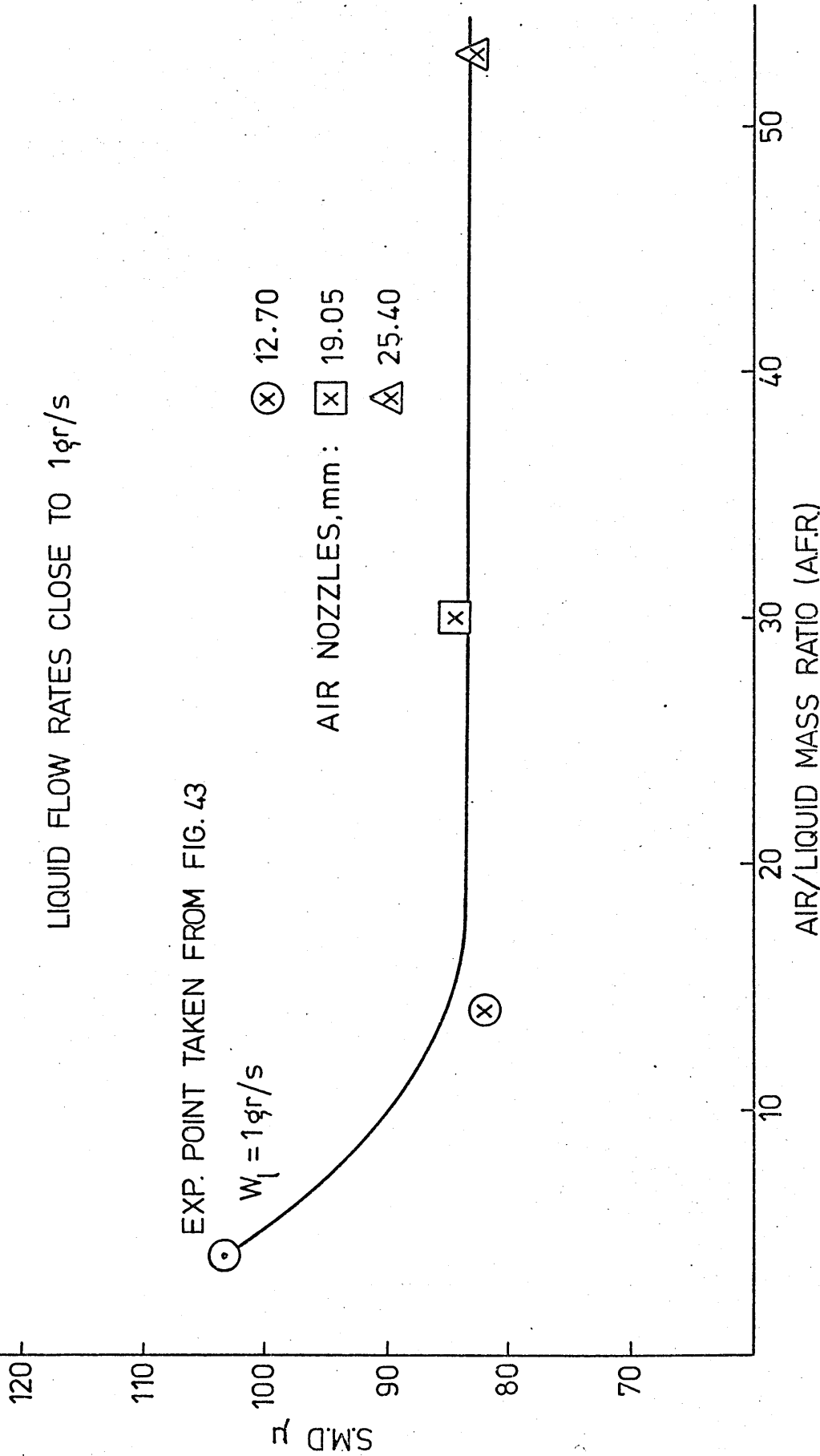
EXP. POINT TAKEN FROM FIG. 43

$W_l = 1 \text{ gr/s}$

⊗ 12.70

⊠ 19.05

⊡ 25.40



INFLUENCE OF AIR/LIQUID RATIO AT LARGE AIR FLOW RATE.

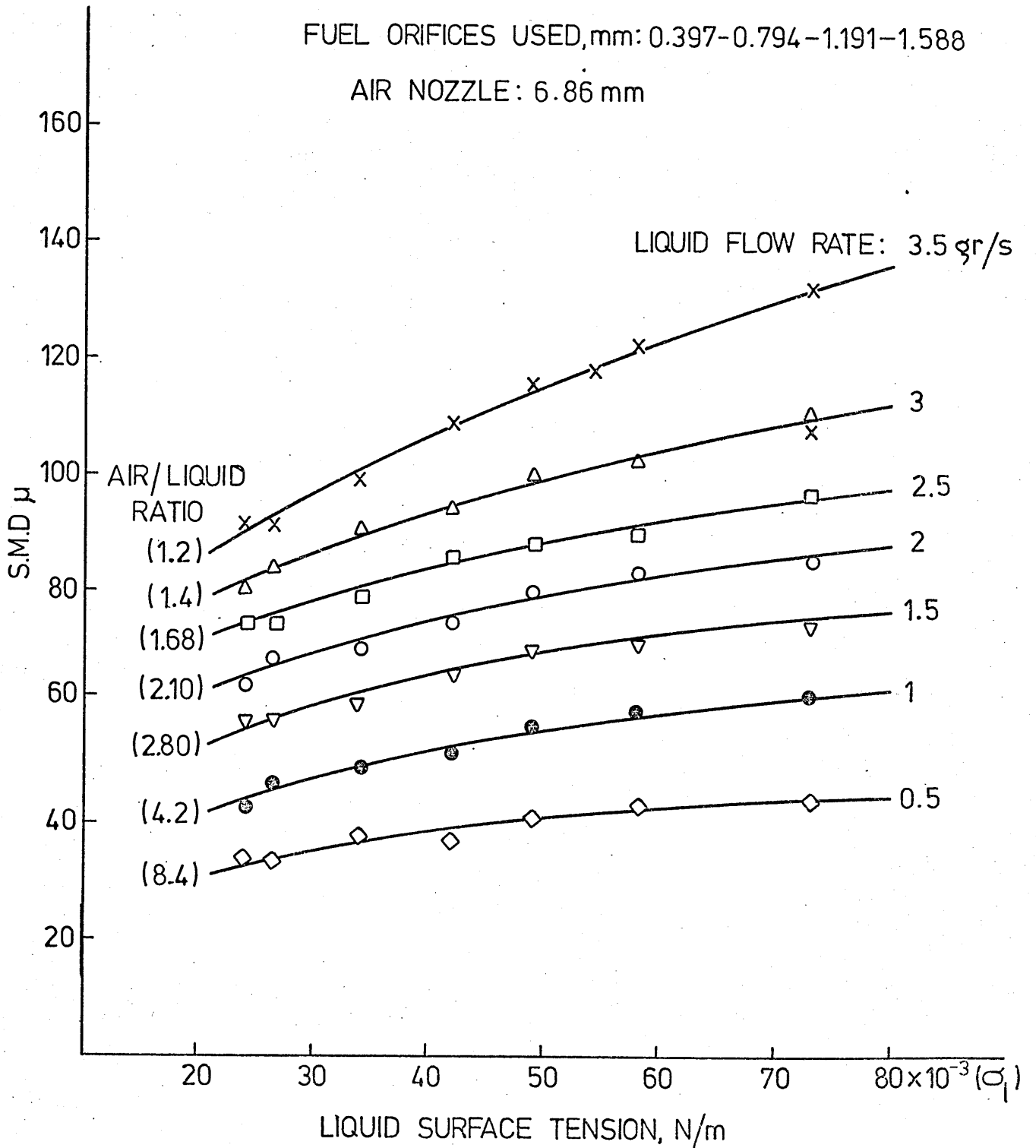
FIG. 45

VARIABLE SURFACE TENSION LIQUIDS

RELATIVE AIR VELOCITY: 100 m/s

FUEL ORIFICES USED, mm: 0.397-0.794-1.191-1.588

AIR NOZZLE: 6.86 mm



INFLUENCE OF LIQUID SURFACE TENSION.

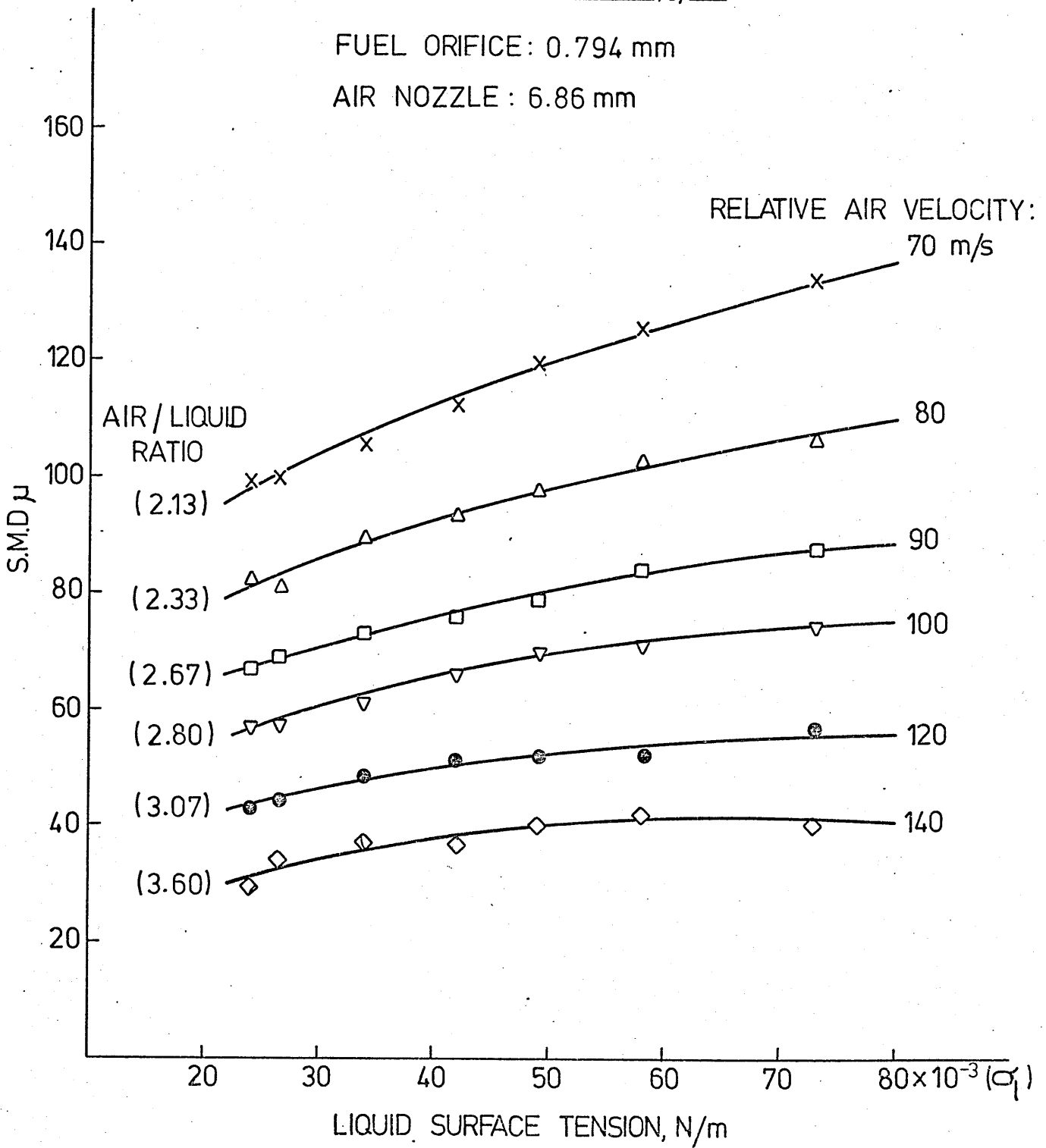
FIG.46

VARIABLE SURFACE TENSION LIQUIDS

LIQUID FLOW RATE : 1.5 gr/s

FUEL ORIFICE : 0.794 mm

AIR NOZZLE : 6.86 mm



INFLUENCE OF LIQUID SURFACE TENSION,

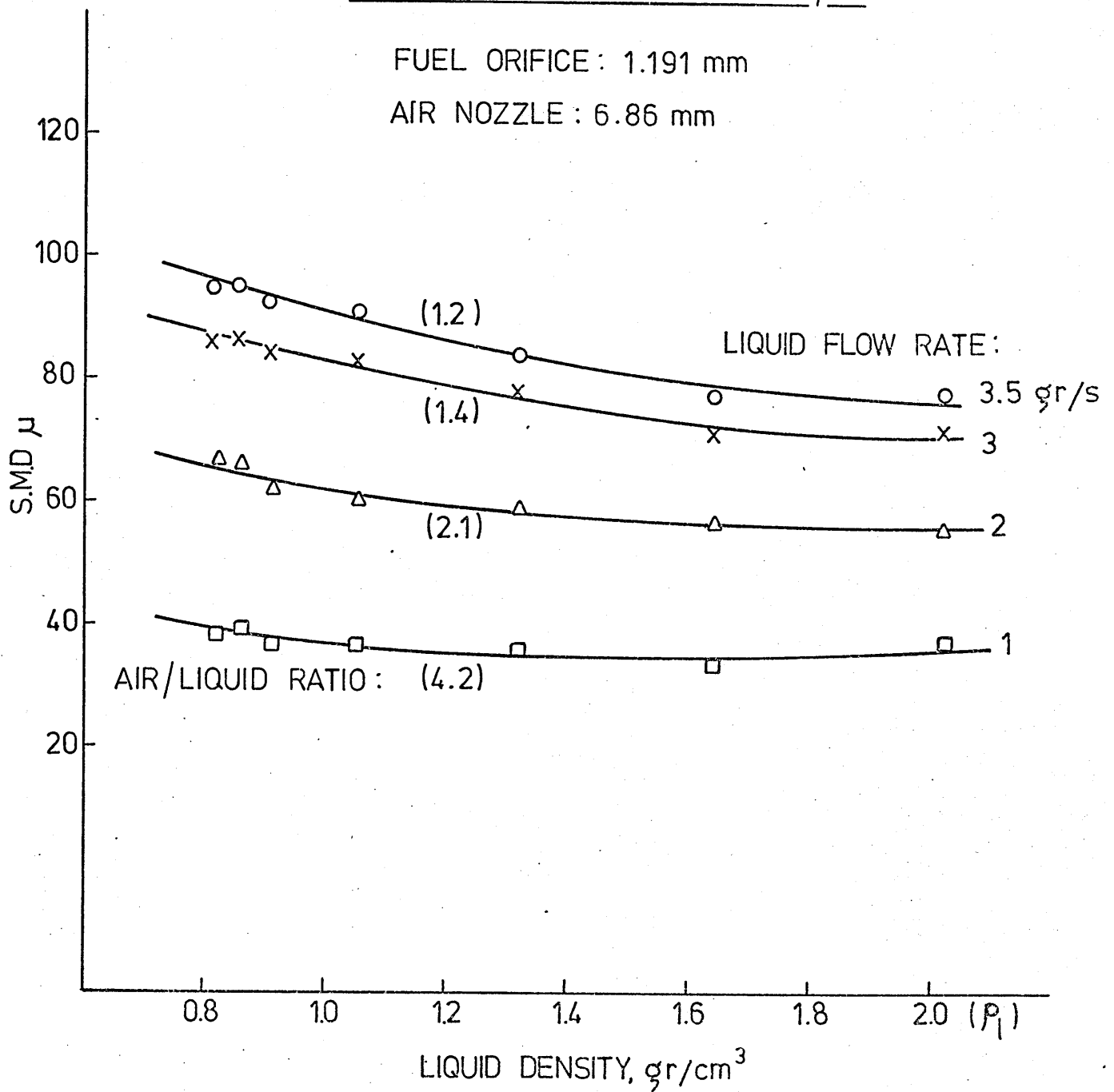
FIG. 47

VARIABLE LIQUID DENSITY

RELATIVE AIR VELOCITY: 100 m/s

FUEL ORIFICE : 1.191 mm

AIR NOZZLE : 6.86 mm



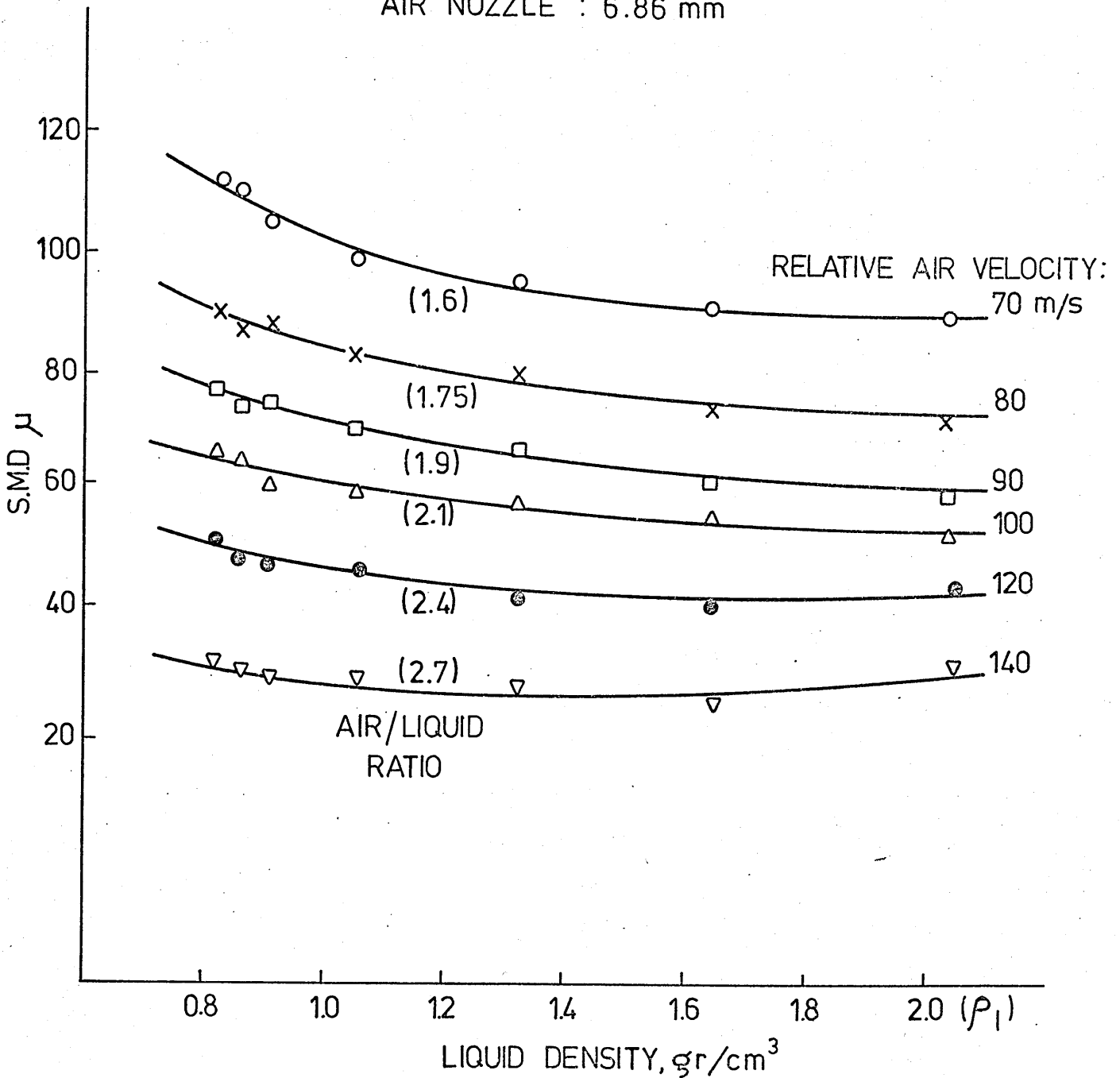
INFLUENCE OF LIQUID DENSITY

VARIABLE LIQUID DENSITY

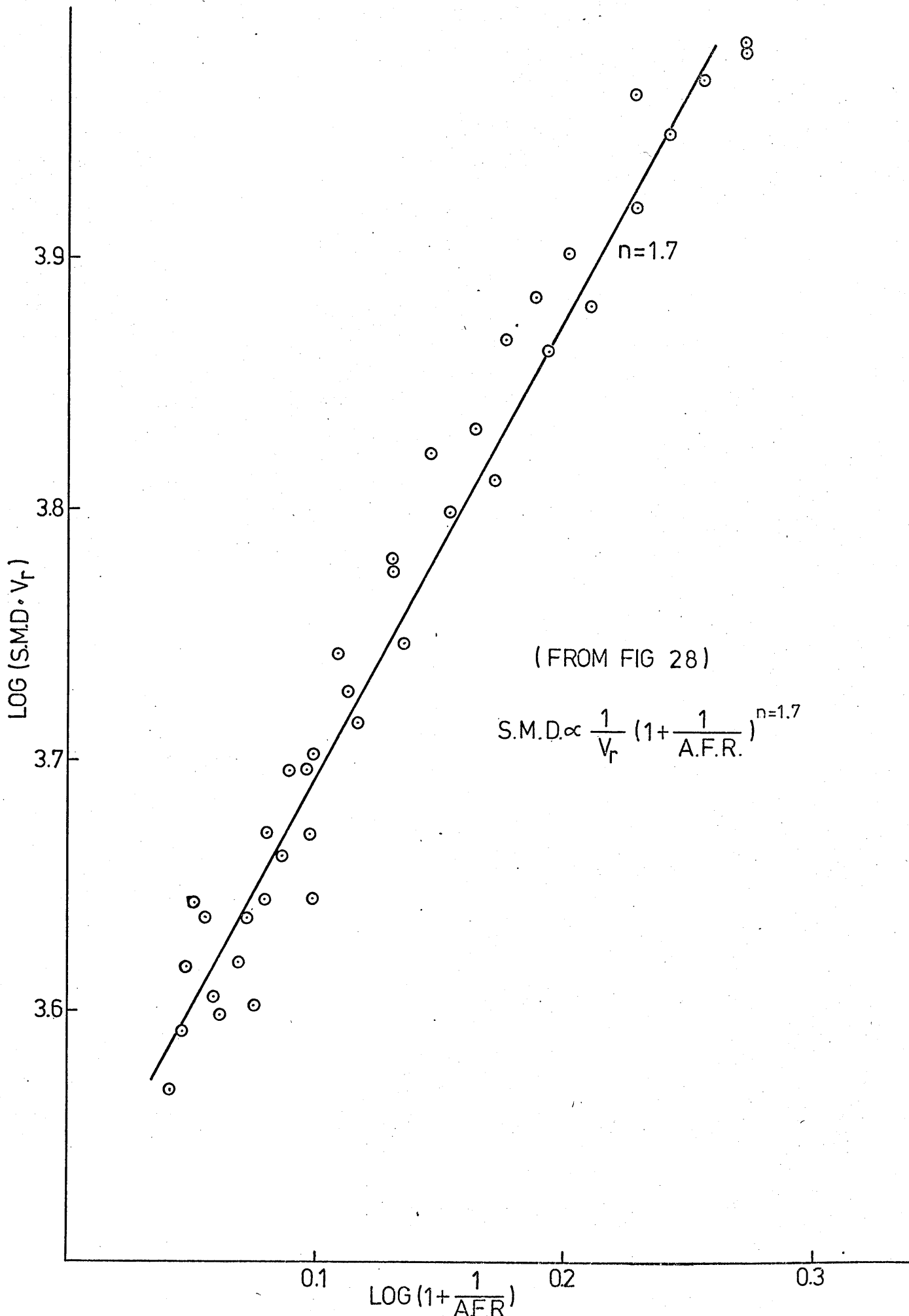
LIQUID FLOW RATE : 2 gr/s

FUEL ORIFICE : 1.191 mm

AIR NOZZLE : 6.86 mm



INFLUENCE OF LIQUID DENSITY.



INFLUENCE OF AIR LIQUID RATIO

FIG. 50

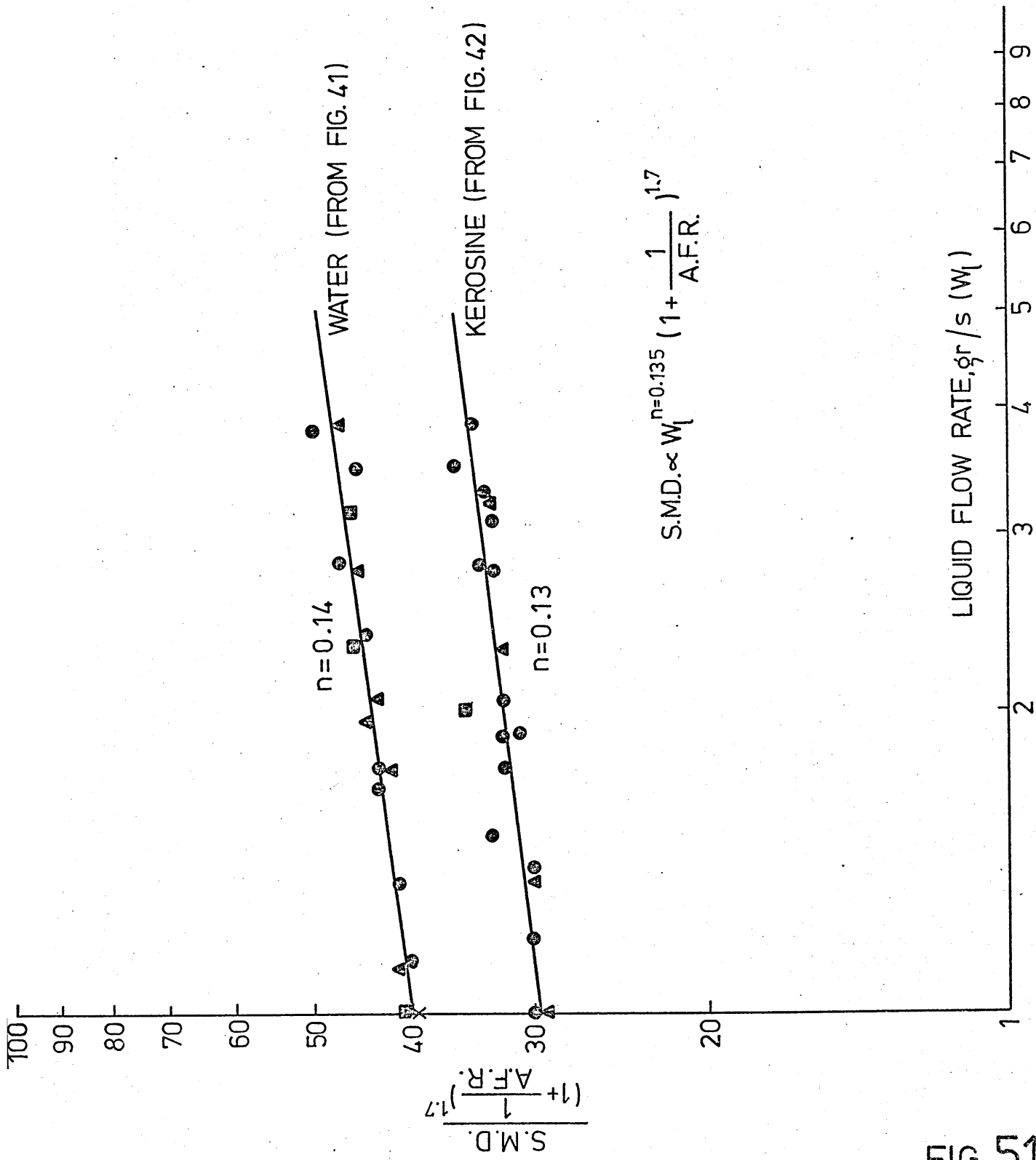


FIG. 51

INFLUENCE OF LIQUID FLOW RATE.

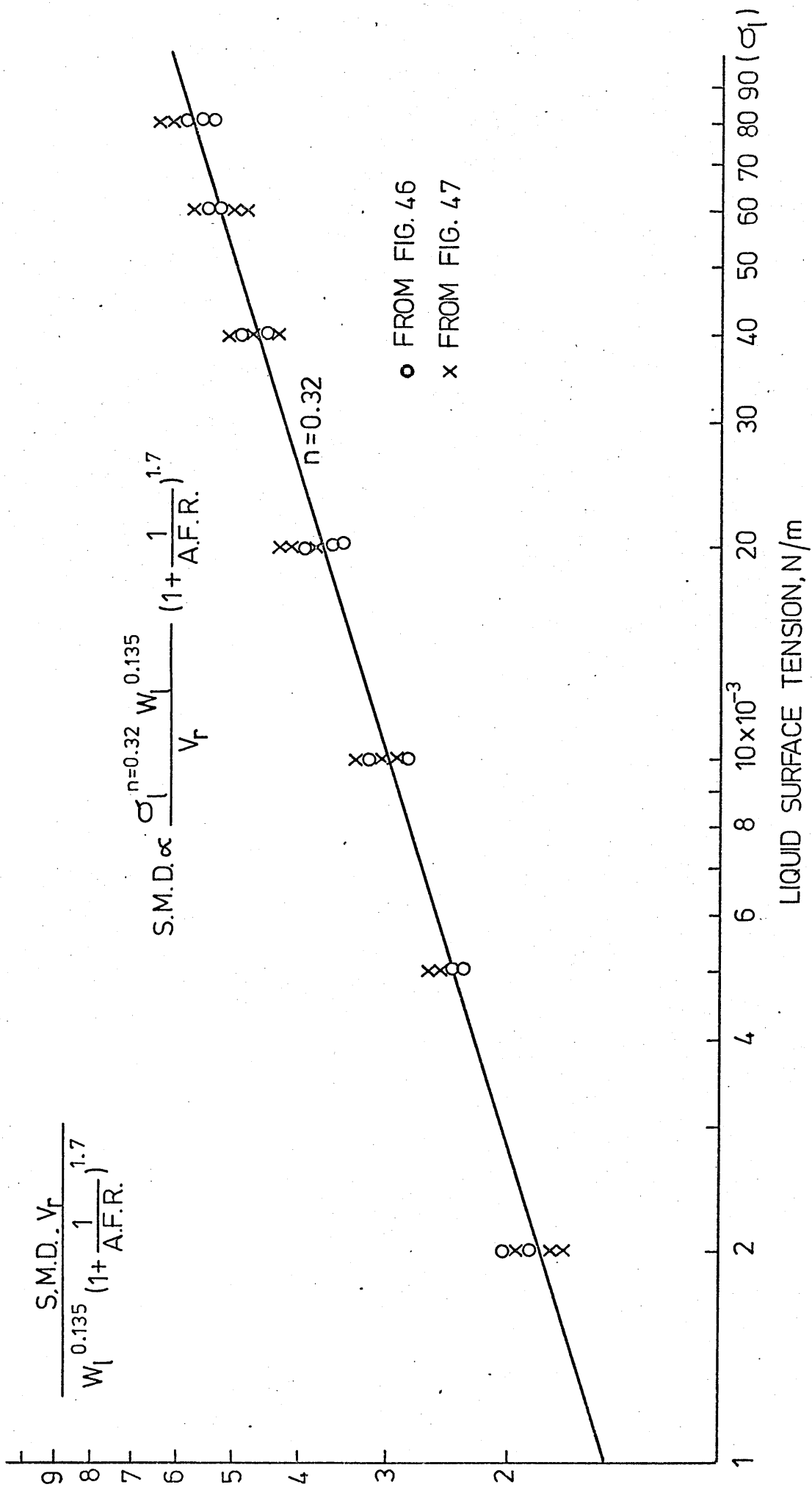
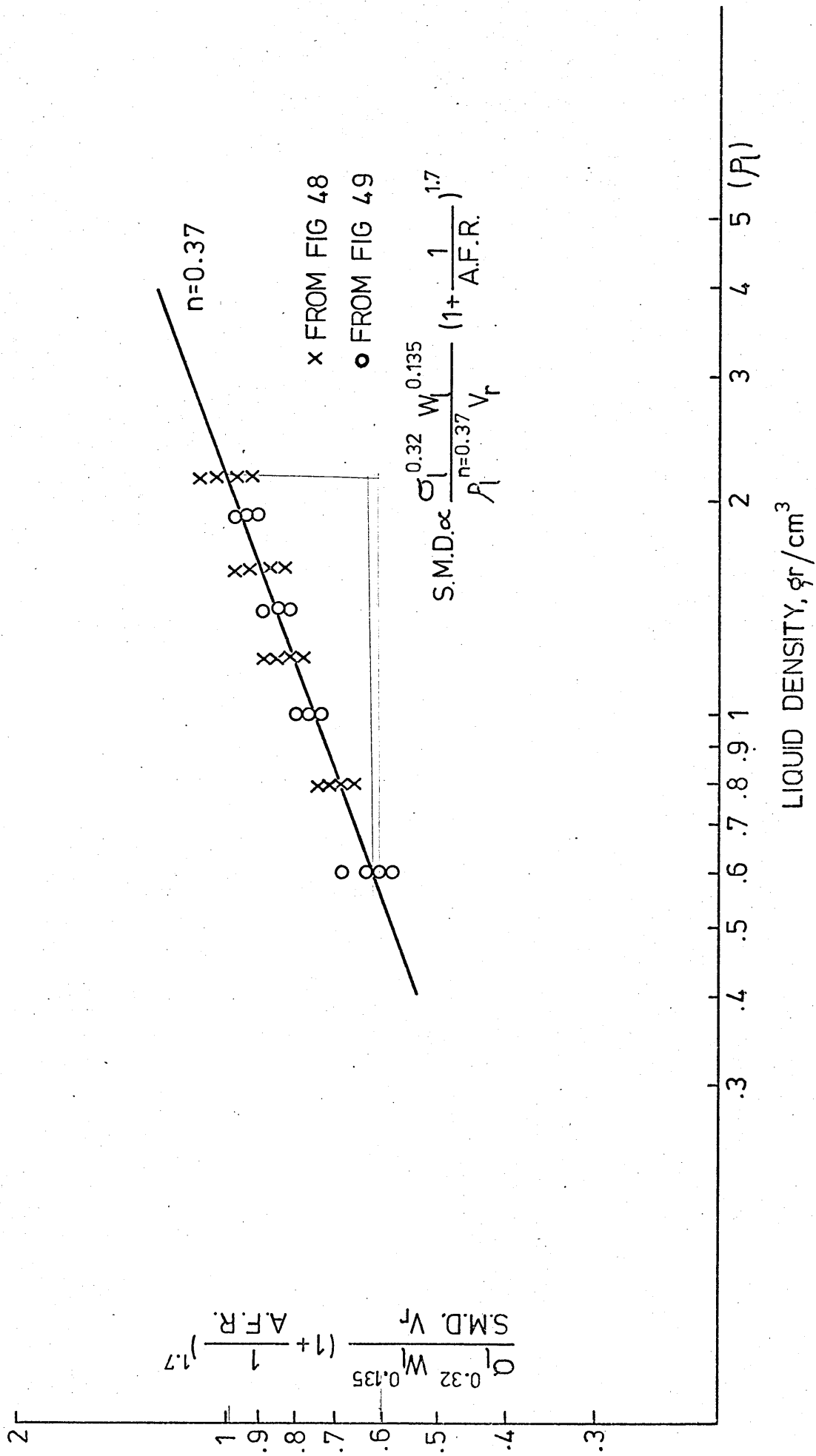


FIG. 52

INFLUENCE OF LIQUID SURFACE TENSION.



INFLUENCE OF LIQUID DENSITY.

FIG. 53

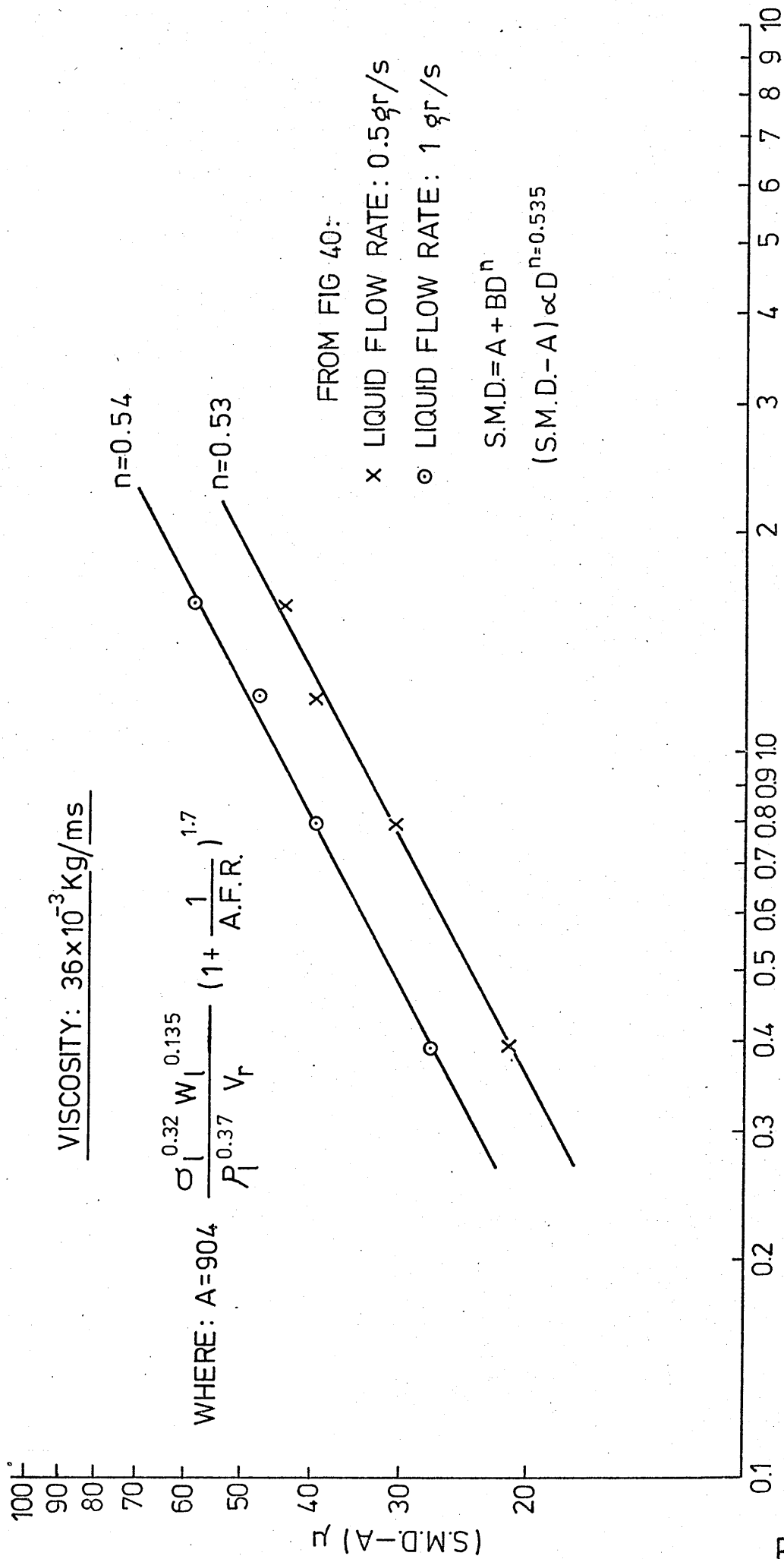


FIG. 54

HIGH VISCOSITY LIQUIDS

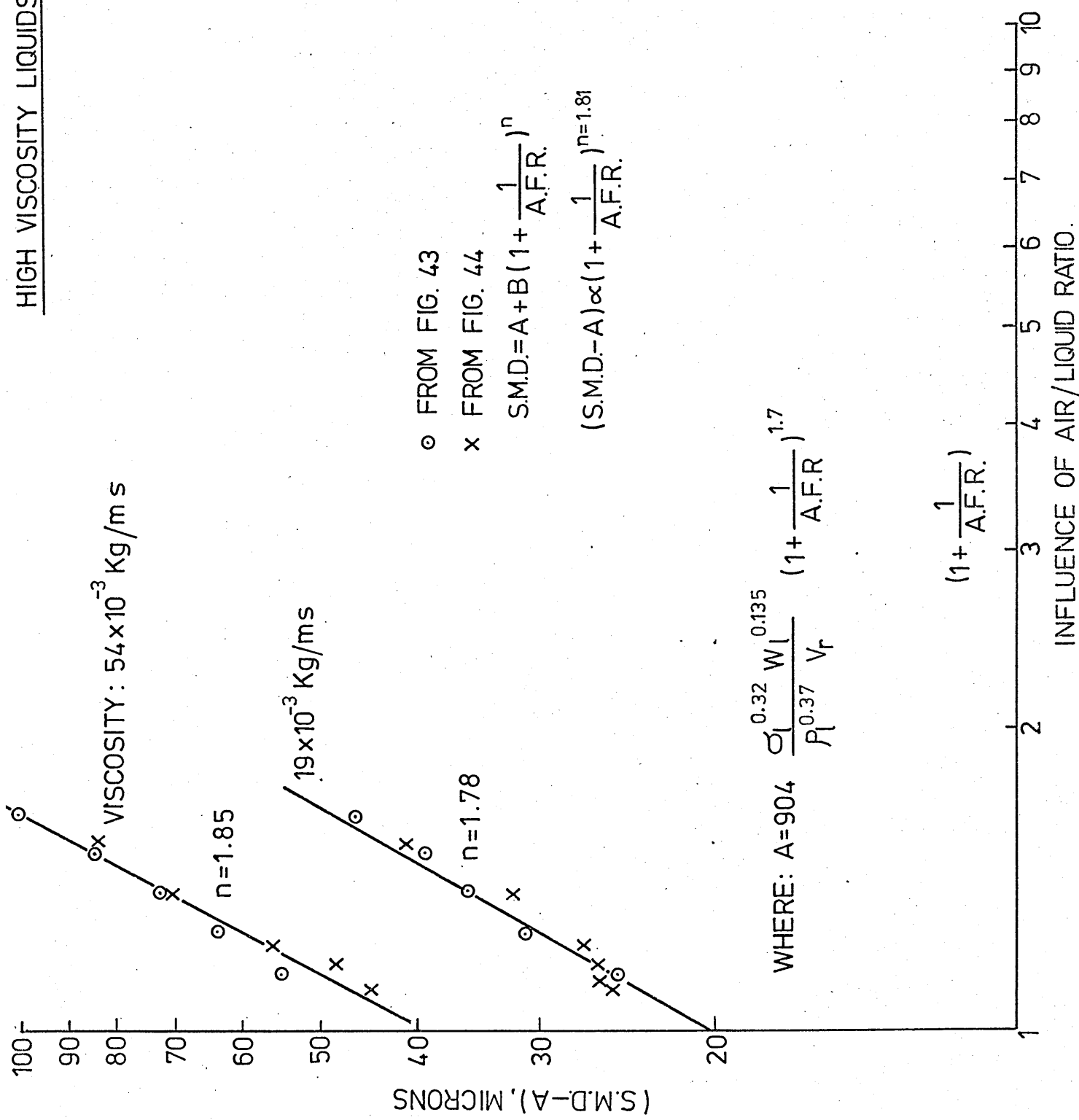
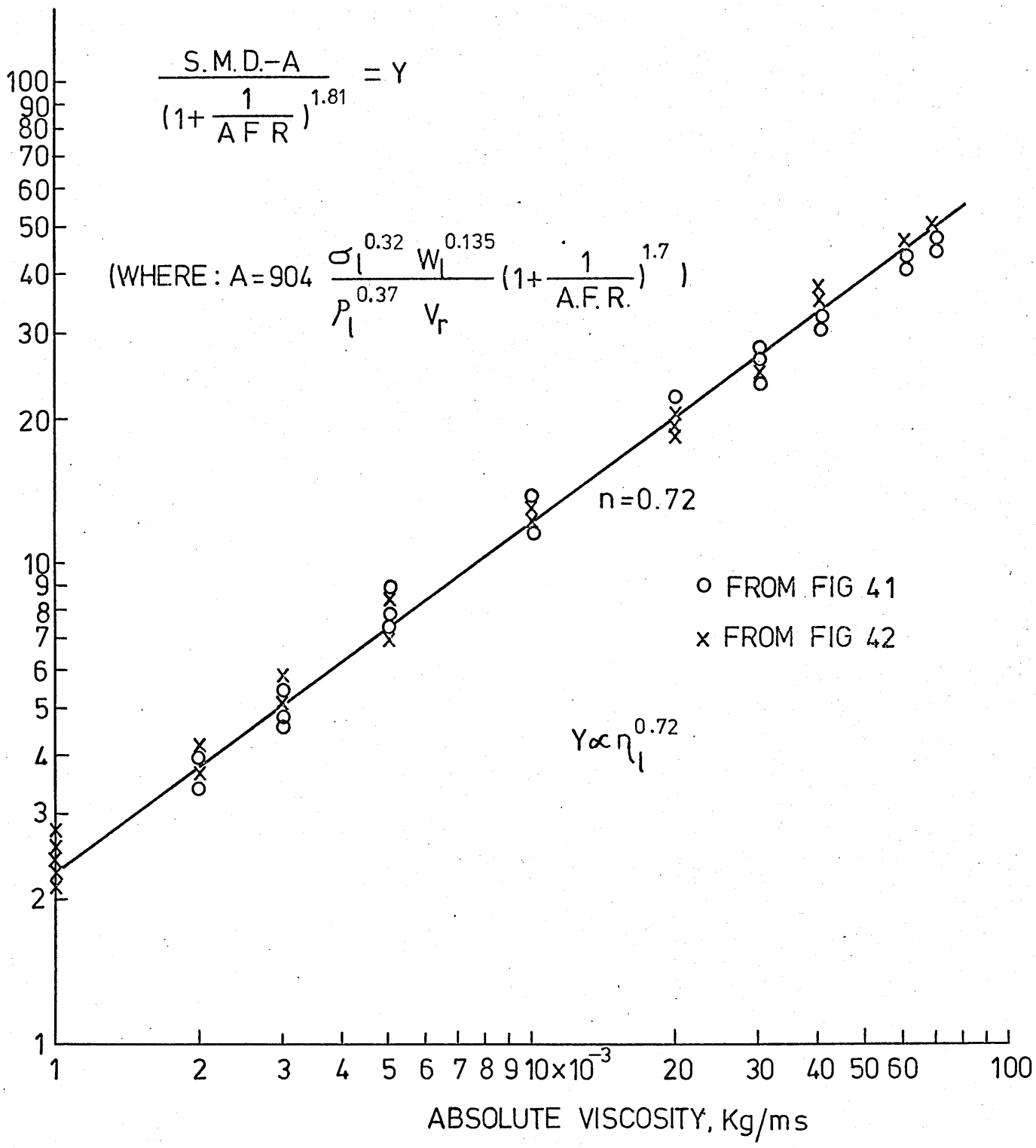


FIG. 55



INFLUENCE OF LIQUID VISCOSITY ON S.M.D.

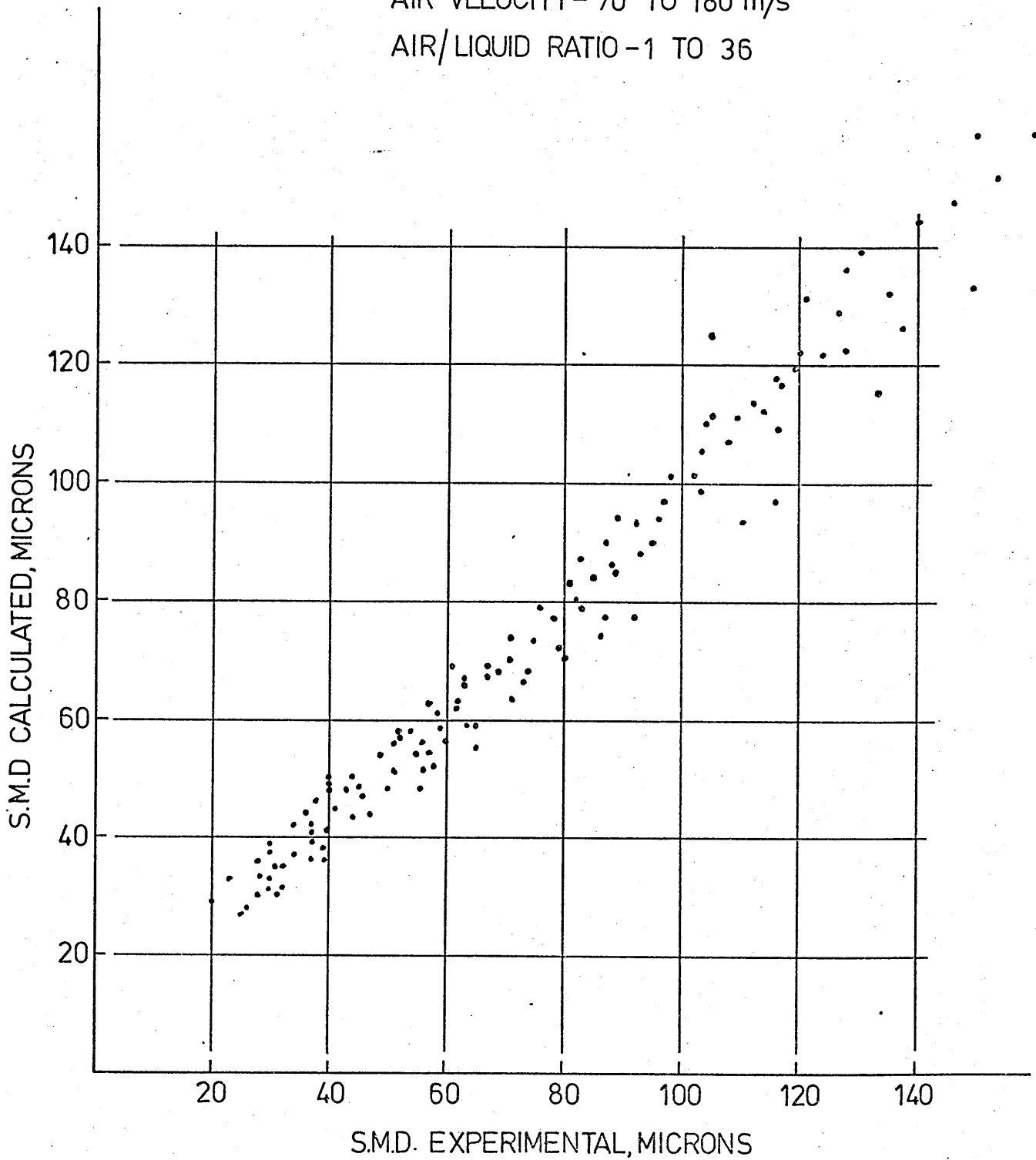
FIG.56

KEROSINE AND WATER DATA

LIQUID FLOW RATE-0.5 TO 3 gr/s

AIR VELOCITY- 70 TO 180 m/s

AIR/LIQUID RATIO-1 TO 36



CALCULATED (Eq. 24) VS MEASURED DATA.

FIG. 57

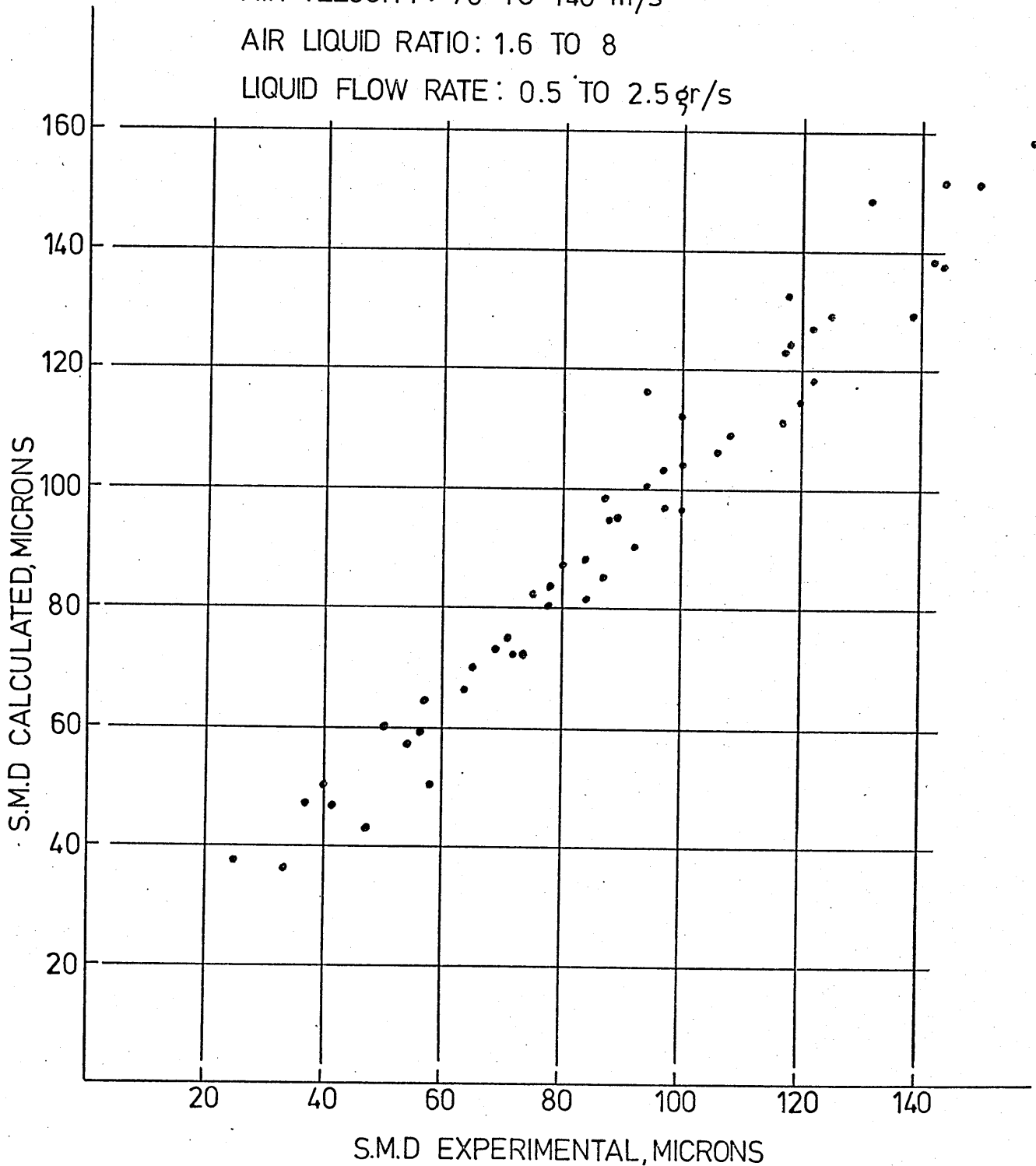
LIQUID VISCOSITY DATA

VISCOSITY: 1.3 TO 76×10^{-3} Kg/ms

AIR VELOCITY: 70 TO 140 m/s

AIR LIQUID RATIO: 1.6 TO 8

LIQUID FLOW RATE: 0.5 TO 2.5 gr/s



CALCULATED (Eq.24) VS MEASURED DATA.

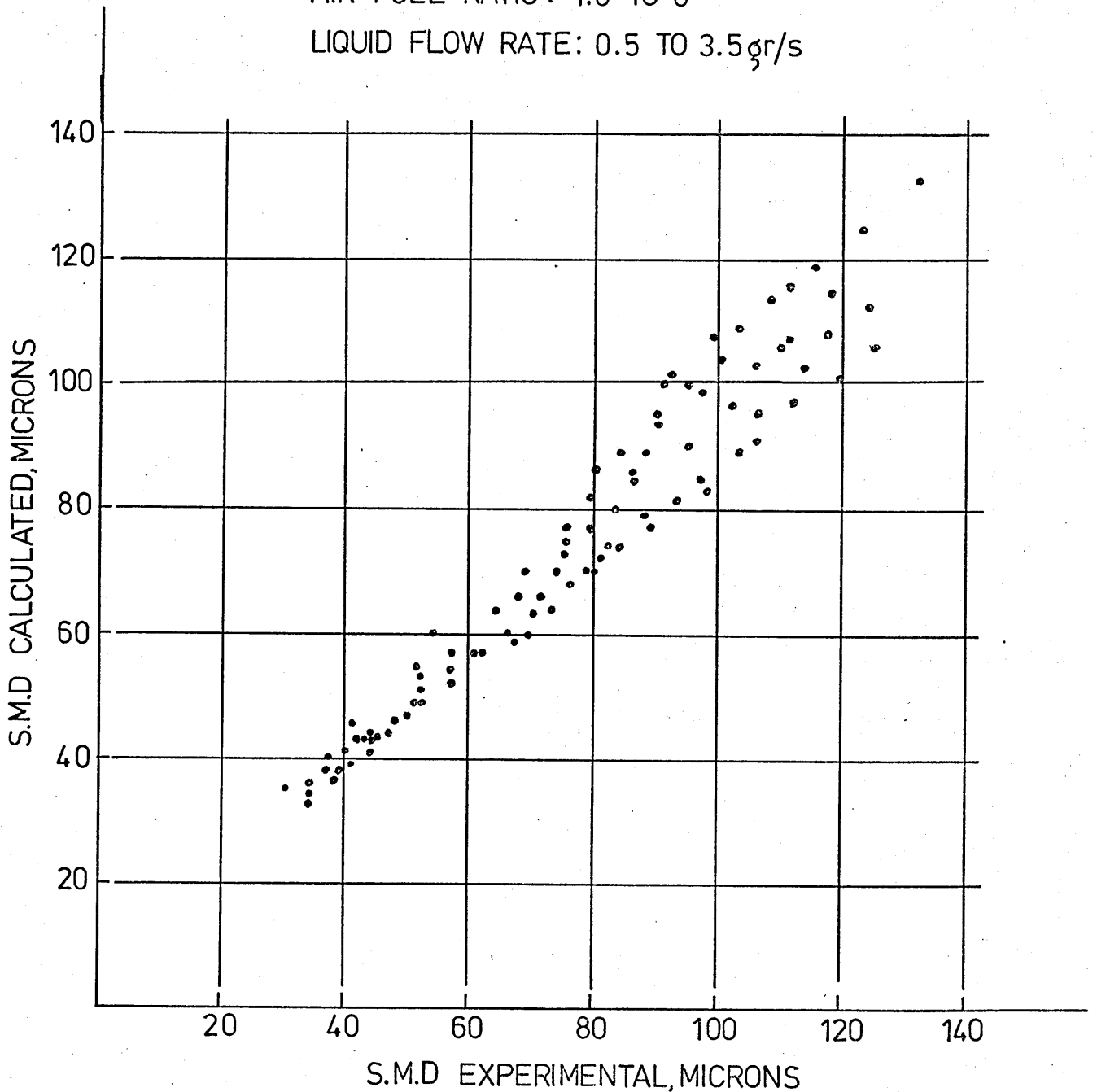
SURFACE TENSION DATA

SURFACE TENSION: 24 TO 73×10^{-3} N/m

AIR VELOCITY: 70 TO 140 m/s

AIR FUEL RATIO: 1.6 TO 8

LIQUID FLOW RATE: 0.5 TO 3.5 gr/s



CALCULATED (Eq.24) VS MEASURED DATA.

FIG.59

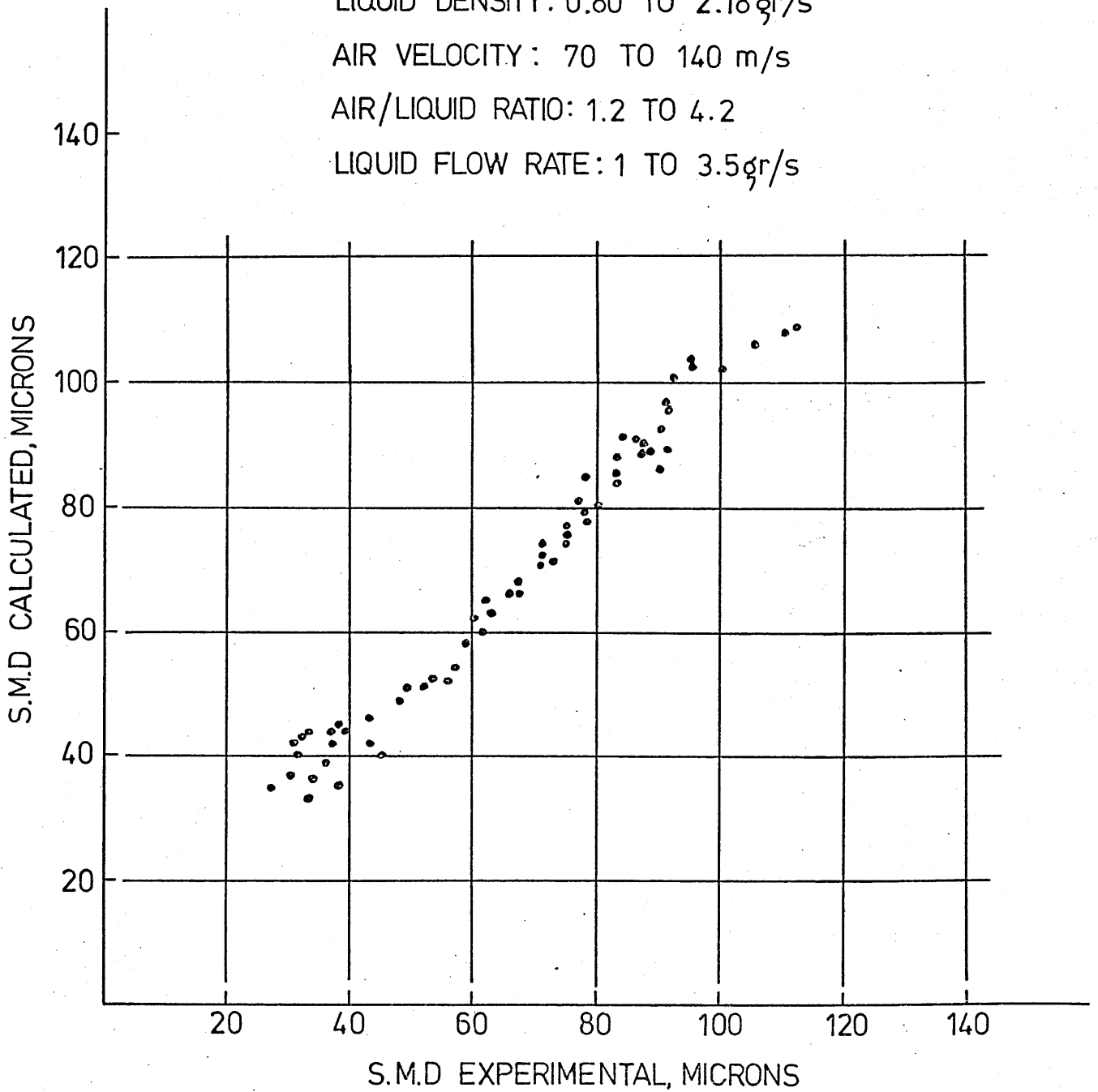
LIQUID DENSITY DATA

LIQUID DENSITY: 0.80 TO 2.18 gr/s

AIR VELOCITY: 70 TO 140 m/s

AIR/LIQUID RATIO: 1.2 TO 4.2

LIQUID FLOW RATE: 1 TO 3.5 gr/s



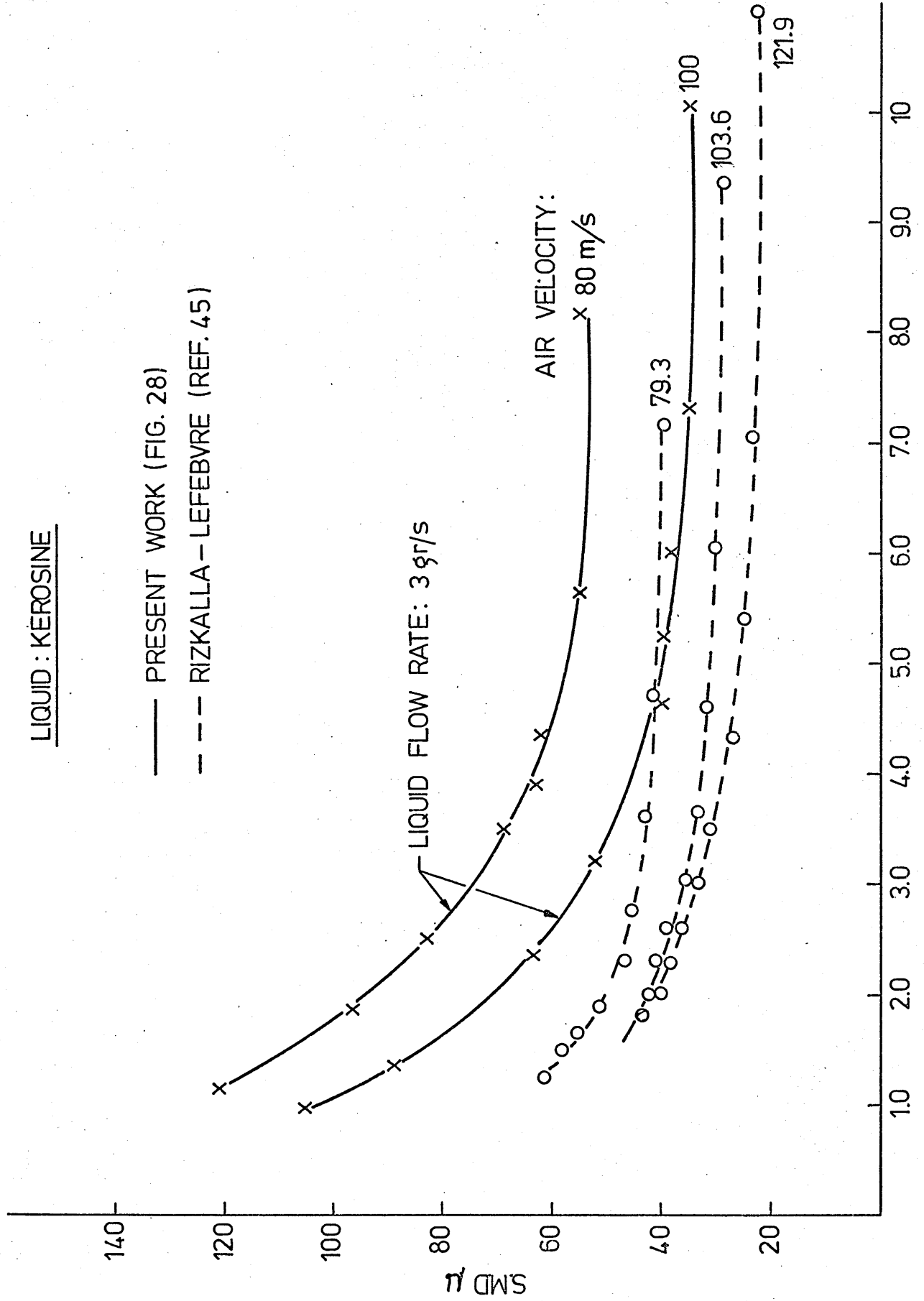
CALCULATED (Eq 24) VS MEASURED DATA.

FIG. 60

LIQUID : KEROSENE

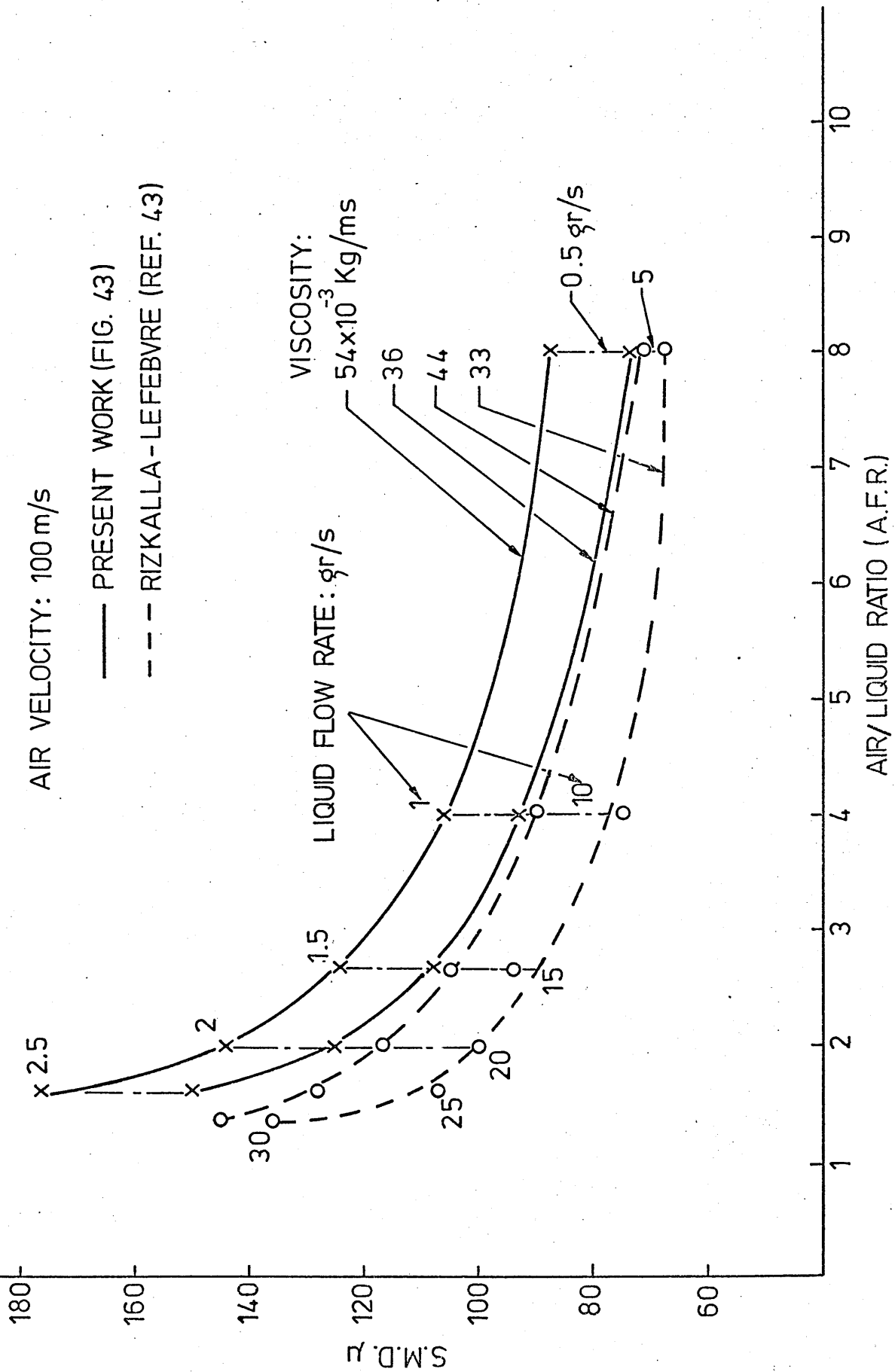
— PRESENT WORK (FIG. 28)

- - - RIZKALLA - LEFEBVRE (REF. 45)



RIZKALLA - LEFEBVRE (REF. 45) VS PRESENT WORK - MEASURED DATA

HIGH VISCOSITY LIQUIDS



RIZKALLA-LEFEBVRE VS PRESENT WORK MEASURED VALUES

FIG.62

LIQUID: KEROSENE

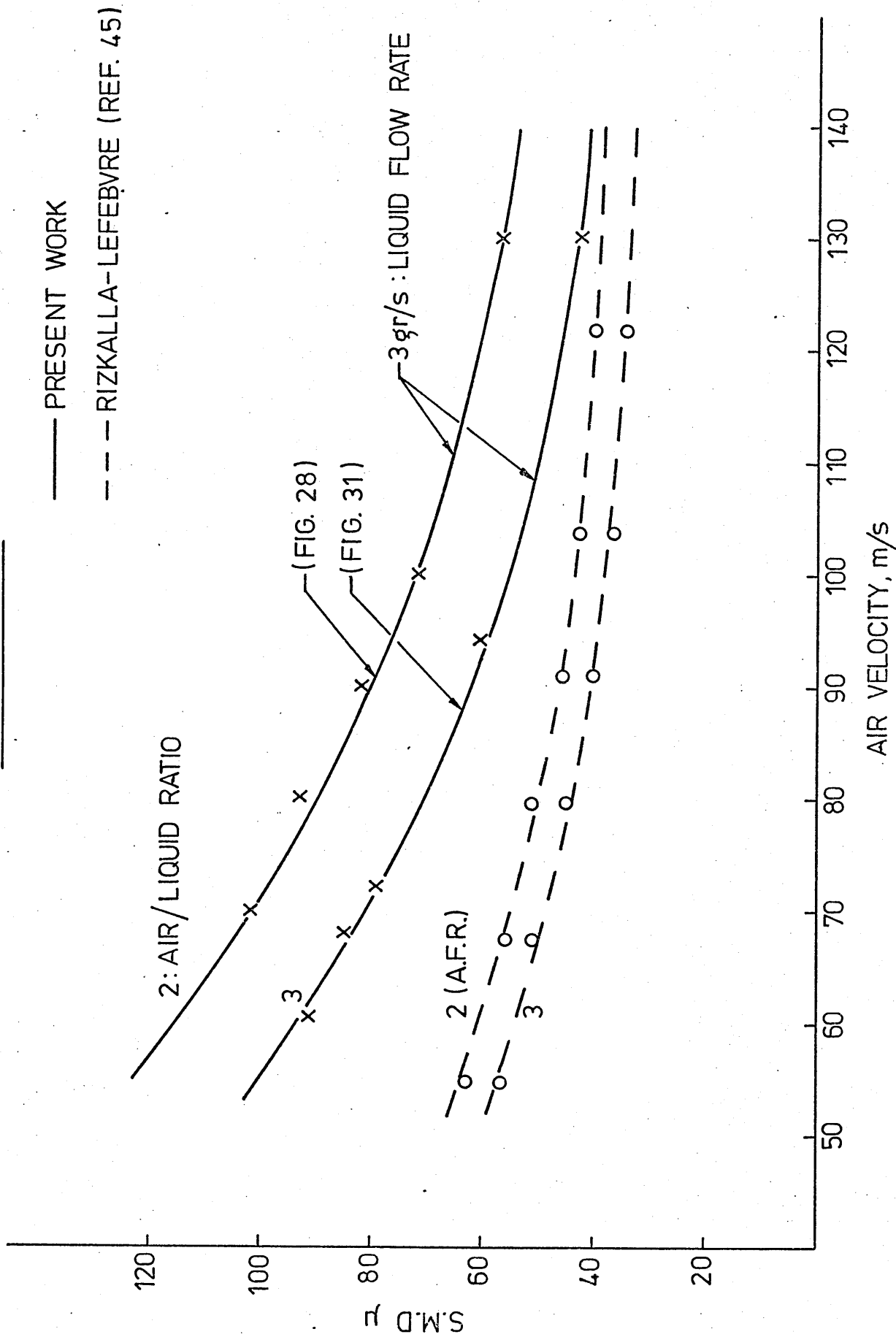
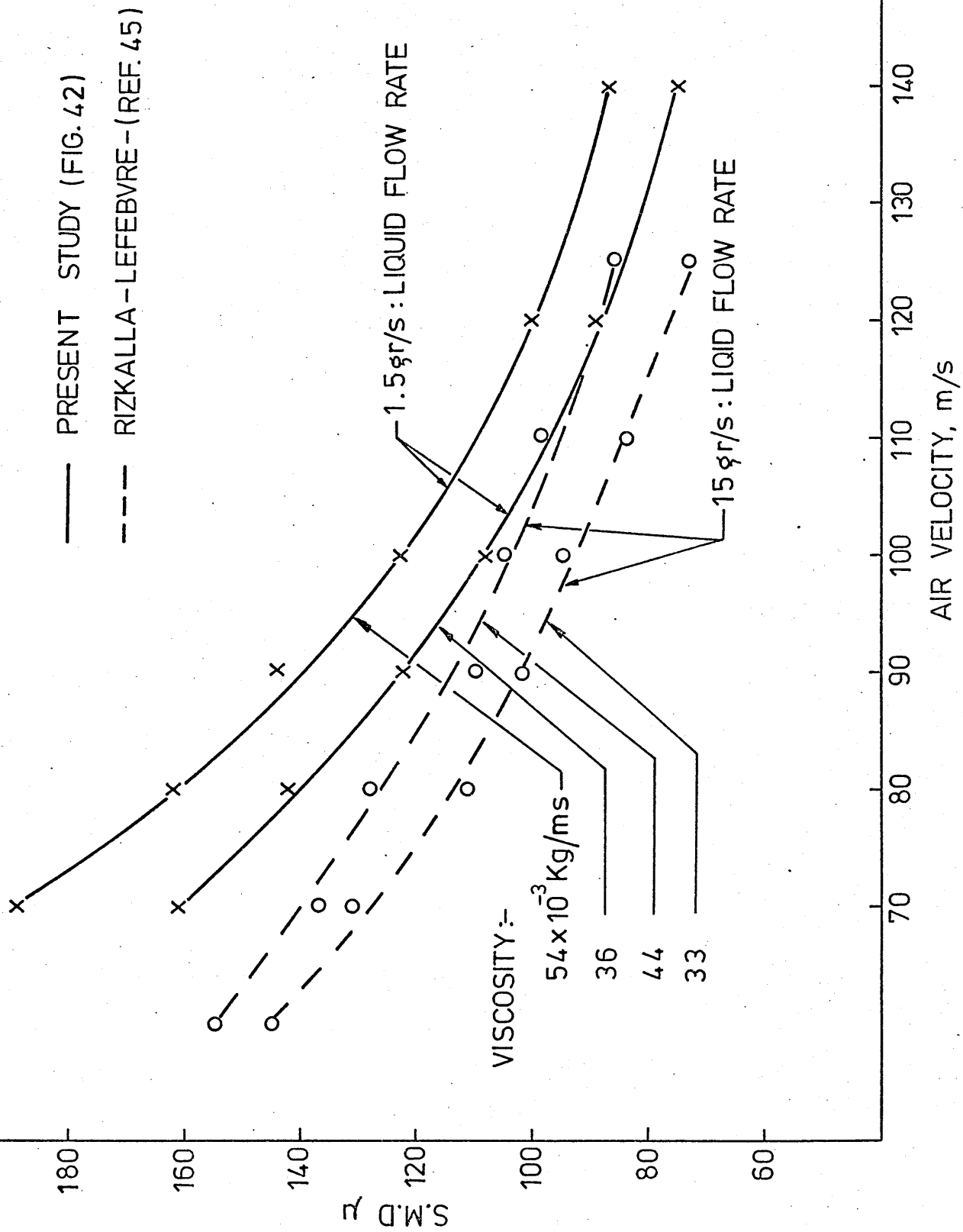


FIG. 63

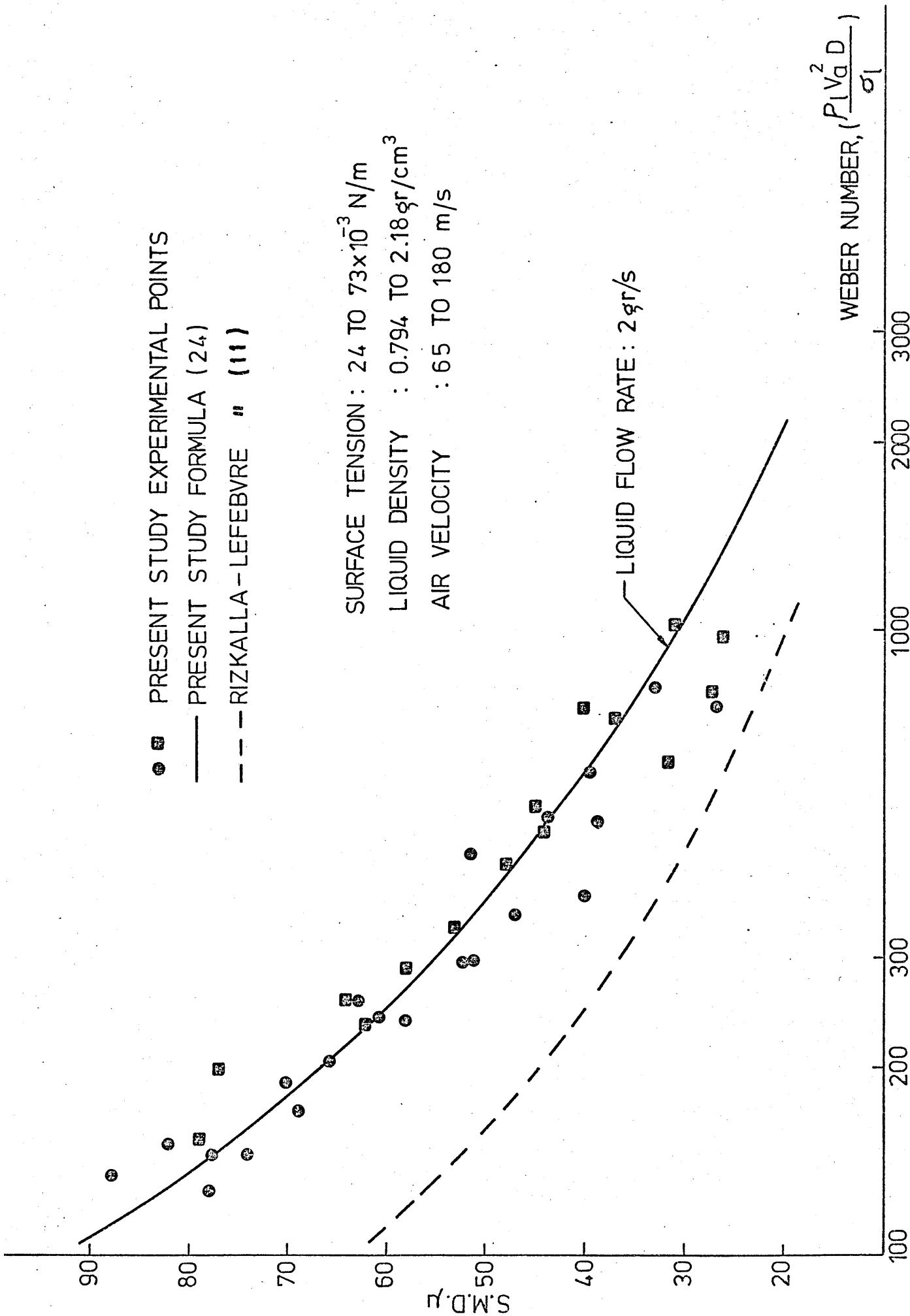
RIZKALLA - LEFEBVRE (REF. 45) VS PRESENT WORK - MEASURED VALUES.

HIGH VISCOSITY LIQUIDS



RIZKALLA-LEFEBVRE (REF. 45) VS PRESENT WORK MEASURED VALUES.

FIG. 64



RIZKALLA - LEFEBVRE (REF. 45) VS PRESENT WORK.

AIR VELOCITY-70 TO 180 m/s
AIR LIQUID RATIO-2 TO 20
LIQUID FLOW RATE-1.5 TO 3 gr/s

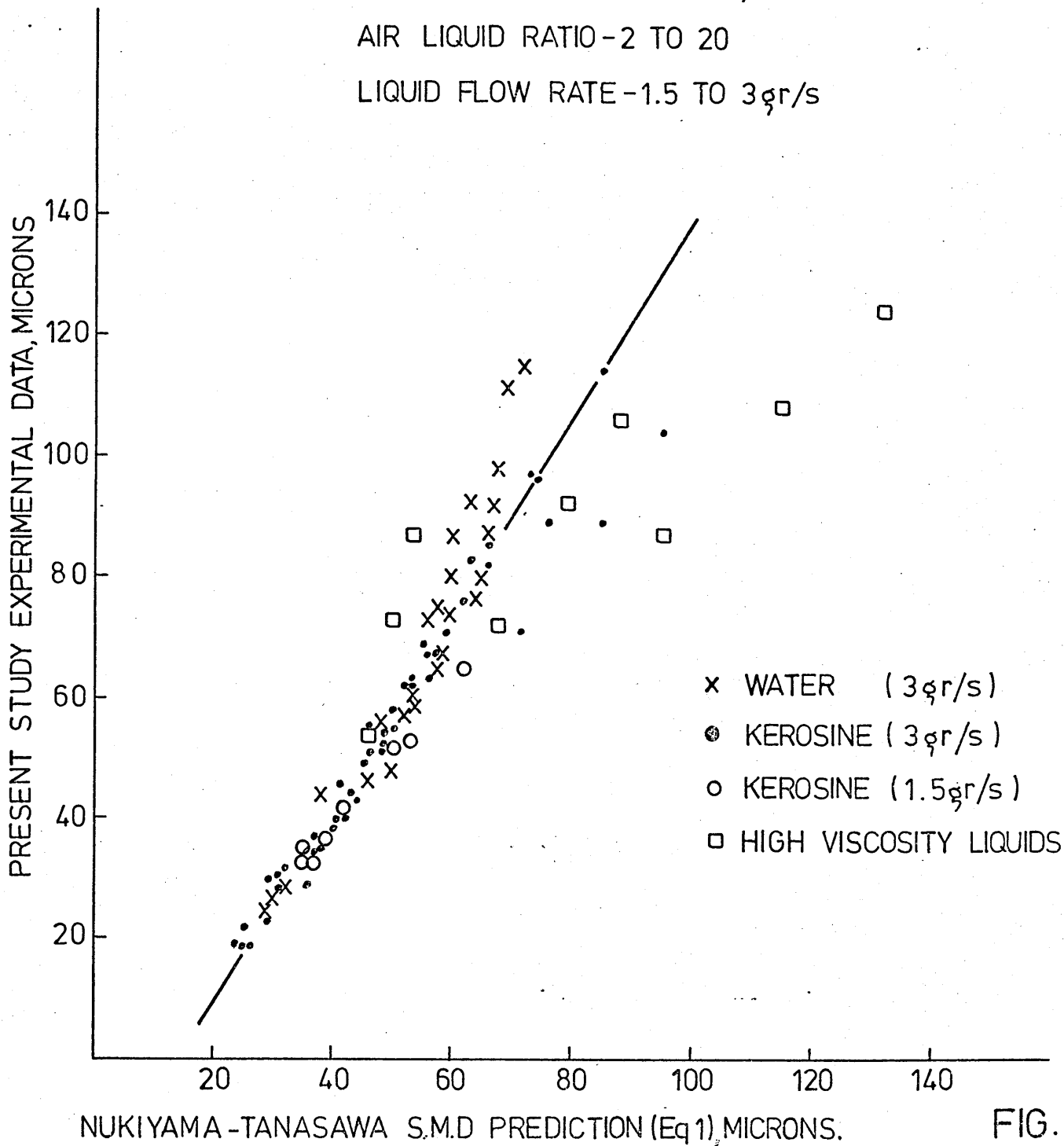


FIG. 60

AIR VELOCITY: 70 TO 180 m/s
AIR LIQUID RATIO: 1.5 TO 10
LIQUID FLOW RATE: 1.5 TO 3 gr/s
ATMOSPHERIC PRESSURE.

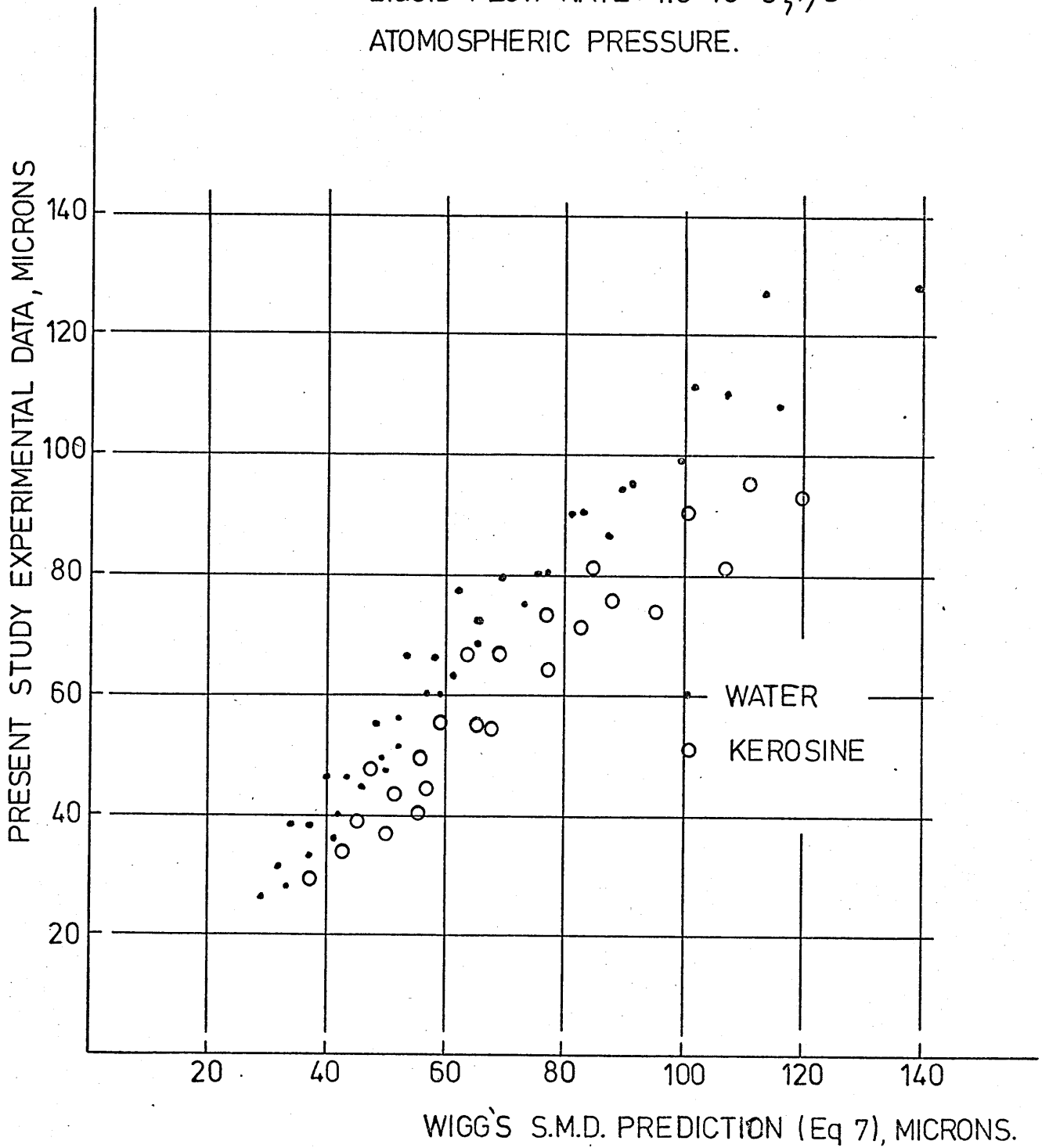
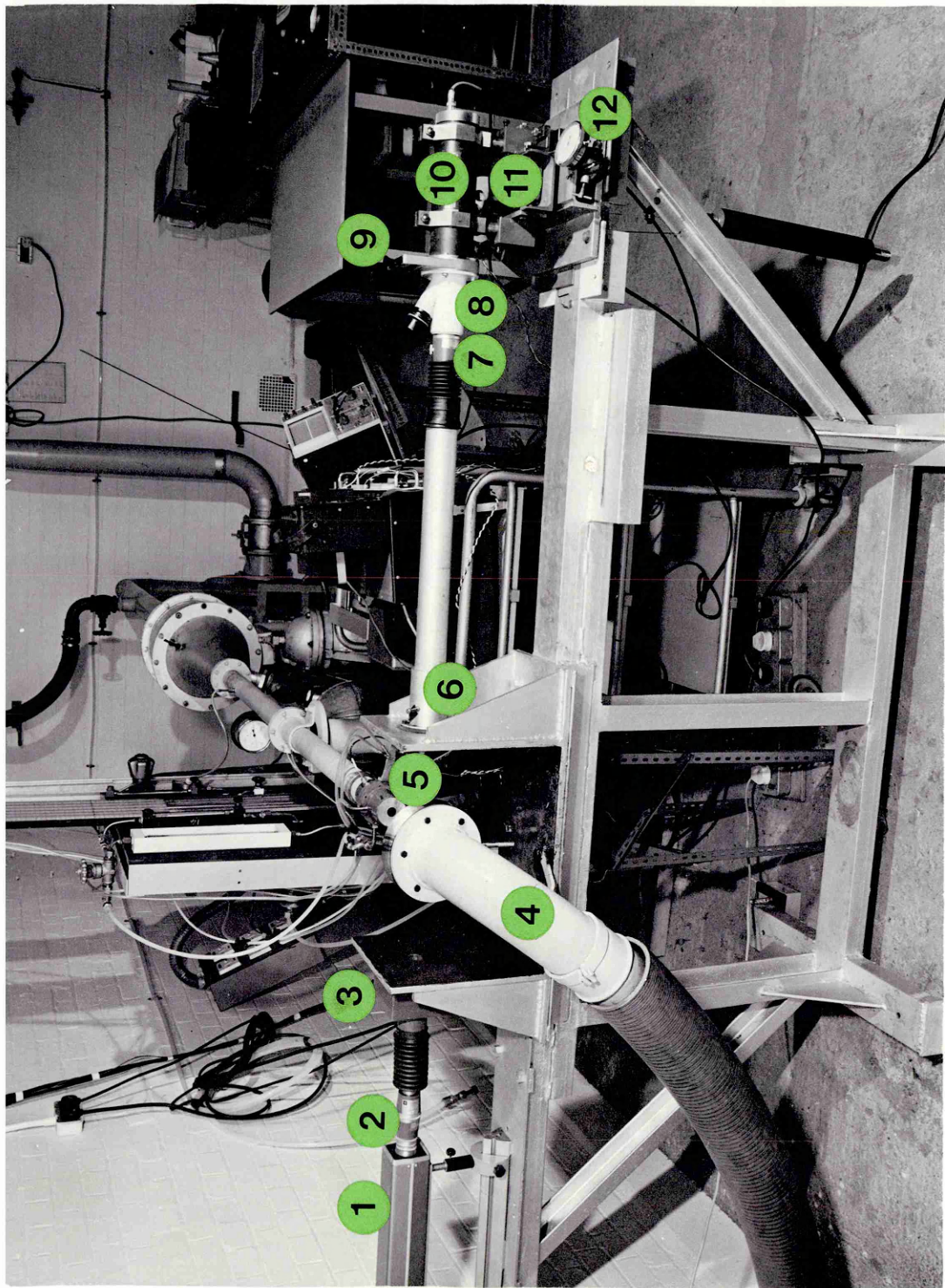


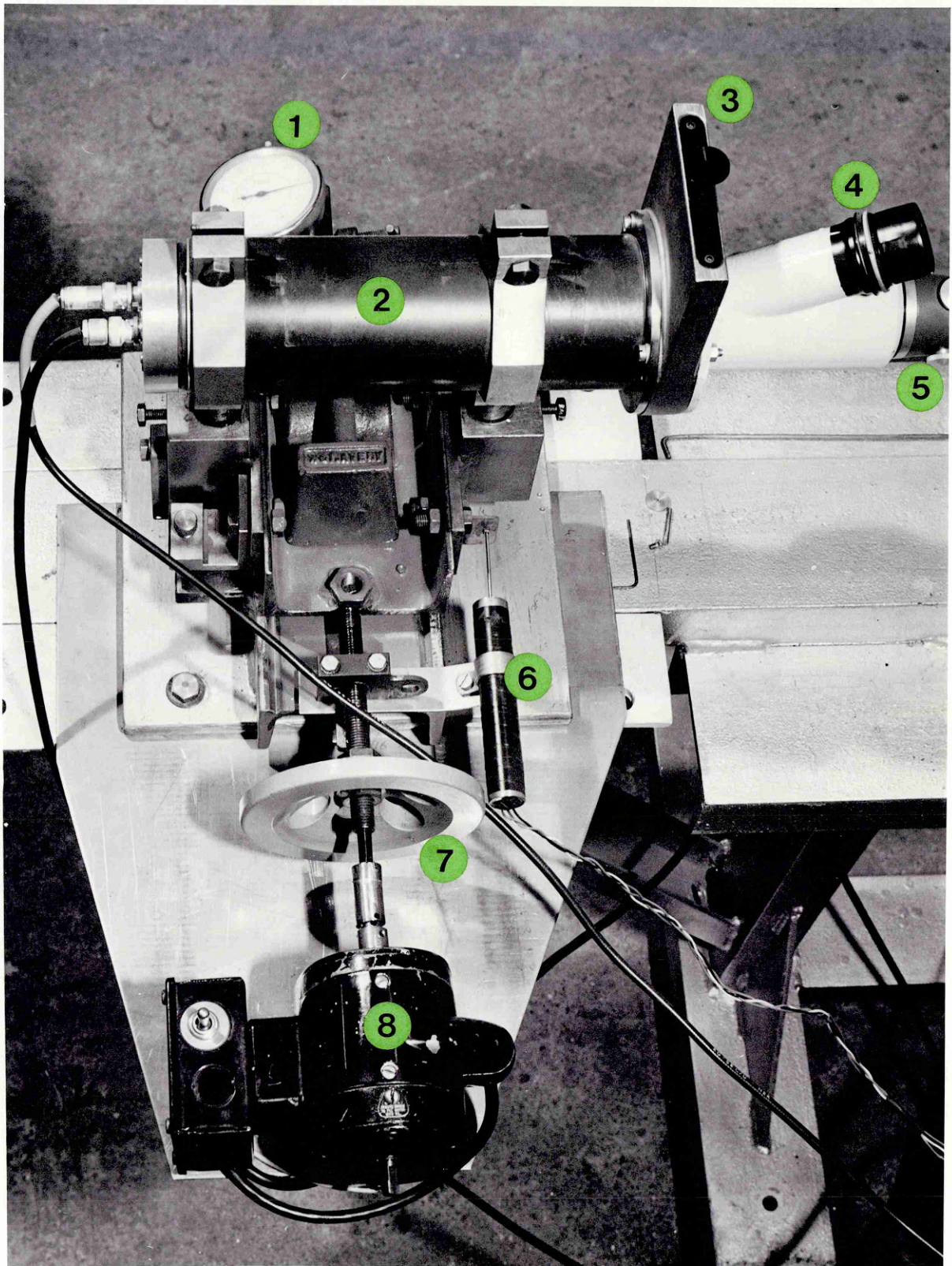
FIG. 67

PLATES



- | | | |
|---------------------|-------------------|--------------------------|
| 1 - LASER | 5 - TEST SECTION | 9 - SHUTTER |
| 2 - TELESCOPE | 6 - RECEIVER LENS | 10 - PHOTOMULTIPLIER |
| 3 - LIGHT CHOPPER | 7 - APERTURE | 11 - TRAVERSING SYSTEM |
| 4 - SPRAY COLLECTOR | 8 - EYEPIECE | 12 - DIAL TEST INDICATOR |

PLATE 1



1 - DIAL TEST INDICATOR

2 - PHOTOMULTIPLIER

3 - SHUTTER

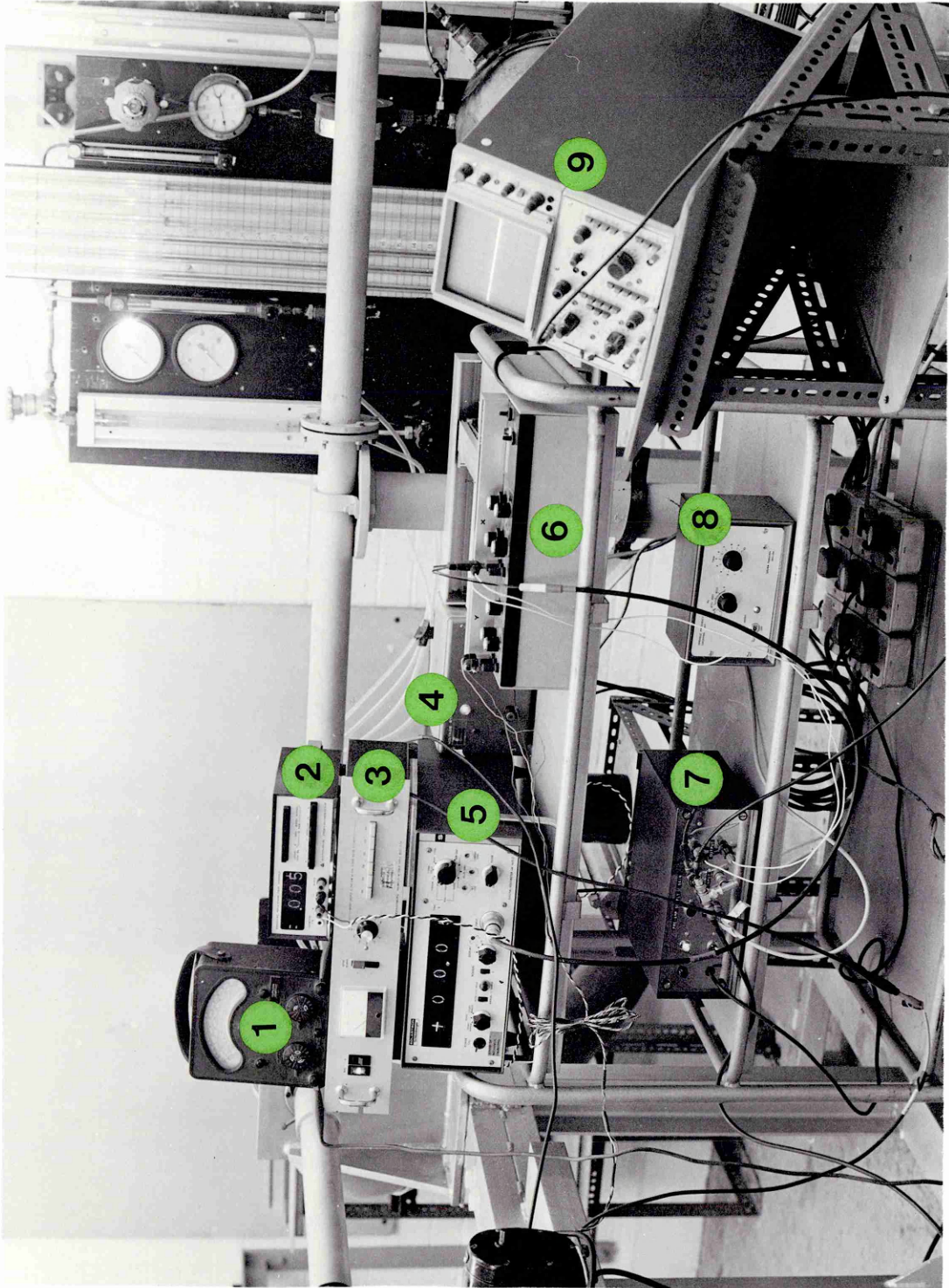
4 - EYEPIECE

5 - APERTURE

6 - X-AXIS TRANSDUCER

7 - TRAVERSING WHEEL

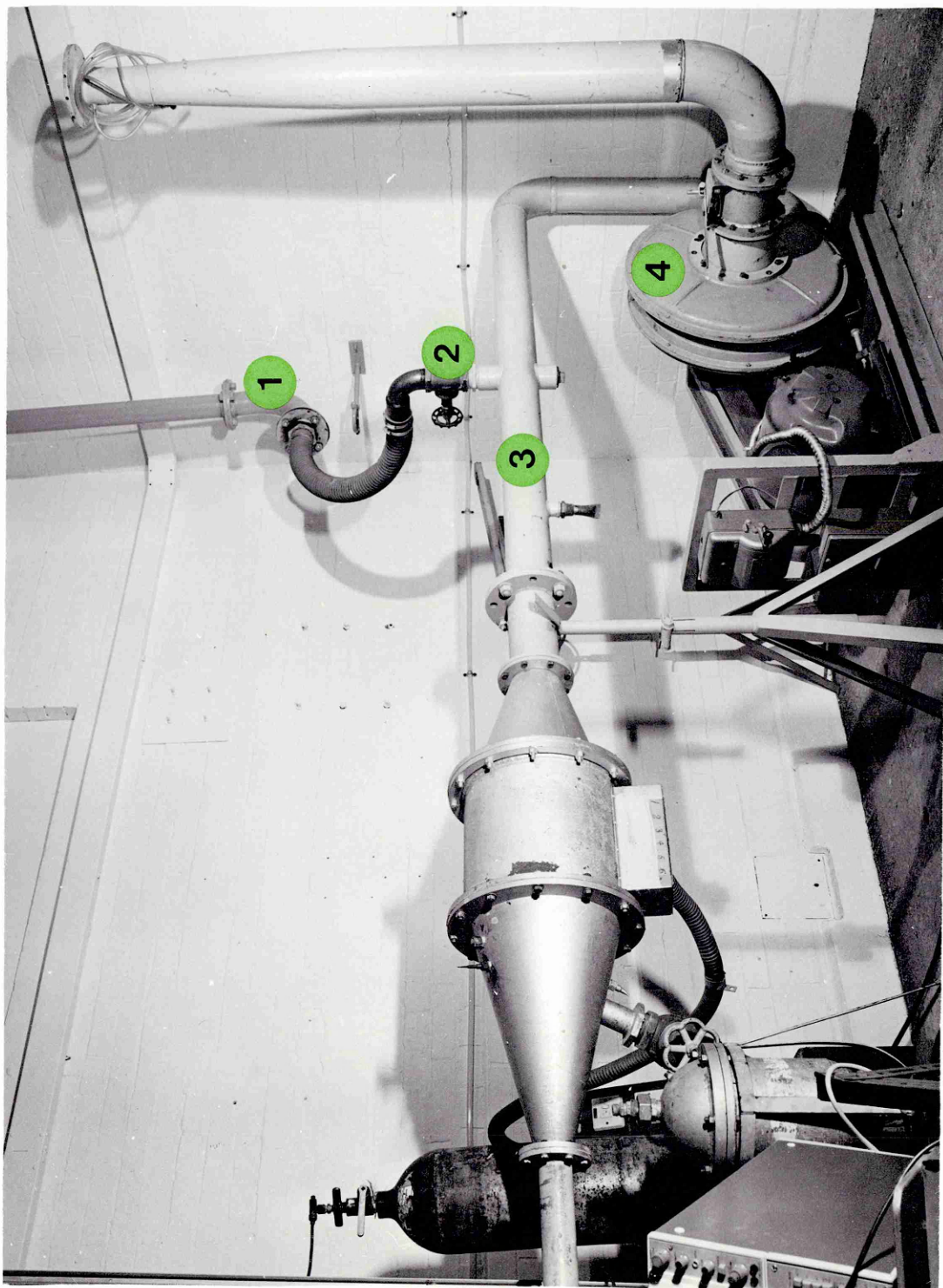
8 - TRAVERSING MOTOR



- 1 - A. V. C.
- 2 - DIGITAL VOLTMETER
- 3 - H. T. SUPPLY TO P. M.
- 4 - X-AXIS POWER SUPPLY
- 5 - DIGITAL VOLTMETER
- 6 - LOG. AMPLIFIER
- 7 - SYNCHRONOUS DEMODULATOR
- 8 - CHOPPER FREQUENCY CONTROL
- 9 - OSCILLOSCOPE

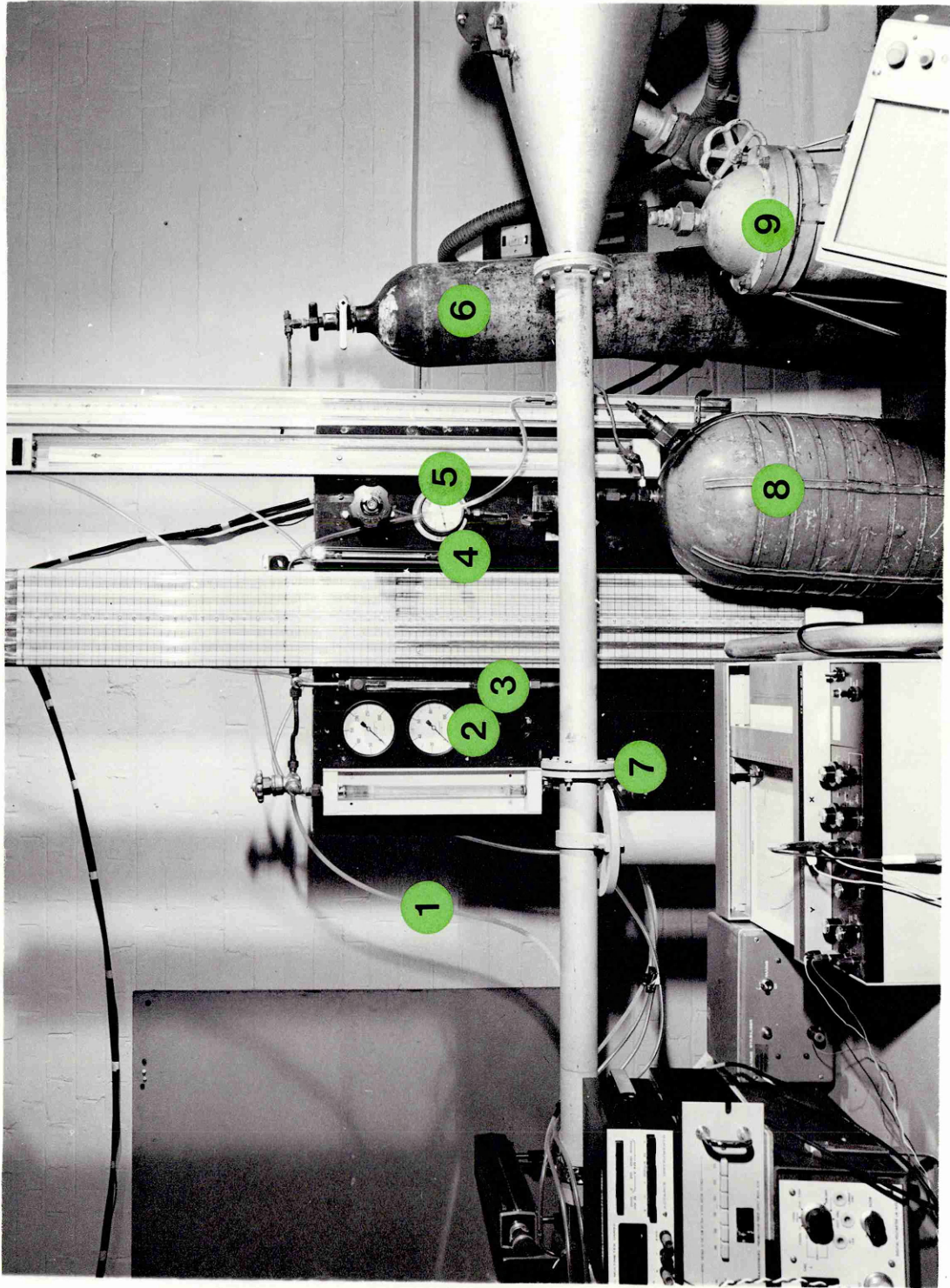
PLATE 3

Handwritten signature



- 1 - EXTERNAL COMPRESSOR LINE
- 2 - SHUT-OFF VALVE
- 3 - MAIN AIR DUCT
- 4 - AIR BLOWER

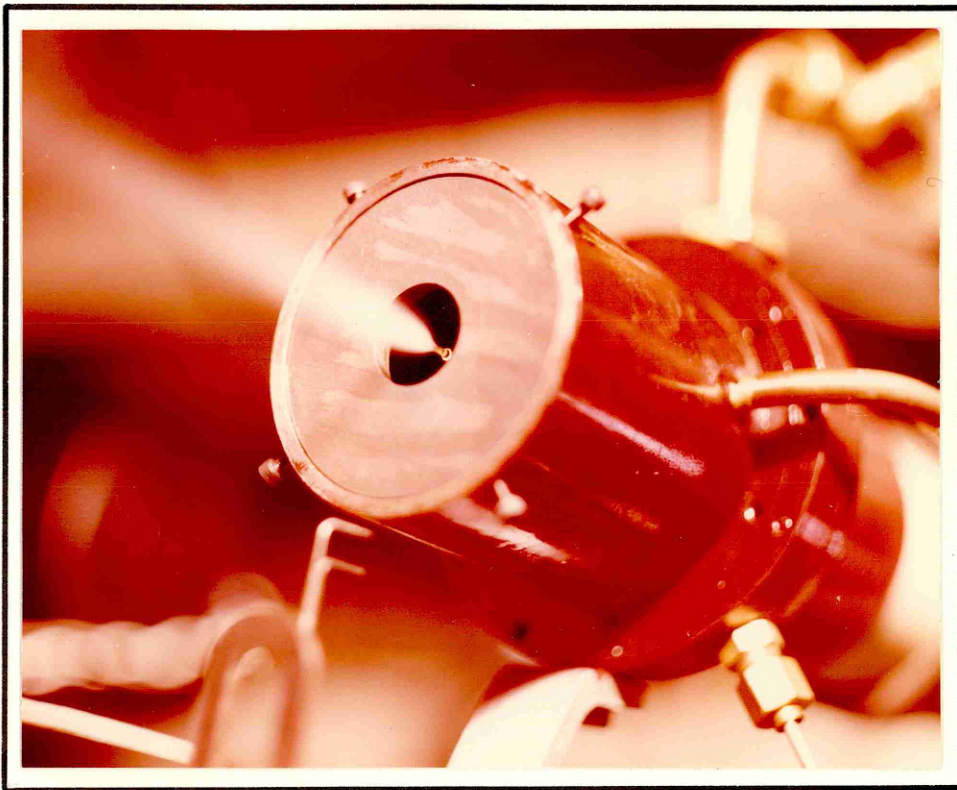
PLATE 4



- | | | |
|---------------------------|-----------------------------------|--------------------------|
| 1 - LIQUID LINE | 4 - FLOW METER | 7 - MAIN AIR DUCT |
| 2 - LIQUID PRESSURE GAUGE | 5 - N ₂ PRESSURE GAUGE | 8 - Kerosine TANK |
| 3 - FLOW METER | 6 - N ₂ BOTTLE | 9 - SPECIAL LIQUIDS TANK |

PLATE 5

PLATE 6

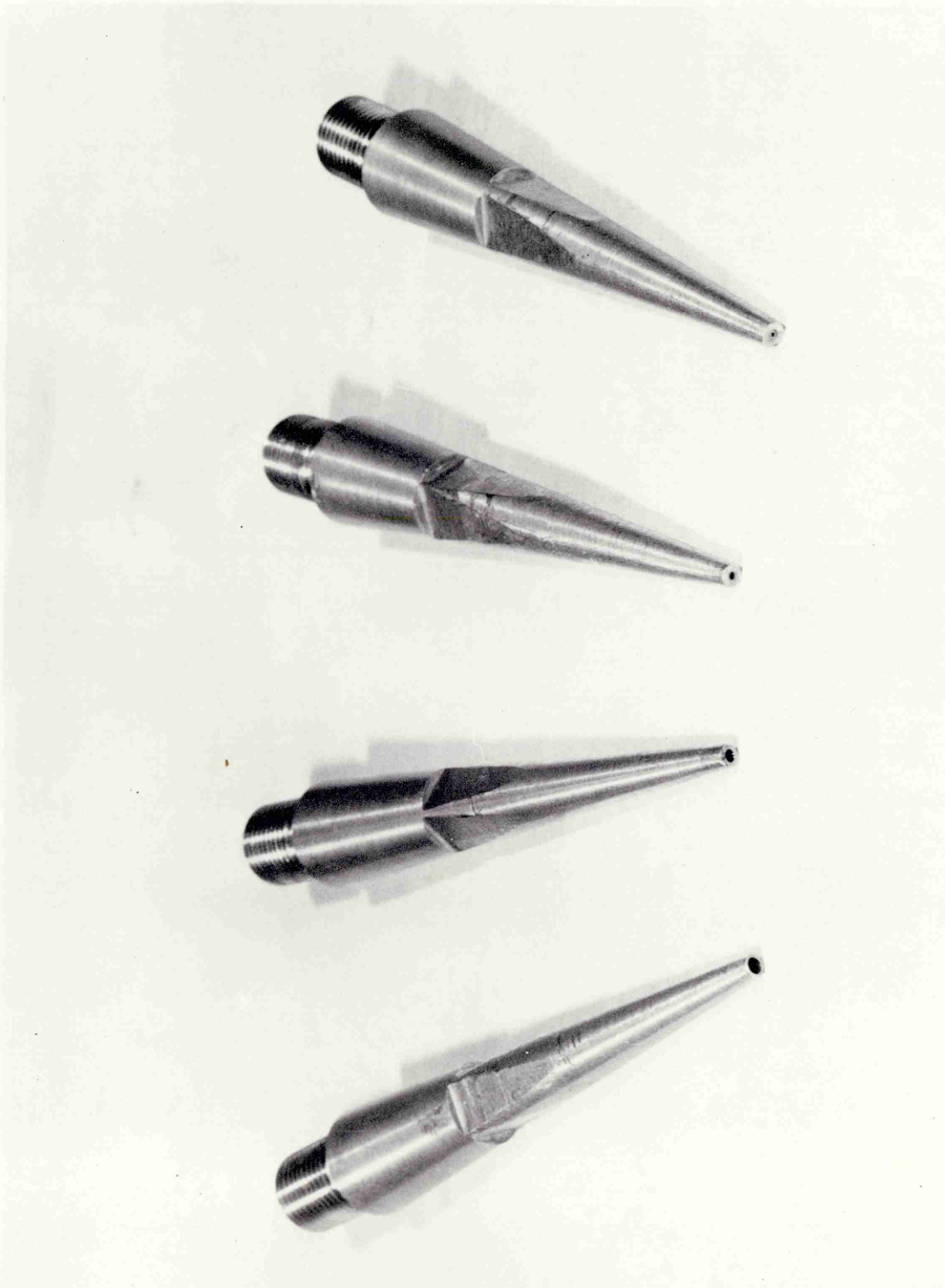


RELATIVE AIR VELOCITY : 120 m/s

KEROSINE FLOW RATE : 2 gr/s

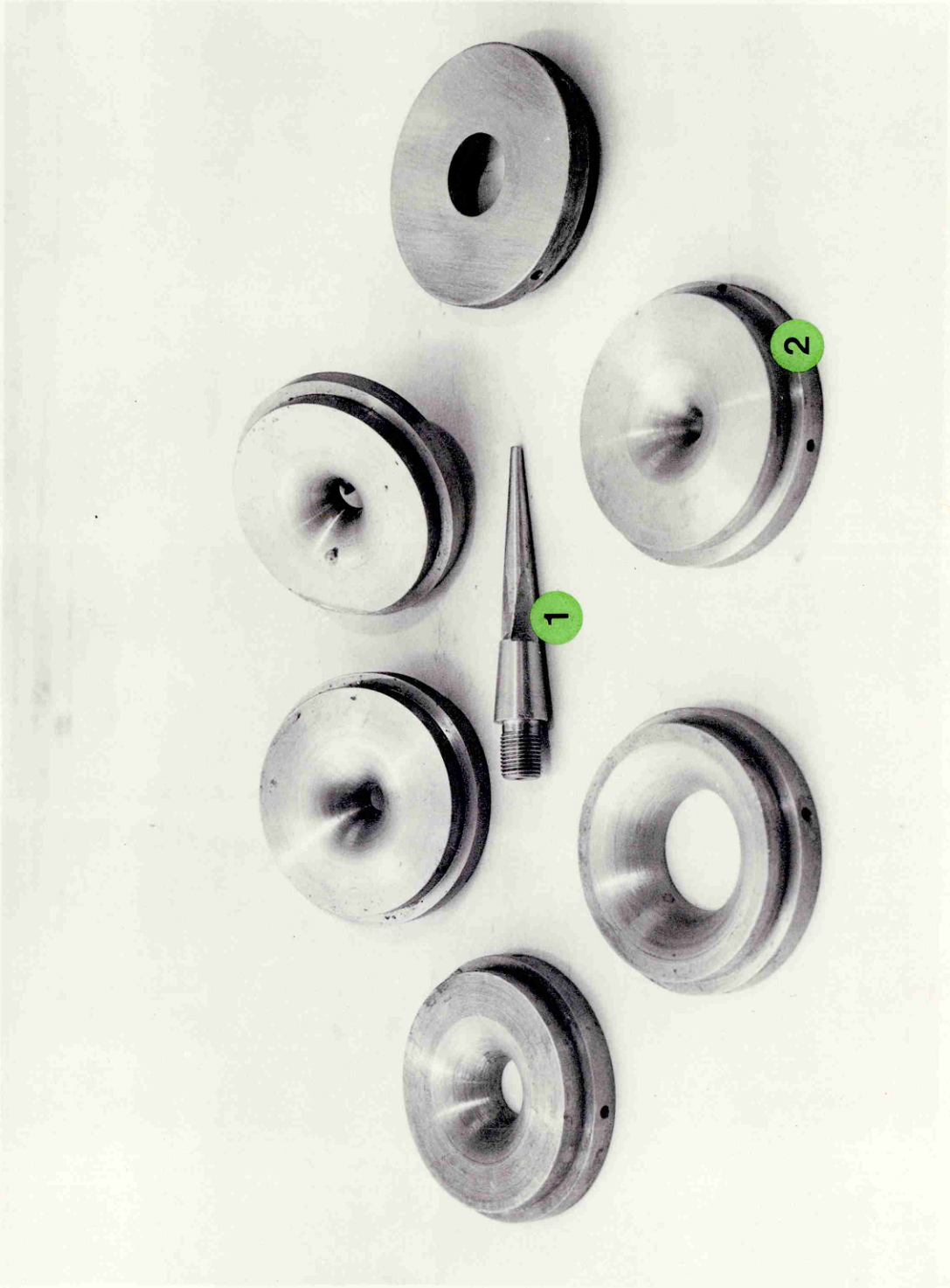
AIR NOZZLE: 19.05 mm - FUEL ORIFICE: 1.588 mm

A.F.R. = 10.05



PLAIN-JET FUEL ORIFICES

PLATE 7



2 - AIR NOZZLES

1 - FUEL ORIFICE

PLATE 8

2

KEROSENE FLOW RATE: 1 gr/s - AIR NOZZLE: 6.85 mm - AIR VELOCITY: 100 m/s - A.F.R. = 4.15

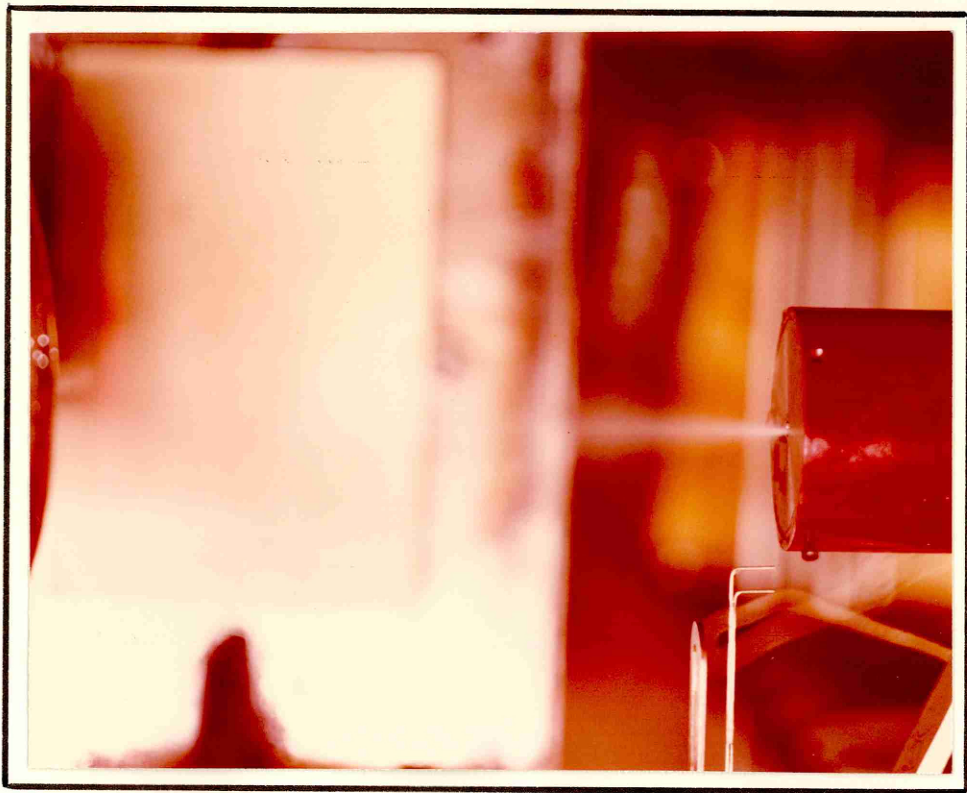


**PLATE
9**

FUEL ORIFICE DIAMETER: 0.794 mm.

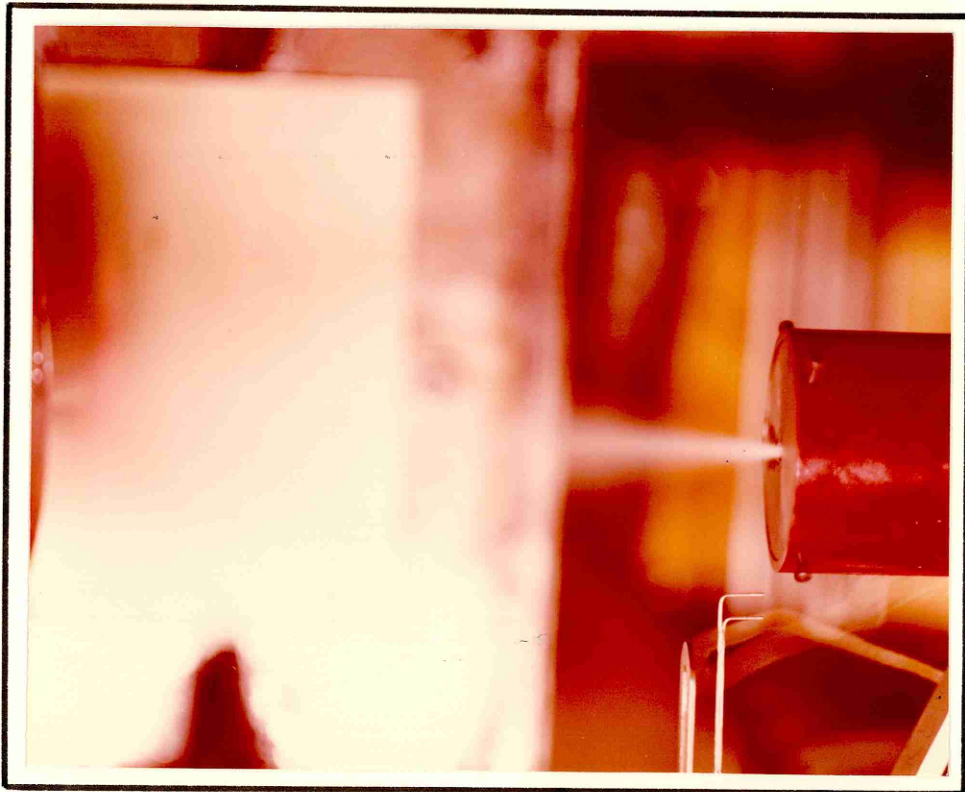


**PLATE
10**

FUEL ORIFICE DIAMETER: 1.588 mm.

KEROSENE FLOW RATE: 2 gr/s - RELATIVE AIR VELOCITY: 100 m/s - FUEL ORIFICE: 1.191 mm



**PLATE
11**

AIR NOZZLE DIAMETER: 5.83 mm - A.F.R. = 1.5



**PLATE
12**

AIR NOZZLE DIAMETER: 6.85 mm - A.F.R. = 2.10



**PLATE
13**

AIR NOZZLE DIAMETER: 12.70 mm - A.F.R. = 7

KEROSENE FLOW RATE: 2 gr/s - AIR NOZZLE: 6.85 mm - FUEL ORIFICE: 1.191 mm



**PLATE
14**

RELATIVE AIR VELOCITY: 70 m/s - A.F.R. = 1.58



**PLATE
15**

RELATIVE AIR VELOCITY: 100 m/s - A.F.R. = 2.10



**PLATE
16**

RELATIVE AIR VELOCITY: 140 m/s - A.F.R. = 2.78